

Modelling of Signal Uncertainty and Control Objectives in Robust Controller Design

Doctor of Philosophy
in
Electronic Engineering

Declan G. Bates

Dublin City University
School of Electronic Engineering

Supervised by Dr. Anthony M. Holohan

April 1996

I hereby certify that this material, which I now submit for assessment on the programme of study leading to the award of Doctor of Philosophy in Electronic Engineering is entirely my own work and has not been taken from the work of others save and to the extent that such work has been cited and acknowledged within the text of my work.

Signed:  ID No.: 92700152

Date: 15/4/96

Acknowledgements

I would like to sincerely thank Dr. Anthony Holohan for his constant guidance, attention and patience over the last four years.

Thanks are also due to Professor Charles McCorkell and the School of Electronic Engineering at Dublin City University for supporting this research.

Finally thanks to my family and friends, without whom...

List of Acronyms

SISO	Single Input Single Output
MIMO	Multi Input Multi Output
MISO	Multi Input Single Output
LQG/LTR	Linear Quadratic Gaussian Control with Loop Transfer Recovery
LTI	Linear Time Invariant
NL	Non Linear
TV	Time Varying
NLTV	Non Linear Time Varying
BIBO	Bounded Input Bounded Output
SGT	Small Gain Theorem
ORDAP	Optimal Robust Disturbance Attenuation Problem
RHP	Right Half Plane
AUR	As-U-Rolls
SVD	Singular Value Decomposition

Abstract

This work develops a new paradigm for optimal robust controller synthesis in the frequency domain. A detailed examination is made of the engineering motivation and engineering efficacy underlying the various strands of robust control theory. The modelling of (a) signal uncertainty and (b) control system objectives in both \mathcal{H}_∞ and \mathcal{L}_1 control theories is considered in particular detail. Based on this examination, a theory which can fairly be described as ‘a modified \mathcal{H}_∞ control theory’ or ‘a frequency domain \mathcal{L}_1 control theory’ is proposed. New signal sets for the modelling of uncertain signals are introduced. It is argued that these models more faithfully capture the way in which uncertain signals act on real physical systems. It is shown that by adopting these new models for uncertain signals, \mathcal{H}_∞ control theory can be used to non-conservatively minimise maximum tracking errors in the time domain, in the SISO case. In the MIMO case, the problem of optimally synthesising a controller to non-conservatively minimise tracking errors in the time domain leads to a modest variation on existing \mathcal{H}_∞ control theory, requiring the usual \mathcal{H}_∞ norm to be modified slightly. It is argued that the proposed paradigm in general achieves a better quality of control and more faithfully expresses the true objectives of feedback control systems. The proposed development is seen to also extend naturally to \mathcal{H}_2 control theory, and indeed provides a new deterministic justification for the \mathcal{H}_2 control problem in the MIMO case.

The question of design transparency in the synthesis of optimal robust controllers for multivariable systems is considered in detail. The implications of the proposed paradigm for transparency of design and weighting function selection are detailed. A decoupling design procedure for robust controller synthesis is proposed which, under certain restrictive conditions, allows the calculation of super-optimal robust controllers on a loop by loop basis. The usefulness of a classical decoupling approach to MIMO control system design in the context of multivariable robust control theory is demonstrated.

A number of design examples are presented which show how the ideas and methods developed in this work can be applied to realistic control problems.

Contents

1	Introduction to Robust Control	1
1.1	Philosophy of the Thesis	2
1.2	Organisation of the Thesis	2
1.3	Fundamental Concepts in Robust Control	3
1.3.1	Norms of Signals	4
1.3.2	Uncertainty in Signals	6
1.3.3	Norms of Systems	8
1.3.4	Uncertainty in Systems	9
1.3.5	A Canonical Form	11
1.3.6	Nominal Performance	14
1.3.7	Robust Stability	15
1.3.8	Robust Performance	17
2	Robust Controller Synthesis: \mathcal{H}_∞ and \mathcal{L}_1 Control theory	18
2.1	\mathcal{H}_∞ Theory: Nominal Performance	19
2.2	\mathcal{H}_∞ Theory: Robust Stability	20
2.3	The Mixed Sensitivity \mathcal{H}_∞ Control Problem	21
2.4	Solutions to the Mixed Sensitivity \mathcal{H}_∞ Control Problem	27
2.5	A Critique of \mathcal{H}_∞ Control Theory	28
2.5.1	(i) The Output Norm and ‘Spikes’	28
2.5.2	(ii) Signal Set and Specification Lumping	32
2.5.3	(iii) Robust Performance	33
2.5.4	(iv) Weighting Function Selection	35
2.6	\mathcal{L}_1 Theory: Nominal Performance	37
2.7	\mathcal{L}_1 Theory: Robust Stability	38
2.8	The Mixed Sensitivity \mathcal{L}_1 Control Problem	39

2.9	Solutions to the Mixed Sensitivity \mathcal{L}_1 Control Problem	41
2.10	A Critique of \mathcal{L}_1 Control Theory	41
2.10.1	(a) The Output Norm: Non Conservative Minimisation of Maximum Tracking Errors in The Time Domain	42
2.10.2	(b) Signal Set and Specification Lumping	43
2.10.3	(c) Robust Performance	44
2.10.4	(d) Weighting Function Selection	44
3	A New Paradigm for Optimal Robust Controller Synthesis in the Frequency Domain	46
3.1	SISO Nominal Performance in \mathcal{H}_∞ : Non Conservative Minimisation of Maximum Tracking Errors in the Time Domain	47
3.1.1	A Sinusoidal Signal Set $\mathcal{D}_w^{(s)}$	47
3.1.2	The Convex Hull is Free	49
3.1.3	A Frequency Domain \mathcal{L}_1 Norm Signal Set	51
3.2	SISO Robust Stability in \mathcal{H}_∞	54
3.3	Interpretations of the \mathcal{H}_∞ Norm	56
3.4	MIMO Nominal Performance in \mathcal{H}_∞ : Non-Conservative Minimisation of Maximum Tracking Errors in the Time Domain	57
3.4.1	Vector Extensions of the Signal Sets $\mathcal{D}_w^{(s)}$ and $\mathcal{D}_w^{(1)}$	57
3.4.2	A New \mathcal{H}_∞ Optimisation Problem	58
3.5	MIMO Robust Stability in \mathcal{H}_∞	64
3.6	A New Approach to \mathcal{H}_∞ Weighting Function Selection	65
3.7	Robust Performance and Relations with Standard \mathcal{H}_∞ Theory	68
3.8	Nominal Performance in \mathcal{H}_2 : Non-Conservative Minimisation of Maximum Tracking Errors in the Time Domain	69
3.8.1	The SISO Case: A Solved Problem	69
3.8.2	An Extension to the MIMO Case	70
3.9	Robust Specifications in \mathcal{H}_2	73
4	A Decoupling Design Method for Super-Optimal Robust Control	74
4.1	Motivation for Decoupling the Design Process	75
4.2	Three Robust Control Problem Formulations	77
4.3	Full Decoupling and Super-Optimality: the Minimum-Phase Case	77
4.4	Half Decoupling: the Non-Minimum-Phase Case	82

4.4.1	Super-Optimal Solutions to the \mathcal{L}_1 and Modified \mathcal{H}_∞ Mixed Sensitivity Problems	82
4.4.2	A Sub-Optimal Solution to the Mixed Sensitivity \mathcal{H}_∞ Control Problem	84
4.5	Discussion	86
5	Multivariable \mathcal{H}_∞ Synthesis via Decoupling and Loopshaping: Some Design Examples	88
5.1	Super-Optimal Pitch Axis Control of a Highly Manoeuvrable Experimental Aircraft	89
5.1.1	Plant Description	89
5.1.2	Closed Loop Design Objectives	91
5.1.3	A Standard \mathcal{H}_∞ Design	91
5.1.4	A Decoupling Controller	92
5.1.5	Super-Optimal Control	97
5.1.6	Discussion and Implications	99
5.2	Loopshaping for Robust Performance and B-Norm Reduction	100
5.2.1	Loopshaping for SISO systems	100
5.2.2	Loopshaping MIMO systems for Improved Robust Performance	102
5.2.3	Loopshaping MIMO systems for Time Domain Objectives . .	109
5.3	Robust Shape Control in a Sendzimir Cold-Rolling Steel Mill - A Decoupling Approach	116
5.3.1	The Control Problem	116
5.3.2	The Sendzimir Mill: Nominal Model	117
5.3.3	Nominal Model Reduction and Decoupling	118
5.3.4	Uncertainty Modelling	120
5.3.5	\mathcal{H}_∞ Controller Synthesis and Performance Analysis	121
5.3.6	Discussion and Implications	127
6	Conclusions	128
6.1	\mathcal{H}_∞ Control Theory and Time Domain ‘Spikes’	129
6.2	Specification Modelling in Robust Control Theory	130
6.3	Uncertain Signal Modelling in Robust Control Theory	130
6.4	Time Domain Specifications and Frequency Domain Design	131
6.5	Weighting Function Selection and Manipulation in \mathcal{H}_∞ Control theory	132

6.6	Connections between \mathcal{H}_∞ and \mathcal{L}_1 Control Theories	133
6.7	A Comparison of the Different Paradigms	134
6.8	Decoupling MIMO Systems for Super-Optimal Robust Controller Design	135
6.9	Loopshaping Decoupled MIMO Systems for Improved Performance . .	136
6.10	Directions for Future Research	136

Chapter 1

Introduction to Robust Control

This chapter introduces in a general way the scope and aims of this work. The research philosophy adopted is outlined and a brief guide to the lay-out of the thesis is given. The remainder of the chapter serves as a brief introduction to some of the most fundamental concepts in robust control theory, with emphasis on those aspects which are most relevant to this thesis.

1.1 Philosophy of the Thesis

In this section we make some preliminary remarks on the scope, philosophy and aims of this thesis. The control philosophy espoused throughout is that of Optimal Robust Controller Synthesis – in particular, the \mathcal{H}_∞ and \mathcal{L}_1 theories are discussed in detail, while the \mathcal{H}_2 theory is also considered. The mathematical techniques required to solve the various optimisation problems which arise in these theories are *not* the subject of this thesis, and these ‘tools’ are therefore not considered in detail. Rather the main subject of the thesis is a consideration of the engineering motivation and engineering efficacy which underlies the various strands of robust control theory. As a consequence, certain rather abstract concepts pertaining to robust control theory are examined in detail. Current techniques for the modelling of uncertainty are evaluated, and in the case of signal uncertainty, new uncertainty sets are proposed. The question of how to express the ‘real’ objectives of feedback control systems as rigorous specifications, which can be met automatically via mathematical optimisation is also considered. Since the particular way in which both uncertainty and control objectives are modelled is essentially at the discretion of the designer, another important issue addressed in the thesis is the effect this ‘choice’ has on the transparency of the design process and the applicability of the theory. Based on the examination of issues such as those outlined above, a new paradigm for optimal robust controller synthesis is proposed which, it is argued, captures the most attractive features of the various approaches presently in use. The emphasis throughout is on multivariable systems. Indeed another aim of the thesis is to examine the relationship between classical multivariable controller design methods and modern multivariable robust control theory. A canonical form for linear controller synthesis is adopted right at the beginning of the thesis in order to emphasise the similarities and differences between the various strands of robust control theory.

1.2 Organisation of the Thesis

The lay-out of the thesis is as follows. This chapter contains some preliminary remarks on the general nature of the thesis. It also contains a brief introduction to some of the most fundamental concepts in robust control theory, with emphasis on those aspects which pertain to this thesis. Chapter 2 contains a detailed examination of the \mathcal{H}_∞ and \mathcal{L}_1 control theories. A critique of both theories is given which seeks not only to

identify their various strengths and limitations but to uncover the root causes of these limitations. Three limitations of \mathcal{H}_∞ control theory in particular are identified – it is argued however that these difficulties are not with \mathcal{H}_∞ control theory *per se*, but with the conventional paradigm which is attached to it. Based on this analysis, Chapter 3 presents a new paradigm for optimal robust controller synthesis. It is argued that the new approach captures the most attractive features of both \mathcal{H}_∞ and \mathcal{L}_1 control theories. The development in Chapters 2 and 3 follows closely that of [1, 2]. Chapter 4 proposes a decoupling design method which under certain conditions allows the design of super-optimal robust controllers. In Chapter 5 a number of design examples are presented which show how the ideas and methods developed in the previous chapters can be applied to realistic control problems. The decoupling design method discussed in Chapter 4 is detailed in [3, 4], while the section in Chapter 5 dealing with Sendzimir mills is an extension of the treatment in [5]. Chapter 6 is a discussion of the most significant observations and results contained in the thesis. Some conclusions are drawn and directions for further research are identified.

1.3 Fundamental Concepts in Robust Control

Underlying all of robust control theory are three fundamental tenets. The first is that uncertainty, both in terms of systems and signals, is inevitable and omnipresent, and thus needs to be explicitly considered from the start of the design process. The second is that the main purpose of feedback is to (a) retain closed loop stability in the face of this uncertainty, and (b) counteract the effect of this uncertainty on system performance. The third is that design methods based on mathematical optimisation are required in order to reveal the limits of performance for systems and thus provide controllers which can be considered optimal in some suitable sense.

The importance given to these concepts in robust control theory has necessitated the development of new models, measures and configurations for control system design. This section will serve as a brief introduction to these basic tools. The development is intended to highlight the fundamental similarities between the various strands of robust control theory.

1.3.1 Norms of Signals

Many of the objectives of controller design are explicitly formulated in terms of the *size* of certain signals. It is clear however that the notion of the size of a signal, whether it be a ‘small tracking error’ or a ‘large input disturbance’, is entirely dependent on the way in which it is measured. Among the many ways in which a signal can be measured, those that satisfy certain geometric properties in a vector space have proved most useful. In mathematical terminology these measures of size are functions called *norms*. Many different signal norms are in common use. For a comprehensive treatment see [6]. In this section we describe only those which are used in \mathcal{H}_∞ , \mathcal{L}_1 and (in a deterministic setting) \mathcal{H}_2 control theories. Note that a signal norm can be defined in the time domain, and/or the frequency domain.

The \mathcal{L}_2 **norm** for scalar signals is

$$\| z(j\omega) \|_2 = \sqrt{\frac{1}{2\pi} \int_{-\infty}^{+\infty} |z(j\omega)|^2 d\omega} \quad (1.1)$$

The \mathcal{L}_2 **norm** for vector signals is

$$\left\| \begin{pmatrix} z_1(j\omega) \\ \vdots \\ z_n(j\omega) \end{pmatrix} \right\|_2 = \sqrt{\frac{1}{2\pi} \int_{-\infty}^{+\infty} \sum_{i=1}^n |z_i(j\omega)|^2 d\omega} = \sqrt{\sum_{i=1}^n \| z_i(j\omega) \|_2^2} \quad (1.2)$$

This norm is also known as the **Euclidean norm** or the **quadratic norm**, and it is the signal norm used in \mathcal{H}_∞ control theory. It is also defined in the time domain but in the context of \mathcal{H}_∞ control theory it is usually considered from a frequency domain perspective. Note that the \mathcal{L}_2 norm cannot be used to measure persistent signals, i.e. signals which do not decay to zero with time. The \mathcal{L}_2 norm corresponds to the total energy in a signal.

The \mathcal{L}_∞ **norm** for real-valued scalar signals is

$$\| z(t) \|_\infty = \sup_{-\infty < t < +\infty} |z(t)| \quad (1.3)$$

This norm describes the size of a signal by its maximum amplitude in the time domain. The size of vector signals can be quantified by combining this norm for scalar signals

with the infinity vector norm.

Thus the \mathcal{L}_∞ **norm** for vector signals is

$$\left\| \begin{pmatrix} z_1(t) \\ \vdots \\ z_n(t) \end{pmatrix} \right\|_\infty = \max_i \| z_i(t) \|_\infty \quad (1.4)$$

This is the signal norm used in \mathcal{L}_1 control theory, and is also called the **maximum amplitude norm** or the **infinity norm**. It is also defined in the frequency domain, but from the perspective of \mathcal{L}_1 control theory it is usually considered in the time domain. Note that this norm can be used to measure persistent signals.

The \mathcal{L}_1 **norm** for scalar signals is

$$\| z(j\omega) \|_1 = \int_{-\infty}^{+\infty} |z(j\omega)| d\omega \quad (1.5)$$

The \mathcal{L}_1 **norm** for vector signals is

$$\left\| \begin{pmatrix} z_1(j\omega) \\ \vdots \\ z_n(j\omega) \end{pmatrix} \right\|_1 = \int_{-\infty}^{+\infty} \sum_{i=1}^n |z_i(j\omega)| d\omega = \sum_{i=1}^n \| z_i(j\omega) \|_1 \quad (1.6)$$

The \mathcal{L}_1 signal norm can also be defined in the time domain where it can be shown to measure total resource consumption, e.g. the total amount of fuel burned by a rocket over the course of its trajectory. In the modified \mathcal{H}_∞ control theory presented in Chapter 3 however, it is considered from a frequency domain point of view.

This thesis will have occasion to discuss many different norms, some of which are defined in the time domain and others in the frequency domain, and this presents notational issues which require comment. Throughout this thesis, systems will be denoted by upper case letters, signals by lower case letters, and sets of systems or signals by upper case script letters. The (i, j) th element of a transfer function matrix $G(s)$ will be denoted by $(G(s))_{ij}$, and similarly for impulse response matrices. Suppose that $G(s)$ is the transfer function of a stable $m \times n$ LTI system, and that $y(t)$ is the output which results from the input $u(t)$. The Fourier transform of a signal $u(t)$ will be denoted by $u(j\omega)$, and similarly for other signals, so that

$$y(j\omega) = G(j\omega)u(j\omega)$$

Then, $G(t)$ denotes the (integrable, causal) impulse response of $G(s)$. Hence,

$$y(t) = G(t) * u(t)$$

where the asterisk denotes convolution. On occasion, the argument t or $j\omega$ will be suppressed in our notation when the specific choice of norm is open and may require either t or $j\omega$. For instance $\|u\|_s$ may mean either $\|u(t)\|_s$ or $\|u(j\omega)\|_s$. After this caution, this slight abuse of notation should not cause confusion later.

1.3.2 Uncertainty in Signals

It is now widely accepted that uncertainty issues constitute a fundamental and unavoidable aspect of the controller design problem. The term **uncertainty** is a loose umbrella term for any sort of limitation in our knowledge of a control system, in whatever form that might take. In physically motivated engineering problems, uncertainty usually arises in two forms. Perhaps it is truer to say that uncertainty issues are generally modelled by control engineers in one of two ways. There is uncertainty in systems and uncertainty in signals. It is interesting that these two different types of uncertainty have very different effects on the closed loop system. For example, system uncertainty can cause a nominally stable system to become unstable, which signal uncertainty cannot do. While the modelling of system uncertainty has received an enormous amount of attention, perhaps it is true to say that the issue of signal uncertainty has been generally under-emphasised in the literature. It is hoped that one of the contributions of this thesis will be to focus in more detail on the different ways in which uncertain signals can be modelled under existing theoretical frameworks. In this subsection we discuss the current methods for describing uncertain signals in robust control theory.

Uncertain signals are input signals to the system which are uncertain, incompletely known, or unpredictable. The physical sources of these signals include disturbances at the input or the output of the plant, measurement noise on feedback signals, command inputs, and a host of other largely unknown inputs due to various environmental factors. It is clear then that in fact *all* of the input signals to a control system are essentially unknown. How then can these signals be described in a formal manner? The first attempts at modelling uncertain signals adopted a probabilistic approach. Signals were viewed as being stochastic in nature but with known spectral densities. This viewpoint led to the so called LQG/LTR control theory [7], which gained signif-

icant popularity in the 1970's. As pointed out in [8] however, a fundamental problem with this theory was the absence of any obvious extension of this approach to deal with modelling of uncertainty in systems. In order to construct a harmonious framework for the modelling of both signal and system uncertainty, the following approach was proposed by Zames in [8].

Consider each input signal as being unknown, but belonging to some set or range of possibilities, denoted by \mathcal{D}_w . This set may be defined in many different ways, depending on the amount of structure required. The simplest and perhaps the most useful way of describing \mathcal{D}_w is to impose a norm bound on the 'size' of the elements of the set. Thus we can write

$$\mathcal{D}_w = \{w(t) \mid \|w(t)\|_s \leq 1\}$$

or

$$\mathcal{D}_w = \{w(j\omega) \mid \|w(j\omega)\|_s \leq 1\}$$

for some signal norm $\|\cdot\|_s$. These correspond to signal sets which are described by the single constraint that w have norm less than or equal to unity in either the time domain or the frequency domain. Such sets can reasonably be described as **unstructured signal sets**. They correspond to the unit ball in the appropriate vector space of signals. Note that even in the SISO case, $w(t)$ and $w(j\omega)$ above will in general be vector quantities, since all the possible uncertain signals acting at various points in the system are 'lumped' together into one vector w . We will have more to say about the implications of this design 'choice' in later chapters.

Describing a class of uncertain signals by the single constraint of a norm bound is insufficiently flexible and too crude for most purposes, and more refined models of uncertain signals are needed. Weighting transfer functions provide much needed flexibility here. Uncertain signals entering the physical system are viewed as the outputs of transfer functions which are driven by inputs having norm less than or equal to one in some signal norm. This is the approach adopted to modelling uncertain signals in \mathcal{H}_∞ and \mathcal{L}_1 control theories. These transfer functions are termed weighting transfer functions, or simply weights. So uncertain signals can be said to be described by **weighted, filtered or coloured** versions of the unit ball in some vector space of signals. The selection of appropriate weighting functions for uncertain input signals is one of the most crucial and difficult steps in robust controller design.

Finally, we remark that the ideal model that captures all the time and frequency domain features of uncertain signals has not yet been developed. Models such as the

ones detailed above based on an entire weighted unit ball may allow for signals which do not exist in practice. As noted in [9], it can be just as limiting to have models which allow signals or perturbations which have no physical motivation but severely degrade performance (of the model), as it is to have models which ignore uncertainty altogether. The problem of finding the optimal trade-off between these two extremes is the subject of ongoing research.

1.3.3 Norms of Systems

In this section we consider ways of measuring the ‘size’ of an LTI system with input w , output z and transfer function matrix T_{zw} , as shown in Figure 1.1

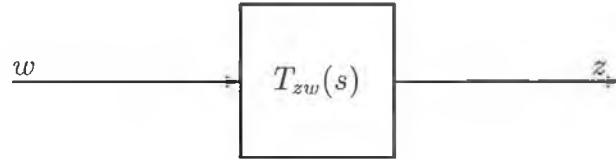


Figure 1.1: LTI System

Many general methods exist for measuring the size of a system in terms of its input and output signals. Just as with signals, we will use functions called norms to do this in a rigorous and consistent way. It will be shown that a natural approach is to measure the size of the system based on the way in which the input and output signals of the system are measured. For a given LTI system

$$z(j\omega) = T_{zw}(j\omega)w(j\omega)$$

when the signal norm is a frequency domain norm, and

$$z(t) = T_{zw}(t) * w(t)$$

when the signal norm is a time domain norm. In the previous subsection we adopted the approach of regarding each input signal w as unknown but belonging to the norm bounded set \mathcal{D}_w . For a given LTI system, this then gives rise to a corresponding well-defined set of possible z 's. Thus in order to define a measure of the system T_{zw}

which takes into account its response to the whole set of possible input signals \mathcal{D}_w , we use the so-called worst case response norm

$$\|T_{zw}(j\omega)\|_{Is} = \sup_{w \neq 0} \frac{\|T_{zw}(j\omega)w(j\omega)\|_s}{\|w(j\omega)\|_s} \quad (1.7)$$

or

$$\|T_{zw}(t)\|_{Is} = \sup_{w \neq 0} \frac{\|T_{zw}(t) * w(t)\|_s}{\|w(t)\|_s} \quad (1.8)$$

System norms of the above form depend completely on the particular signal norm $\|\cdot\|_s$, and will therefore be referred to as **induced norms**. Note that they arise very naturally in the present control context. The norm $\|\cdot\|_{Is}$ is said to be induced by $\|\cdot\|_s$. Whether or not the term induced norm requires the numerator (or output side) norm and the denominator (or input side) norm to be the same is just a matter of definition. In this thesis, the requirement that they are identical is taken to be a part of the definition. Induced norms quantify the maximum possible “gain” of the system from w to z , in terms of a certain signal norm. Expressions of the form

$$\|T_{zw}(j\omega)\|_{Irs} = \sup_{w \neq 0} \frac{\|T_{zw}(j\omega)w(j\omega)\|_r}{\|w(j\omega)\|_s} \quad (1.9)$$

or

$$\|T_{zw}(t)\|_{Irs} = \sup_{w \neq 0} \frac{\|T_{zw}(t) * w(t)\|_r}{\|w(t)\|_s} \quad (1.10)$$

also define norms. Note however that different signal norms appear on the numerator and the denominator. System norms of this type can reasonably be referred to as **semi-induced norms**, and this terminology will be used later. The system norms induced by the various signal norms detailed earlier will be discussed in detail as they arise, in Chapter 2.

1.3.4 Uncertainty in Systems

It is entirely obvious that real-life physical systems cannot be modelled perfectly. The behaviour predicted by a model of the system and the actual behaviour of the physical system will always differ. In most engineering problems, such differences are so substantial that they cannot be ignored. Limitations in our ability to model systems can be thought of as uncertainty in the system, since the actual behaviour of the physical system is then partly unknown, partly uncertain.

In classical feedback design the problem of system uncertainty was tackled by prescribing stability margins in terms of the gain, phase or peak M values of the

closed loop system. The use of such margins revealed an implicit assumption about the nature of system uncertainty, i.e. that it is unstructured. This means that no attempt is made to trace the origins of the uncertainty to specific points in the system; all that is assumed is some knowledge of a bound on its ‘size’. In this section we detail the various models available in robust control theory to *explicitly* describe unstructured system uncertainty. In cases where a significant amount of information is available regarding the source of the uncertainty, a more structured model may be appropriate, and this can be handled under the framework of μ analysis and synthesis. This theory however is beyond the scope of this thesis.

The three most commonly used models of unstructured system uncertainty in robust control theory are as follows. Let $P_0(s)$ be the transfer function matrix corresponding to the nominal plant, i.e. a best estimate in some sense of the true plant behaviour. Let $P(s)$ be the transfer function matrix corresponding to the true plant. Then

$$P(s) = P_0(s) + \Delta_a(s) \quad (1.11)$$

$$P(s) = P_0(s) (I + \Delta_i(s)) \quad (1.12)$$

$$P(s) = (I + \Delta_o(s)) P_0(s) \quad (1.13)$$

where Δ_a represents an **additive uncertainty**, Δ_i an **input multiplicative uncertainty** and Δ_o an **output multiplicative uncertainty**. Of course Δ_i and Δ_o are equivalent in the SISO case. Now just like with the modelling of uncertain signals, the three Δ ’s above are viewed as being unknown but belonging to some well defined set.

This scenario raises the question of what sort of uncertainty sets to use, i.e. of how to describe system uncertainty sets. Again as with signal sets, we restrict our attention to sets which are described by a single norm bound. Also, we consider only induced norms. These limitations (in optimal *synthesis* problems) are necessitated by the mathematical tools available at present. Some terminology is needed. A system T_{yx} with input x and output y is said to be **bounded input bounded output (BIBO) stable** in the $\| \cdot \|_s$ -sense (or s-stable for short) if there is a finite constant M such that

$$\| y \|_s \leq M \| x \|_s$$

for all inputs x . In this thesis the term stability always means BIBO stable in some signal norm $\| \cdot \|_s$, and the norm in use should be clear from the context. Then for

each of the three models above the particular uncertainty Δ_a , Δ_i or Δ_o is considered to belong to a set of the form

$$\mathcal{D}_\Delta = \{\Delta \mid \Delta \text{ is s-stable, LTI, and } \|\Delta\|_{Is} \leq r\}$$

where r is some scalar and $\|\Delta\|_{Is}$ means

$$\|\Delta(j\omega)\|_{Is} = \sup_{a \neq 0} \frac{\|\Delta(j\omega)a(j\omega)\|_s}{\|a(j\omega)\|_s} \quad \text{or} \quad \|\Delta(t)\|_{Is} = \sup_{a \neq 0} \frac{\|\Delta(t) * a(t)\|_s}{\|a(t)\|_s}$$

and where $\|\cdot\|_s$ is some signal norm. This sort of plant uncertainty is called **unstructured system uncertainty**, because Δ is constrained only by a single induced norm bound. This set can be viewed as a set of possible perturbations to the plant model. So the plant to be controlled is viewed as a *set* of possible systems, rather than as a single system which is completely and perfectly known. As was the case with signal uncertainty, our unstructured models of system uncertainty can be made more flexible and refined by including weighting transfer functions to reflect the likely spectral content of the uncertainty in the given plant. This is done by setting

$$\Delta = W\tilde{\Delta} \tag{1.14}$$

where W is a stable minimum phase transfer function or transfer function matrix. Thus $\|\tilde{\Delta}\|_{Is}$ can always be normalised to be ≤ 1 . Both input and output multiplicative uncertainty models are needed since multiplication of transfer function matrices is non-commutative. In effect the former assumes that all the uncertainty occurs at the plant input while the latter assumes that it all occurs at the output.

1.3.5 A Canonical Form

The previous four subsections have detailed the ways in which robust control theory measures and models signals, systems and uncertainty. A standard configuration for feedback controller design which includes these various sources of uncertainty is shown in Figure 1.2. Uncertain input signals are represented by disturbances at the output of the plant and measurement noise on the feedback signal. Plant uncertainty is unstructured and multiplicative, acting at the input of the plant.

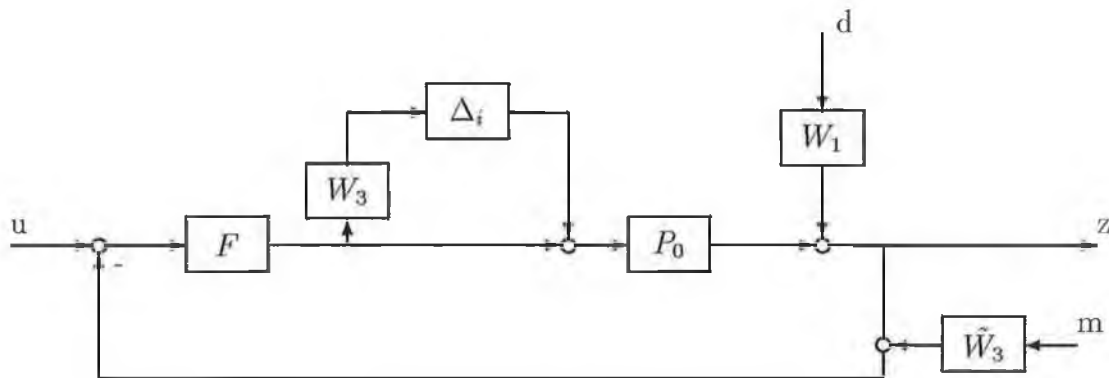


Figure 1.2: A Standard Configuration for Linear Controller Synthesis

This configuration has the advantage of being intuitively appealing from a physical point of view; disturbances at the output of the plant are drawn at the plant output etc. In order to cast the design problem in the framework of mathematical optimisation however, it is useful to have a single canonical form which includes as special cases all the different systems resulting from variations in the form and location of uncertainty. This subsection describes such a canonical form for linear time-invariant (LTI) controller synthesis problems. This canonical form is well known, and is widely used in the robust control literature [6, 44]. Consider the feedback configuration shown in Figure 1.3.

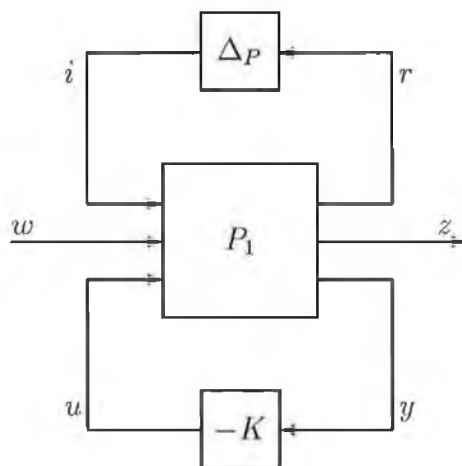


Figure 1.3: A Canonical Form for Linear Controller Synthesis with both Signal and System Uncertainty.

As is well known from the μ analysis literature [9], any feedback system of the form shown in Figure 1.2 can be transformed into this configuration via block diagram manipulations. Referring to the figure, the block P_1 is called the **nominal augmented plant**, and Δ is an uncertainty block which is unstructured but norm bounded. In this formulation, P_1 includes the nominal plant together with dynamics associated with the weighting transfer functions used to model signal and system uncertainty. P_1 then, together with Δ is the actual system to be controlled. The block $-K$ is the **controller**, and it consists of all the subsystems which the control system designer is free to choose. The vector signal w is called the vector of **exogenous inputs**. It consists of all external signals entering the system, and typically includes external disturbances, measurement noise signals and command inputs. This configuration allows us therefore to ‘lump’ all sources of signal uncertainty into a single vector w . The signal z is called the **regulated outputs**, and is *not* simply the physical outputs of the system. It is in fact all the signals in the system which are needed to write down the control problem’s specifications. Thus, it generally includes tracking errors, and may also include the plant input, system state variables, and so on. The signal u is called the **actuator inputs**, and is the vector of all input signals to P_1 which the controller can manipulate. Finally, the vector y is called the **sensor outputs**. It contains all the signals which the controller has access to. This canonical form is, in terms of abstraction, further removed from the ‘real’ physical system than that given in Figure 1.2. Its advantage however is that it easily allows controller design to be formulated in terms of mathematical optimisation problems. Note also that under this framework the purpose of feedback is clearly to attenuate the effects of both signal and system uncertainty on the system. Even the problem of command tracking is formulated in terms of the attenuation of the effect of an uncertain signal (the command input) on the appropriate regulated variables (tracking errors).

For the above configuration, any specification is said to be obeyed **nominally** if the nominal system, the system with $\Delta = 0$, obeys it. It is said to be obeyed **robustly** if it is satisfied for every Δ in the uncertainty set \mathcal{D}_Δ . In robust control theory, specifications are given in terms of the stability or the performance of the closed loop system. In the following subsections we show how nominal performance, robust stability and robust performance specifications can be cast as mathematical optimisation problems under the above canonical framework. We note however that in full generality, the only type of specifications which \mathcal{H}_∞ and \mathcal{L}_1 optimal synthesis can handle robustly are stability specifications.

1.3.6 Nominal Performance

Performance Specifications in robust control theory are generally given in terms of the attenuation of the effect of uncertain input signals on the regulated variables of the system, subject to internal closed loop stability. Nominal performance specifications can be cast as mathematical optimisation problems under the above canonical framework as follows. Consider Figure 1.4.

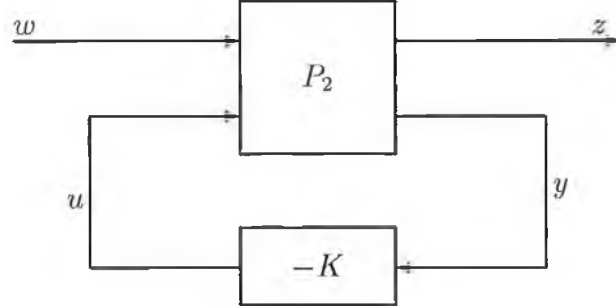


Figure 1.4: A Canonical Form for Linear Controller Synthesis with Signal Uncertainty.

Note that in the above configuration Δ_P is zero, and P_2 is the nominal plant augmented with dynamics associated with the weighting transfer functions used to model signal uncertainty. It is natural to partition P_2 conformally with its inputs w and u and with its outputs z and y . Thus,

$$\begin{pmatrix} z \\ y \end{pmatrix} = P_2 \begin{pmatrix} w \\ u \end{pmatrix} = \begin{pmatrix} P_{11} & P_{12} \\ P_{21} & P_{22} \end{pmatrix} \begin{pmatrix} w \\ u \end{pmatrix}$$

The closed loop transfer function from w to z in Figure 1.4 will be denoted by T_{zw} , and is

$$T_{zw} = P_{11} - P_{12}K(I + P_{22}K)^{-1}P_{21} \quad (1.15)$$

Then the **Optimal Nominal Performance Problem** is given by

$$\inf_K \sup_{w \in \mathcal{D}_w} \|z\|_s$$

where the infimum is over all LTI controllers which stabilise the closed loop system. This problem can also be written in the form

$$\inf_K \|T_{zw}\|_{I_s} \text{ or } \inf_K \|T_{zw}\|_{I_{rs}}$$

where the infimum is over all stabilising controllers, and the system norms in question are induced by the appropriate signal norms. The optimal nominal performance problem can clearly be regarded as a set of optimisation problems (depending on which signal norms are chosen), and it has received a great deal of attention in the robust control literature. In standard \mathcal{H}_∞ control theory reliable software packages are available which can be used to solve this problem in both the SISO and MIMO cases. It will be argued in the sequel however that the particular paradigm on which these solutions are based is flawed from an engineering point of view. In \mathcal{L}_1 control theory complete theoretical solutions to the optimal nominal performance problem do exist for most cases. However, no reliable software for the design of optimal controllers is commercially available.

1.3.7 Robust Stability

As mentioned earlier, only system uncertainty can destabilise a nominally stable plant. Therefore, the first issue to be addressed in terms of system uncertainty is robust stability. Consider the configuration of Figure 1.5.

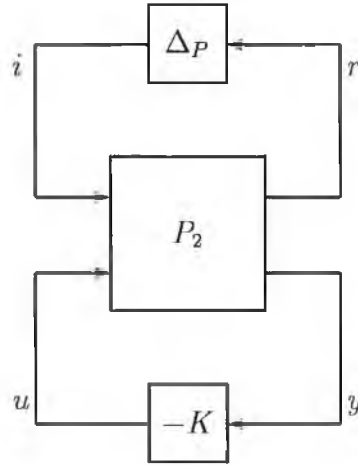


Figure 1.5: A Canonical Form for Linear Controller Synthesis with Plant Uncertainty.

Denote by T_{ri} the transfer function from input i to output r , with Δ_P removed. So T_{ri} is the transfer function ‘seen’ by Δ_P . Robust stability specifications can be cast as mathematical optimisation problems under the above canonical framework by using the Small Gain Theorem [11, 44], which is a fundamental result in robust control theory. Applying the SGT to the set-up of Figure 1.5 yields the following [11, 12].

Theorem 1.1 *Suppose that the system of Figure 1.5 is nominally stable, and that α is a positive real number. If*

$$\|T_{ri}\|_{Is} < \alpha$$

then the system of Figure 1.5 is BIBO stable in the $\|\cdot\|_s$ -norm sense for every Δ_P which obeys

$$\|\Delta_P\|_{Is} \leq \alpha^{-1}$$

This theorem gives a sufficient condition for robust stability for the uncertainty set \mathcal{D}_Δ defined above. The great utility of the SGT comes from two facts. Firstly, it holds equally well for any induced norm. Note however that it does not apply to semi-induced norms, and this observation will be seen to be fundamentally important in the sequel. The second great advantage of the SGT is that it applies also to systems which are non-linear (NL) and/or time-varying (TV). On the robust stability question, this translates into the following. The theorem also guarantees stability for all Δ_P ’s in the set

$$\widehat{\mathcal{D}}_\Delta = \{\Delta_P \mid \Delta_P \text{ is s-stable, and } \|\Delta_P\|_{Is} \leq 1\}$$

So the condition $\|T_{ri}\|_{Is} < 1$ ensures robust stability in the face of a class of NL and/or TV Δ_P ’s too, and the requirement in \mathcal{D}_Δ that Δ_P must be LTI can be dropped. However, considerable mathematical subtleties arise when Δ_P is NL and/or TV, and care is needed when extending the notion of induced norm to NLTV operators, as in “ $\|\Delta_P\|_{Is}$ ” in the above definition of $\widehat{\mathcal{D}}_\Delta$. In the interests of brevity, robust stability results will be given only for LTI Δ_P ’s, and the more general case of NLTV Δ_P ’s will not be discussed in detail. Rather, it suffices to inform the reader that the SGT and the concept of induced norm can be extended to the NLTV case, but some extra mathematical machinery is needed [11]. In any case, our use of the SGT is standard and routine, and all the robust stability results stated in this thesis may be extended to cover Δ_P ’s which are NL and/or TV.

Motivated by the SGT, we have the **Optimal Robust Stability Problem**

$$\inf_K \|T_{ri}\|_{Is}$$

where the infimum is over all stabilising controllers, and the system norms in question are induced by the appropriate signal norms. It can fairly be argued that the Robust Stability Problem is substantially solved in both the \mathcal{H}_∞ and \mathcal{L}_1 control theories. The condition in the SGT is sometimes but not always necessary as well as sufficient for robust stability with the relevant uncertainty sets. The problem of settling the necessity question depends on the norms in use.

1.3.8 Robust Performance

In the previous subsection the effect of system uncertainty on the stability of the closed loop system was considered. Once the question of robust stability has been settled, the next most important consideration is obviously to minimise the impact of system uncertainty on the performance of the system. Indeed it can reasonably be argued that robust performance is the ultimate goal of robust control theory. Robust performance specifications can be cast as mathematical optimisation problems under the above canonical framework as follows. With reference to Figure 1.3, consider the problem of robustly minimizing the induced norm of the transfer function from the uncertain input signal w to the system output z when the plant uncertainty \mathcal{D}_Δ is unstructured. This is called the **Optimal Robust Performance Problem** and can be stated as

$$\inf_K \sup_{\Delta \in \mathcal{D}_\Delta} \|T_{zw}(s, K, \Delta)\|_{Is}$$

where the infimum is over all LTI controllers which are robustly stable for \mathcal{D}_Δ . This problem is a hard problem and is the subject of ongoing research in the robust control community. In full generality it is unsolved in both the \mathcal{L}_1 and \mathcal{H}_∞ control theories, the major difficulty obviously being the requirement of dealing with both signal and system uncertainty simultaneously.

Chapter 2

Robust Controller Synthesis: \mathcal{H}_∞ and \mathcal{L}_1 Control theory

As outlined in Chapter 1, many desirable feedback system properties and corresponding specifications amount to requiring certain closed loop transfer functions to have small induced norm. This suggests that it would be highly desirable to minimize the induced norm of the closed loop system over all LTI stabilizing controllers. What controller optimization problems of this general type have already been solved? To date, only two major problems of this type have been fully and comprehensively solved at an analytical level, corresponding to the \mathcal{H}_∞ and \mathcal{L}_1 control theories. This chapter gives a brief outline of these theories. The development is intended to highlight the similarities as well as the differences between them. Some detailed comments are made on certain aspects of both \mathcal{H}_∞ and \mathcal{L}_1 control theory. These observations provide the motivation for the development of the modified $\mathcal{H}_\infty / \mathcal{H}_2$ control theories presented in Chapter 3.

2.1 \mathcal{H}_∞ Theory: Nominal Performance

In this section we discuss the issue of nominal performance under the framework of \mathcal{H}_∞ control theory. This thesis will have occasion to discuss many system norms. One such norm is the \mathcal{H}_∞ **norm** or the **infinity norm in the frequency domain**, which is given by

$$\|T_{zw}(s)\|_\infty = \sup_{-\infty < \omega < +\infty} |T_{zw}(j\omega)|$$

in the SISO case, and by

$$\|T_{zw}(s)\|_\infty = \sup_{-\infty < \omega < +\infty} \bar{\sigma}(T_{zw}(j\omega))$$

in the MIMO case, where $\bar{\sigma}(T_{zw}(j\omega))$ denotes the maximum singular value of $T_{zw}(j\omega)$. With reference to Figure 1.4, the \mathcal{H}_∞ **Nominal Performance Problem** is given by

$$\inf_K \|T_{zw}(s)\|_\infty$$

where the infimum is over all LTI stabilizing controllers. The engineering motivation for this problem rests on the following theorem, which is fundamental in \mathcal{H}_∞ control theory [13].

Theorem 2.1 *Suppose that $z(j\omega) = T_{zw}(j\omega)w(j\omega)$, and that $T_{zw}(s)$ is the transfer function matrix of a stable LTI system. Then*

$$\|T_{zw}(s)\|_\infty = \sup_{w \neq 0} \frac{\|z(j\omega)\|_2}{\|w(j\omega)\|_2}$$

This theorem says that the \mathcal{H}_∞ system norm is induced by the \mathcal{L}_2 signal norm. To see the engineering relevance of this, define

$$\mathcal{D}_w^{(e)} = \{w(j\omega) \mid \|w(j\omega)\|_2 \leq 1\} = \mathcal{BL}_2^n(j\omega) \quad (2.1)$$

(with “e” for energy), where $\mathcal{BL}_2^n(j\omega)$ denotes the unit ball in $\mathcal{L}_2^n(j\omega)$. The set $\mathcal{D}_w^{(e)} = \mathcal{BL}_2^n(j\omega)$ consists of all n -vector signals having energy less than or equal to one. As $w(j\omega)$ ranges through $\mathcal{D}_w^{(e)}$, it gives rise to a well defined set of possible system outputs. Specifically, the signal $z(j\omega)$ then ranges through

$$\mathcal{D}_z^{(e)} = \{z(j\omega) \mid z(j\omega) = T_{zw}(j\omega)w(j\omega), \|w(j\omega)\|_2 \leq 1\} \quad (2.2)$$

which may be written succinctly as

$$= T_{zw}(j\omega)\mathcal{BL}_2^n(j\omega)$$

Hence, the maximum possible size of the undesirable signal z , as measured by the \mathcal{L}_2 signal norm, and as w ranges throughout the set $\mathcal{D}_w^{(e)}$, is

$$\sup_{w(j\omega) \in \mathcal{D}_w^{(e)}} \|z(j\omega)\|_2 = \sup_{w \in \mathcal{BL}_2^n(j\omega)} \|T_{zw}(j\omega)w(j\omega)\|_2$$

The above expression is easily recognized from Theorem 2.1, so that

$$\sup_{w(j\omega) \in \mathcal{D}_w^{(e)}} \|z(j\omega)\|_2 = \|T_{zw}(s)\|_\infty$$

Hence, minimizing $\|T_{zw}(s)\|_\infty$ corresponds to minimizing the worst case $\|z(j\omega)\|_2$ as w ranges through $\mathcal{D}_w^{(e)} = \mathcal{BL}_2^n$. This observation motivates the optimal controller synthesis problem of minimizing the system norm $\|T_{zw}(s)\|_\infty$, and this is a solved problem. Indeed, software for solving this problem is commercially available [71].

Previous work in the area of \mathcal{H}_∞ control theory has been based on the use of the \mathcal{L}_2 norm on both the input and the output side, since the \mathcal{L}_2 norm appears on both the denominator and numerator in Theorem 2.1 above. On the input side, exogenous inputs are taken to be square integrable signals which have energy less than or equal to unity. On the output side, this approach minimizes the worst case \mathcal{L}_2 norm of the output. This viewpoint can reasonably be referred to as the **energy paradigm** for \mathcal{H}_∞ , and this terminology will be used below.

2.2 \mathcal{H}_∞ Theory: Robust Stability

Let us turn now to the issue of system uncertainty, and the problem of ensuring closed loop stability in the presence of this uncertainty under the framework of \mathcal{H}_∞ control theory. We restrict our attention to so-called unstructured uncertainty, wherein Δ_P is constrained only by a single induced norm bound. Thus, define

$$\mathcal{D}_{\Delta_P}^{(e)} = \{\Delta_P(j\omega) \mid \Delta_P(j\omega) \text{ is 2-stable, LTI, and } \|\Delta_P(j\omega)\|_\infty \leq 1\}$$

The following result is well known [13].

Theorem 2.2 *Suppose that the system of Figure 1.5 is nominally stable, and that α is a positive real number. Then the system of Figure 1.5 is BIBO stable in the \mathcal{L}_2 norm sense for every LTI $\Delta_P(j\omega)$ which obeys*

$$\|\Delta_P(j\omega)\|_\infty = \sup_{a \neq 0} \frac{\|\Delta_P(j\omega)a(j\omega)\|_2}{\|a(j\omega)\|_2} \leq \alpha^{-1}$$

if and only if

$$\| T_{ri}(s) \|_{\infty} < \alpha$$

Hence, the condition $\| T_{ri}(s) \|_{\infty} < 1$ guarantees robust stability for the uncertainty set $\mathcal{D}_{\Delta_P}^{(e)}$ above. It is necessary as well as sufficient for robust stability with this uncertainty set. Applying the SGT to the set-up of Figure 1.5, and specializing to the \mathcal{L}_2 signal norm, immediately establishes sufficiency. Necessity is proved by exhibiting a destabilizing Δ_P when $\| T_{ri}(s) \|_{\infty} \geq 1$. Such a Δ_P which is LTI can always be found [14, 15]. It is also necessary and sufficient for the uncertainty set

$$\hat{\mathcal{D}}_{\Delta_P}^{(e)} = \{\Delta_P \mid \Delta_P \text{ is 2-stable, and } \|\Delta_P\|_{\infty} \leq 1\}$$

where the requirement that Δ_P be LTI has been dropped. This robust stability result motivates the \mathcal{H}_{∞} **Robust Stability Problem** given by

$$\inf_K \| T_{ri}(s) \|_{\infty}$$

where the infimum is over all LTI stabilizing controllers. This problem can be thought of as maximizing stability robustness. It can be cast in the canonical form of Figure 1.4, by allowing the input i (respectively, the output r) in Figure 1.5 to play the role of w (resp. z) in Figure 1.4. So this is a solved problem.

2.3 The Mixed Sensitivity \mathcal{H}_{∞} Control Problem

The previous two sections have detailed the Nominal Performance Problem and the Robust Stability Problem in \mathcal{H}_{∞} control theory. We have noted that both problems are ‘solved’ from a mathematical point of view, and in the next section references to the various methods of solving \mathcal{H}_{∞} optimisation problems are given. In this section however, we concentrate on the issue of controller *design*. It is entirely obvious that in any realistic design problem, the controller must effectively counteract both signal *and* system uncertainty. Therefore, in this section we consider a problem formulation which combines both nominal performance and robust stability - The Mixed Sensitivity \mathcal{H}_{∞} Control Problem. We first of all define the following terms, which will be seen to be instrumental in the design process.

For a given nominal plant G_o with stabilising controller K , denote by S_o the **Nominal Sensitivity Function**, where

$$S_o = \frac{1}{1 + G_o K} \quad (\text{SISO})$$

and

$$S_o = (I + G_o K)^{-1} \quad (\text{MIMO})$$

Denote by T_o the **Nominal Complementary Sensitivity Function**, where

$$T_o = \frac{G_o K}{1 + G_o K} \quad (\text{SISO})$$

and

$$T_o = G_o K (I + G_o K)^{-1} = (I + G_o K)^{-1} G_o K \quad (\text{MIMO})$$

We also define the function R_o , where

$$R_o = \frac{K}{1 + G_o K} \quad (\text{SISO})$$

and

$$R_o = K (I + G_o K)^{-1} \quad (\text{MIMO})$$

R_o has no common name in the literature, and will be referred to here as the **Nominal Control Sensitivity Function**. Note carefully that

$$S_o + T_o = I \quad (2.3)$$

Now in Section 2.1, and with reference to Figure 1.4, the \mathcal{H}_∞ Nominal Performance Problem was shown to be given by

$$\inf_K \|T_{zw}(s)\|_\infty$$

where the infimum is over all LTI stabilizing controllers. What exactly is the transfer function matrix $T_{zw}(s)$? The answer to this question obviously depends on the type and location of the various uncertain signals entering the system. Consider the vector of exogenous inputs w given by

$$w = \begin{pmatrix} d_a \\ d_b \\ c \\ m \end{pmatrix}$$

where d_a and d_b denote disturbances acting at the input and output of the nominal plant respectively, c is an uncertain command signal, and m is measurement noise acting on the feedback signal. This vector includes all the possible sources of uncertain

signals likely to be considered in most typical controller design problems. Recall that the vector of regulated variables is defined as including all signals which are necessary to write down the specifications for the design. Since design specifications are usually given in terms of the output and control signals, let the vector of regulated variables z be given by

$$z = \begin{pmatrix} y \\ u \end{pmatrix}$$

where y is the output of the nominal plant and u is the control signal. Then it is easy to show that for

$$z = T_{zw}w$$

the transfer function matrix T_{zw} is given by

$$T_{zw} = \begin{pmatrix} W_{1a}S_oG_o & W_{1b}S_o & T_o & W_2T_o \\ -W_{1a}R_oG_o & -W_{1b}R_o & R_o & -W_2R_o \end{pmatrix}$$

Note that each term of the matrix T_{zw} involves one of the sensitivity functions S_o , T_o or R_o . Note also that the weighting functions present in the matrix arise from the modelling of the various uncertain signals, and that these have been absorbed into the augmented plant.

Now recall that in Section 3.2, and with reference to Figure 1.5, the \mathcal{H}_∞ Robust Stability Problem was shown to be given by

$$\inf_K \|T_{ri}(s)\|_\infty$$

where the infimum is over all LTI stabilizing controllers. Again the transfer function or transfer function matrix T_{ri} will depend on the way in which the uncertainty in the plant is modelled. Table 2.1 below gives T_{ri} for each of the three possible types of uncertainty. Note that the plant uncertainty weighting function W_3 has again been absorbed into the augmented plant.

Δ	T_{ri} (SISO)	T_{ri} (MIMO)
Δ_a	$-W_3 \frac{T_o}{G_o}$	$-W_3 G_o^{-1} T_o$
Δ_i	$-W_3 T_o$	$-W_3 G_o^{-1} T_o G_o$
Δ_o	$-W_3 T_o$	$-W_3 T_o$

Table 2.1. T_{ri} for different types of Plant Uncertainty

The full extent of the complexity of the design process now becomes clear, since satisfaction of nominal performance and robust stability specifications must inevitably involve the minimisation of interdependent sensitivity functions. Indeed, inspection of the matrix T_{zw} reveals that the nominal performance problem *alone* places conflicting demands on the values of S_o , T_o and R_o . In typical controller design problems however a detailed study of the physics of the system in question together with some engineering insight on the part of the designer usually allows some simplification of the problem. We briefly detail the most significant issues.

1. In most designs it is not realistic to consider all possible types and sources of uncertainty. In general system uncertainty can be modelled as *either* additive or input or output multiplicative. Significant disturbances are usually present at the input *or* the output of the system and so on.
2. Design specifications often only place conflicting demands on certain sensitivity functions over *different* frequency ranges. For example, the attenuation of output disturbances and measurement noise in the nominal performance problem requires both S_o and T_o respectively to be made small. From (2.3), this is obviously not possible. However since output disturbances usually occur at low frequencies and measurement noise generally becomes significant at high frequencies, careful selection of the weighting functions W_1 and W_3 will allow both specifications to be satisfied over disjoint frequency bands. Similarly, command signals are usually confined to the lower end of the frequency spectrum, and thus command tracking and disturbance attenuation are actually complementary specifications.
3. The requirement that the control signal be kept small is dependent on the value of R_o , and since all real plants are strictly proper, this means that the controller K should roll off at high frequencies. Clearly, this is compatible with the above requirements on S_o and T_o .
4. Finally, it is almost always the case that our knowledge of the dynamic behaviour of the plant deteriorates significantly at high frequencies. This means that the plant uncertainty weighting function W_3 is generally small at low frequencies and increases with increasing frequency. Choosing for example a multiplicative output uncertainty as our model then requires the complementary sensitivity function T_o to roll off at

high frequencies. Again, this is compatible with the requirements arising from the specifications above.

The above discussion highlights the nature of the design process in \mathcal{H}_∞ controller synthesis. Clearly, modelling of uncertainty is crucial, in terms of choosing which sensitivity functions should be minimised over which frequency bands. Thus the selection of the uncertainty weighting functions W_{1a} , W_{1b} , W_2 and W_3 is an important step in the actual controller design process.

We turn now to the problem of simultaneously achieving nominal performance and robust stability specifications. The discussion above along with our characterisation of the matrices T_{zw} and T_{ri} naturally leads to the following popular approach. Once the various *uncertainty* weighting functions have been selected for the particular system, they can be used together with any relevant design specifications to choose *design* weighting functions W_S , W_T and W_R for each of the three sensitivity functions S_o , T_o , and R_o . For example, W_S would be chosen based on W_{1a} and/or W_{1b} together with any command following specifications for the closed loop system. W_T would be chosen to satisfy robust stability specifications given by W_3 as well as including measurement noise attenuation properties. In this way the weighting functions change from being simply models of uncertainty to actual dynamic design parameters. Once the design weighting functions have been chosen, commercially available software packages such as [71] can be used to solve the so-called **Mixed Sensitivity \mathcal{H}_∞ Control Problem** given by

$$\inf_K \| J(s) \|_\infty$$

where the infimum is over all LTI stabilizing controllers, and J is a matrix cost function given by

$$J = \begin{pmatrix} W_S(s)S_o(s) & W_R(s)R_o(s) & W_T(s)T_o(s) \end{pmatrix}$$

In many designs the control signal u can actually be constrained by shaping the complementary sensitivity function T_o , so that with a suitably chosen W_T , the cost function J becomes simply

$$J = \begin{pmatrix} W_S(s)S_o(s) & W_T(s)T_o(s) \end{pmatrix}$$

Then it can be shown that

$$\frac{1}{\sqrt{2}} \| J(s) \|_\infty \leq \max (\| W_S(s)S_o(s) \|_\infty, \| W_T(s)T_o(s) \|_\infty) \leq \| J(s) \|_\infty \quad (2.4)$$

and thus it is easy to see that the cost function J effectively captures both nominal performance and robust stability specifications. The construction of the mixed sensitivity cost function given above also clearly reveals the inherent trade-off between *performance* and *robustness* which is present in every design.

A number of detailed comments are made in the sequel concerning aspects of \mathcal{H}_∞ controller design. In addition the design examples presented in Chapter 5 should serve to illustrate the various issues which arise in practical design problems. For the moment we confine ourselves to the following observations.

1. No systematic methods of choosing either the uncertainty or the design weighting functions exist. Choosing the uncertainty weighting functions can be difficult and time consuming and in general requires a good understanding of the physical characteristics of the particular plant and its operating environment, as well as a fair degree of engineering intuition. Subsequently constructing the design weighting functions is also non-trivial, and depends to a large extent on the relative importance given by the designer to often conflicting specifications in the final design.
2. The mixed sensitivity \mathcal{H}_∞ control problem does not have a solution for all possible combinations of weighting functions. The selection of weighting functions which correspond to specifications which are too ambitious, or which violate certain rank conditions required by state space solutions to the mathematical optimisation problem, will result in the failure of the software to compute a controller. The size of the ‘crossover gap’, i.e. the frequency interval between the 0 db crossover frequency of the weighting functions W_S and W_T is particularly crucial.
3. The approximations required by the selection of a single design weighting function for each sensitivity function, together with the necessity of including different specifications in a single matrix cost function J , generally means that the final controller will be the result of an iterative process. Weighting functions will usually have to be adjusted and closed loop behaviour validated by simulation before a satisfactory design is achieved.
4. The mixed sensitivity problem formulation guarantees nominal performance only - the effect of plant uncertainty on the *performance* of the system is not considered.

5. All design is done in the frequency domain.
6. The order of the \mathcal{H}_∞ optimal controller is not explicitly constrained in the design process. In general the controller will have higher order than is necessary and thus model reduction techniques can usually be used to reduce the complexity of the control law without degrading closed loop performance.
7. \mathcal{H}_∞ controller synthesis has become a widely accepted design technique among the control community, and has proved particularly successful in problems involving multivariable plants operating in a hostile environment.

2.4 Solutions to the Mixed Sensitivity \mathcal{H}_∞ Control Problem

After more than 15 years of intensive research there are now several distinct theories which may be used to solve \mathcal{H}_∞ optimisation problems. The mathematical theory required in each case can fairly be described as difficult and involved, and the resulting software algorithms tend to be computationally demanding. This thesis is not concerned with the mathematical solutions of \mathcal{H}_∞ optimisation problems per se, but with the control engineering motivation underlying the different robust control methodologies, and so below we simply list the various theories together with the relevant references.

1. Nevanlinna-Pick Interpolation Theory [16, 17, 18]
2. Vector Space Duality Theory [19, 20, 21, 22]
3. Kwakernaak's Theory [25, 26]
4. Sarason's Theory [27, 28]
5. Convex Optimisation [6]
6. Optimal Hankel Norm Model Reduction Theory [23, 24]

Currently available commercial software packages such as [71, 78] use Optimal Hankel Norm Model Reduction Theory to compute \mathcal{H}_∞ optimal controllers. The advantages of this method include the fact that explicit state space formulas for the controller are available, as well as the fact that all computations can be done in state space, making the resulting algorithms more numerically robust. The more recent numerical approach of convex optimisation has also provided some promising results, especially in terms of revealing the limits of performance for a given system.

2.5 A Critique of \mathcal{H}_∞ Control Theory

This section contains certain comments on \mathcal{H}_∞ control theory. Our purpose is to detail what we regard as limitations of the theory, and to explore the root causes of these limitations. Later in the chapter, an analagous examination of \mathcal{L}_1 control theory is made. These contrasting observations motivate the development of a modified \mathcal{H}_∞ control theory, detailed in Chapter 3.

2.5.1 (i) The Output Norm and ‘Spikes’

Consider now applying standard \mathcal{H}_∞ control theory to the problem of minimizing a system’s output due to an uncertain input signal, as described earlier. Previous work in the area of \mathcal{H}_∞ control theory has been based on the use of the \mathcal{L}_2 signal norm on both the input and the output sides. Applying this conventional or standard \mathcal{H}_∞ approach then leads to the problem of finding the LTI stabilizing controller which minimizes $\|T_{zw}(s)\|_\infty$. Now, it follows immediately from Theorem 2.1 that

$$\|z(j\omega)\|_2 \leq \alpha \quad \forall w \in \mathcal{D}_w^{(e)} \Leftrightarrow \|T_{zw}(s)\|_\infty \leq \alpha \quad (2.5)$$

Hence, if the \mathcal{L}_2 norm of z must be kept smaller than α , the condition needed is

$$\|T_{zw}(s)\|_\infty \leq \alpha$$

Note that this condition is necessary and sufficient for ensuring that the effect of a class of exogenous inputs on the system’s output is bounded, in a certain precise sense. Present day \mathcal{H}_∞ software [71], will effectively deliver the controller which yields the smallest possible value of α in eqn. (2.5), thereby yielding the best possible upper bound on the energy of the output signal for all possible inputs in the set

$\mathcal{D}_w^{(e)} = \mathcal{BL}_2^n(j\omega)$. So standard \mathcal{H}_∞ control theory effectively minimizes the impact of uncertain input signals on the system's outputs in a certain precise sense.

While this may appear impressive, it will now be shown that it does not prohibit the possibility of “spikes” in the system's output $z(t)$ with arbitrarily large amplitude in the time domain. Obviously, even moderately large ‘spikes’ in the amplitude of $z(t)$ would be completely intolerable in many applications. A pedagogy for controller design which permits large ‘spike-like’ excursions in $z(t)$ runs in the face of the very objectives and function of a control system.

Lemma 2.1 *Suppose that the LTI controller K minimizes*

$$\lambda_\infty = \|T_{zw}(s)\|_\infty = \sup_{w \in \mathcal{D}_w^{(e)}} \|T_{zw}(j\omega)w(j\omega)\|_2$$

over all LTI stabilizing controllers. Then there exists a sequence of exogenous inputs $w_k(j\omega) \in \mathcal{D}_w^{(e)}$ such that

$$\|z_k(t)\|_{t=0} \rightarrow \infty \text{ as } k \rightarrow \infty$$

where $z_k(t)$ denotes the system's output due to the exogenous input $w_k(j\omega)$, and where $\mathcal{D}_w^{(e)}$ is defined in eqn. (2.1).

Proof

We may suppose that $T_{zw}(s)$ is SISO. The proof will be seen to extend to the general MIMO \mathcal{H}_∞ -problem without difficulty. Define the sequence of exogenous inputs w_k , $k = 1, 2, \dots$ by

$$w_k(j\omega) = \begin{cases} T_{zw}^{-1}(j\omega) \sqrt{\frac{\pi}{k}} \alpha_0 & \text{for } -k \leq \omega \leq k \\ 0 & \text{otherwise} \end{cases}$$

where α_0 is a positive real scalar. Let us suppose that the controller K is the \mathcal{H}_∞ -optimal controller, so it is the solution of

$$\lambda_\infty = \inf_K \|T_{zw}(s)\|_\infty$$

As is well known, the optimal $T_{zw}(s)$ is all-pass, meaning that

$$\|T_{zw}(j\omega)\| = \lambda_\infty (= \text{constant}) \quad \forall \omega$$

Take α_0 to be λ_∞ . To see that $w_k \in \mathcal{D}_w^{(e)}$, note that

$$\|w_k(j\omega)\|_2^2 = \frac{1}{2\pi} \int_{-k}^{+k} |T_{zw}^{-1}(j\omega)|^2 d\omega = \frac{\pi}{k} \lambda_\infty^2$$

Using the all-pass property gives

$$\| w_k(j\omega) \|_2^2 = \frac{1}{2\pi} \lambda_\infty^{-2} 2k \frac{\pi}{k} \lambda_\infty^2 = 1$$

so that $w_k \in \mathcal{D}_w^{(e)}$. Let z_k be the response of the system to the input w_k . Then,

$$z_k(j\omega) = \begin{cases} \sqrt{\frac{\pi}{k}} \lambda_\infty & \text{for } -k \leq \omega \leq k \\ 0 & \text{otherwise} \end{cases}$$

Inverse Fourier transforming gives

$$\begin{aligned} z_k(t) &= \frac{1}{2\pi} \sqrt{\frac{\pi}{k}} \lambda_\infty \int_{-k}^{+k} e^{j\omega t} d\omega \\ &= \lambda_\infty \sqrt{\frac{k}{\pi}} \frac{\sin kt}{kt} \end{aligned}$$

so that

$$\lim_{t \rightarrow 0} z_k(t) = \lambda_\infty \sqrt{\frac{k}{\pi}}$$

which is unbounded as $k \rightarrow \infty$, as claimed. \square

Although this lemma may seem a little startling at first, its practical significance must not be over-emphasized. Obviously, the above lemma only proves that an infinite amplitude ‘spike’ in $z(t)$ is hypothetically possible, and only in the sense of a limit. Also, optimal \mathcal{H}_∞ controllers satisfy the all-pass property only over a finite bandwidth, and the sequence of inputs used in the above proof are themselves ‘spike-like’. Moreover, there are bounds which relate the A norm (the system norm used in \mathcal{L}_1 control theory to give a hard bound on the \mathcal{L}_∞ norm of the output signal) to the \mathcal{H}_∞ system norm. In [9] for example it is shown that

$$\| G(s) \|_\infty \leq \| G(t) \|_A \leq d \| G(s) \|_\infty \quad (2.6)$$

where d is the Smith-McMillan degree of $G(s)$, while in Section 3.5 below bounds are given which may be used to argue that very large ‘spikes’ will not occur in practice. However, it is clear that the above bounds are not very attractive for high order systems.

Another way of looking at the difficulty is as follows. There are no bounds relating the \mathcal{L}_2 norm and the \mathcal{L}_∞ norm of signals. Specifically, we have the following.

Lemma 2.2 *There exists no finite constant M such that*

$$\|z(t)\|_2 \leq M \|z(t)\|_\infty \quad \forall z(t) \in \mathcal{L}_2^n(t) \cap \mathcal{L}_\infty^n(t)$$

and similarly there exists no finite constant N such that

$$\|z(t)\|_\infty \leq N \|z(t)\|_2 \quad \forall z(t) \in \mathcal{L}_2^n(t) \cap \mathcal{L}_\infty^n(t)$$

Proof

For the proof, it suffices to consider scalar signals which are very wide or very narrow rectangular pulses. Consider the sequence of signals defined by

$$w_k(t) = \begin{cases} 1/\sqrt{2k} & \text{for } -k \leq t \leq +k \\ 0 & \text{otherwise} \end{cases}$$

Then $\|w_k(t)\|_2 = 1$ and $\|w_k(t)\|_\infty = 1/\sqrt{2k}$ which is unbounded as $k \rightarrow 0$. For the other part, define

$$w_k(t) = \begin{cases} 1 & \text{for } -k \leq t \leq +k \\ 0 & \text{otherwise} \end{cases}$$

Then $\|w_k(t)\|_\infty = 1$ and $\|w_k(t)\|_2 = \sqrt{2k}$ which is unbounded as $k \rightarrow \infty$. \square

So a bound on the \mathcal{L}_2 norm of a signal (on its own) does not prohibit the signal from having ‘spikes’ of arbitrarily large time domain amplitude, and more generally does not allow *any* bound on its \mathcal{L}_∞ norm to be inferred.

There are several arguments for talking one’s way around the ‘spike’ problem, including those outlined above. These can be used to argue that in practical applications the ‘spike’ difficulty will not be as severe as Lemma 2.1 superficially suggests. Although it is fair to say that practitioners are aware that extremely large spikes will not occur in practice, nonetheless the formal theory permits such behaviour at a hypothetical level and does not rule it out. Further, the arguments needed to do so are not a part of standard \mathcal{H}_∞ control theory, and are informal and/or conservative. For instance, optimizing sub-optimal bounds as in eqn. (2.6) is not completely satisfactory, and cannot be accepted as the final word. This suggests that the underlying problem formulation is flawed, and that the arguments needed should be fully integrated into the formal theory in a manner which is non-conservative and exact. Doing so is one aim of this thesis. The crucial point is that standard \mathcal{H}_∞ control theory cannot guarantee a good upper bound on the amplitude of the output signal $z(t)$ in

the time domain with $w(j\omega) \in \mathcal{D}_w^{(e)}$. This lemma raises the question of whether the problem stems from \mathcal{H}_∞ -control theory *per se*, or whether it stems from the control theoretic paradigm which is conventionally attached to it. We will have more to say on this important issue later.

2.5.2 (ii) Signal Set and Specification Lumping

Recall that in standard \mathcal{H}_∞ theory, the vector of exogenous inputs belongs to the unit ball in $\mathcal{L}_2^n(j\omega)$. When T_{zw} is $m \times n$, the signal $w(j\omega)$ is an n -vector, say

$$w(j\omega) = (w_1(j\omega), \dots, w_n(j\omega))^T$$

Suppose now that each vector element $w_i(j\omega)$ is *individually* modelled in the usual \mathcal{H}_∞ way, i.e. as the unit ball in $\mathcal{L}_2(j\omega)$. In this situation, the signal $w(j\omega)$ ranges through $\mathcal{D}_w^{(2)}$, where

$$\begin{aligned} \mathcal{D}_w^{(2)} &= \{w(j\omega) \mid w(j\omega)^T = (w_1(j\omega), \dots, w_n(j\omega)), \parallel w_i(j\omega) \parallel_2 \leq 1\} \\ &= \mathcal{BL}_2(j\omega) \times \dots \times \mathcal{BL}_2(j\omega) \end{aligned}$$

If the \mathcal{L}_2 norm is used also on the output side, the resulting synthesis problem for this signal set, i.e. that of choosing the controller that minimizes the largest $\parallel z(j\omega) \parallel_2$ as w varies through $\mathcal{D}_w^{(2)}$, is *not* a standard \mathcal{H}_∞ problem. To obtain a standard \mathcal{H}_∞ problem, the collection of n individual unit balls $\mathcal{D}_w^{(2)}$ must be replaced by a single unit ball in $\mathcal{L}_2^n(j\omega)$. In other words, $\mathcal{D}_w^{(2)}$ must be covered by $\mathcal{D}_w^{(e)}$, meaning that

$$\mathcal{D}_w^{(2)} \subset \sqrt{n} \mathcal{D}_w^{(e)}$$

This step is conservative and highly undesirable. This disadvantage can reasonably be called **signal set lumping**. To obtain a standard \mathcal{H}_∞ problem all exogenous inputs must, so to speak, be lumped in together.

Consider, for instance, a plant with several outputs. Each plant output has a sensor or transducer to produce an on-line measurement of the value of that output. Imperfections in sensors are generally modelled as additive noise. Such sensor noise signals arising from independent sensors are necessarily independent of each other, as in $\mathcal{D}_w^{(2)}$. When using $\mathcal{D}_w^{(e)}$, the w_i 's are not independent. In most applications, the elements of w are independent of each other, and the \mathcal{L}_2 norm i.e. the signal norm on which standard \mathcal{H}_∞ theory is based, cannot effectively capture this situation. Similarly, each plant output and/or plant input may have significant unknown external

disturbances acting on it, and these disturbances may be physically independent of each other. Again, the corresponding elements of w are then independent of each other, and standard \mathcal{H}_∞ control theory cannot effectively capture this situation.

Similar remarks apply to the output side. With reference to Figure 1.4, different elements of z generally need to be controlled to different levels of precision. Applying a weighting function to z to differentially emphasize distinct elements of z is only a partial solution. Minimizing $\|z(j\omega)\|_2$ still involves averaging over distinct plant outputs, as well as over frequency or time. This obscures which elements are or are not being effectively controlled. Independent constraints on the worst case \mathcal{L}_2 norm of each z_i cannot be imposed. This limitation can reasonably be termed **specification lumping**.

2.5.3 (iii) Robust Performance

The presence of substantial plant uncertainty impacts on many facets of controller design, not merely on closed loop stability. Recall that the canonical form for linear controller synthesis given in Figure 1.3 allows both signal and system uncertainty to be included in the problem formulation. The motivation for minimizing the \mathcal{H}_∞ norm however was given in terms of two theorems, one dealing with nominal performance and the other with robust stability. These problem formulations can be thought of as corresponding to two ‘special cases’ of the general canonical form, and are given in Figures 1.4 and 1.5. It is obvious that the fact that each theorem deals separately and disjointly with signal and system uncertainty is unfortunate, and represents a serious shortcoming.

It would therefore be highly desirable to be able to handle performance specifications in the presence of both signal and system uncertainty simultaneously and in a rigorous way. In this regard, the simplest and most obvious \mathcal{H}_∞ robust performance problem is as follows. With reference to Figure 1.3, consider the problem of robustly minimizing the worst case \mathcal{H}_∞ norm of the transfer function matrix from the uncertain input signal w to the system output z when the plant uncertainty $\mathcal{D}_{\Delta P}^{(e)}$ is unstructured. This is called the \mathcal{H}_∞ **Optimal Robust Performance Problem** and can be stated as

$$\inf_K \sup_{\Delta_P \in \mathcal{D}_{\Delta P}^{(e)}} \|T_{zw}(s, K, \Delta_P)\|_\infty$$

where the infimum is over all LTI controllers which are robustly stable for $\mathcal{D}_{\Delta P}^{(e)}$. This

problem is unsolved.

If the transfer function to be minimized is the sensitivity function, then this problem is called the optimal **Robust Disturbance Attenuation Problem** (RDAP or ORDAP), and there is a literature on it [21, 22, 34, 35]. Previous renditions of the RDAP problem for the MIMO case [22, 35], are not especially attractive formulations of the problem, because they suffer from (i) and (ii) above, but try to avoid (iii). Analytical solutions to this problem are not available.

In fact, the only robust specification which can be optimized by standard \mathcal{H}_∞ control theory is robust stability. No robust *performance* problem is solved non-conservatively by standard \mathcal{H}_∞ -control theory. Heuristic approaches to avoiding this limitation of \mathcal{H}_∞ have been suggested. Perhaps the best known procedure of this variety is so-called μ -synthesis [36, 37]. Unfortunately, convergence is not guaranteed by this procedure [38].

Alternatively, one can settle for suboptimal approaches to the problem. In [39], formal bounds are given which limit the deterioration of the performance of the closed loop system due to plant uncertainty, in the SISO case. This result together with loopshaping techniques is used in [75] to improve robust performance in SISO systems. In the case of MIMO systems the situation is more complicated, and in [70] the authors show that very small levels of plant uncertainty can result in a totally unacceptable deterioration in system performance. On the other hand a result in [40] for MIMO systems can be used to show that as long as performance specifications are only given over a finite frequency interval called an operating band, the degradation in terms of robust performance over this band is small, provided that (a) the associated nominal performance is sufficiently good, and (b) the level of plant uncertainty is sufficiently small. In [30], a controller design algorithm is presented which generates a sequence of controllers which solve the so-called Robust \mathcal{H}_∞ Almost Disturbance Decoupling Problem, under certain assumptions. In the most general case however the design algorithms become complicated optimisation based procedures.

The issue of robust performance in MIMO systems will be considered again in Chapter 5. For the moment however it is sufficient to note that since from an applications point of view, the vast majority of control problems require both signal and system uncertainty to be considered when designing for performance specifications, it seems clear from the above discussion that all in all standard \mathcal{H}_∞ control theory at present does quite poorly with robust performance problems.

2.5.4 (iv) Weighting Function Selection

As noted in [29], the effectiveness of any given design procedure depends to a large extent on how well the relationship between design parameters and design specifications is understood. In \mathcal{H}_∞ control theory the design parameters are the weighting functions, and the selection of these functions can fairly be regarded as the most important and difficult step in the design process.

In the \mathcal{H}_∞ literature, there are two viewpoints regarding the weighting functions which lead to two distinct approaches to the design problem. In the first, weights are regarded as fixed quantities obtained from physical reasoning, in effect *models* of the possible signal and/or system uncertainty, and are therefore not subject to iterative manipulation by the designer. In the second, the weights are chosen to attempt to satisfy frequency dependent specifications on the magnitude of the system's closed loop transfer functions directly, generally the system's nominal sensitivity function S_o and complementary sensitivity function T_o . The weights can thus be manipulated iteratively to emphasise or shape the robustness or performance qualities of the design at various frequencies.

The first approach is undoubtedly more straightforward, especially if a reasonable amount of information can be obtained as to the nature of the uncertainty in the system. See [31] for an example of this approach. Since each weighting function represents the best possible model of each individual source of signal or system uncertainty, there is no iterative manipulation of the weights. However, note that (i) the approach does not prohibit 'spikes' at the output, even at optimum, (ii) the approach suffers from signal set and specification lumping, and (iii) closed loop transfer functions must be replaced by their nominal values, so that performance specifications are met nominally, not robustly. The consequence is that if standard \mathcal{H}_∞ software is used, the resulting design may very well be entirely unacceptable.

Thus as noted in Section 2.3 on the mixed sensitivity \mathcal{H}_∞ control problem, the original *uncertainty* weighting functions will usually have to be manipulated into *design* weighting functions, which can be used by the designer to satisfy various specifications on the closed loop system. This leads to the second viewpoint in which the weighting functions are regarded as 'tuning knobs' to be used in trading off between feedback properties over different frequency ranges and different vector directions. The weights then represent direct *specifications* on the modulus (or the maximum singular value in the MIMO case) of $S_o(j\omega)$ and $T_o(j\omega)$ (typically), at various fre-

quencies and in various vector directions, rather than information about signal or system uncertainty. However, this does not mean that their selection is automatic. On the contrary, and as noted in [32], there still do not exist systematic and analytic ways of choosing \mathcal{H}_∞ weighting functions to satisfy design specifications. It is true that for SISO minimum phase systems, weighting function manipulation is relatively straightforward. However for unstable and/or non-minimum phase systems, and especially in the MIMO case, the situation becomes significantly more complicated. Firstly, the relationship between the weighting function matrices and the resulting ‘optimal’ design is far from transparent from the designer’s point of view. Various design features and limitations, such as those due to right half plane poles and zeros, impose some fairly complicated design tradeoffs [33]. Secondly, the prospect of choosing, let alone iteratively manipulating, a 7×7 matrix of weighting transfer functions for example, is certainly a daunting one. In practice, the selection tends to be based on past experience and trial and error methods.

In summary then we make the following points. The current situation regarding weighting function selection in standard \mathcal{H}_∞ control theory is obviously far from perfect. It can reasonably be argued that the observations (i) to (iii) above go some way towards identifying the source of the difficulty. Firstly, the model on the output side (i.e. the model of or statement of the objectives of control systems) is flawed. The essential content of Lemma 2.1 is that the \mathcal{L}_2 signal norm gives a poor mathematical model of the objectives of a control system. Secondly, accurate models on the input side (i.e. models of signal uncertainty based on physical reasoning) must be abandoned because of (ii) above. Accurate models of signal uncertainty would have to be covered by a single unit ball anyway, thereby significantly reducing their descriptive value. Thirdly robust performance specifications cannot be handled well. It can be argued that it is precisely because of the above limitations that a \mathcal{H}_∞ design based on uncertainty weighting functions may well produce an unacceptable final design. Consequently, the weighting functions generally need to be iteratively modified before a suitable design is obtained. One of the motivations for the modified \mathcal{H}_∞ theory presented in Chapter 3 is therefore to ease the difficulty of weighting function selection by attempting to avoid the various limitations detailed above.

2.6 \mathcal{L}_1 Theory: Nominal Performance

The discussion of \mathcal{H}_∞ control theory given above adopted the perspective of continuous time systems only, as the entire development carries over without difficulty to the discrete time case. In \mathcal{L}_1 control theory however, considerable differences emerge between problems formulated in continuous and discrete time. Therefore in our treatment we will give details for both where appropriate. In the literature, discrete time problems are usually denoted by the symbol l_1 . In our treatment however, the symbol \mathcal{L}_1 is used throughout - the discrete or continuous nature of the problem will be stated explicitly as appropriate.

In this section we discuss the issue of nominal performance under the framework of \mathcal{L}_1 control theory. The system norm used in \mathcal{L}_1 control theory is given by

$$\|T_{zw}(t)\|_A = \int_{-\infty}^{+\infty} |T_{zw}(t)| dt$$

in the SISO case, and by

$$\|T_{zw}(t)\|_A = \max_i \sum_{j=1}^n \int_{-\infty}^{+\infty} |(T_{zw}(t))_{ij}| dt = \max_i \sum_{j=1}^n \|(T_{zw}(t))_{ij}\|_1$$

in the MIMO case, where $(T_{zw}(t))_{ij}$ denotes the inverse Laplace transform of the (i, j) th element of $T_{zw}(s)$. So $T_{zw}(t)$ is the impulse response or impulse response matrix from w to z . The system norm $\|\cdot\|_A$ will be referred to as the **A norm**, and is seen to be the \mathcal{L}_1 norm over time t combined with the max-row-sum matrix norm. Note that for continuous time systems, the equivalent norm in the Laplace transform domain is \hat{A} , which is defined as

$$\|T_{zw}(s)\|_{\hat{A}} = \|T_{zw}(t)\|_A$$

where $T_{zw}(s)$ is the Laplace transform of $T_{zw}(t)$ [42]. Similarly for discrete time systems, the equivalent norm in the Z transform domain is \hat{A} , defined as

$$\|\hat{T}_{zw}\|_{\hat{A}} = \|T_{zw}(k)\|_A$$

where \hat{T}_{zw} is the Z transform of $T_{zw}(k)$ [43].

Therefore with reference to Figure 1.4, the **\mathcal{L}_1 Nominal Performance Problem** is given by

$$\inf_K \|T_{zw}(s)\|_{\hat{A}}$$

for continuous time systems, and

$$\inf_K \| \hat{T}_{zw}(z) \|_{\hat{A}}$$

for discrete time systems, where the infimum is over all LTI stabilizing controllers. The engineering motivation for this problem relies on the following theorem, which is fundamental in \mathcal{L}_1 control theory [44].

Theorem 2.3 *Suppose that $z(t) = T_{zw}(t) * w(t)$, and that $T_{zw}(t)$ is the impulse response matrix of a stable LTI system. Then*

$$\| T_{zw}(t) \|_A = \sup_{w \neq 0} \frac{\| z(t) \|_{\infty}}{\| w(t) \|_{\infty}}$$

This theorem says that the \mathcal{L}_{∞} norm on signals induces the A norm on systems. In order to see the engineering relevance of this theorem, let us restate it as follows. Identical reasoning to that used previously shows that

$$\| T_{zw}(t) \|_A = \sup_{w(t) \in \mathcal{D}_w^{(m)}} \| z(t) \|_{\infty}$$

where

$$\mathcal{D}_w^{(m)} = \{w(t) \mid \| w(t) \|_{\infty} \leq 1\} = \mathcal{BL}_{\infty}^n(t)$$

(with “m” for max-amplitude). In the \mathcal{L}_1 approach, w belongs to the signal set $\mathcal{D}_w^{(m)} = \mathcal{BL}_{\infty}^n(t)$, which consists of all signals having amplitude less than or equal to one at all times. The above theorem can be stated equivalently as

$$\| T_{zw}(t) \|_A \leq \alpha \Leftrightarrow \| z(t) \|_{\infty} \leq \alpha \quad \forall w(t) \in \mathcal{D}_w^{(m)}$$

This observation motivates the optimal controller synthesis problem of choosing K to minimize the worst case output z , as quantified by the \mathcal{L}_{∞} norm, and as w ranges through $\mathcal{BL}_{\infty}^n(t)$. This corresponds to the \mathcal{L}_1 **Nominal Performance Problem** and it is essentially a solved problem.

2.7 \mathcal{L}_1 Theory: Robust Stability

Because the A norm is an induced norm, there is a SGT result analagous to that in \mathcal{H}_{∞} theory for this system norm, and it is an important result in \mathcal{L}_1 control theory. Applying the SGT to the set-up of Figure 1.5, and specializing to the \mathcal{L}_{∞} norm, yields the following [44].

Theorem 2.4 *Suppose that the system of Figure 1.5 is nominally stable, and that α is a positive real number. Then the system of Figure 1.5 is BIBO stable in the \mathcal{L}_∞ norm sense for every LTI $\Delta_P(t)$ which obeys*

$$\| \Delta_P(t) \|_A = \sup_{a \neq 0} \frac{\| \Delta_P(t) * a(t) \|_\infty}{\| a(t) \|_\infty} \leq \alpha^{-1}$$

if

$$\| T_{ri}(t) \|_A < \alpha$$

This robust stability theorem is non-conservative only if Δ_P is allowed to be TV and/or NL, as in

$$\hat{\mathcal{D}}_{\Delta_P}^{(n_i)} = \{ \Delta_P \mid \Delta_P \text{ is } \infty\text{-stable, and } \| \Delta_P \|_A \leq 1 \}$$

When Δ_P is constrained to being LTI, this condition is conservative [45, 44]. In contrast, this does not hold for the analogous \mathcal{H}_∞ result. This theorem motivates the **\mathcal{L}_1 Robust Stability Problem** given by

$$\inf_K \| T_{ri}(s) \|_A$$

for continuous time systems, and

$$\inf_K \| \hat{T}_{ri}(z) \|_{\hat{A}}$$

for discrete time systems, where the infimum is over all LTI stabilising controllers. This problem corresponds to maximizing stability robustness, and it is a solved problem.

2.8 The Mixed Sensitivity \mathcal{L}_1 Control Problem

The **Mixed Sensitivity \mathcal{L}_1 Control Problem** for continuous time systems is given by

$$\inf_K \| J(s) \|_A$$

where the infimum is over all LTI stabilizing controllers, and $J(s)$ is a matrix cost function given by

$$J = \begin{pmatrix} W_S(s)S_o(s) & W_R(s)R_o(s) & W_T(s)T_o(s) \end{pmatrix}$$

The equivalent problem for discrete time systems is

$$\inf_K \| \hat{J}(z) \|_{\hat{A}}$$

where the infimum is over all LTI stabilizing controllers, and \hat{J} is a matrix cost function given by

$$J = \begin{pmatrix} \hat{W}_S \hat{S}_o & \hat{W}_R \hat{R}_o & \hat{W}_T \hat{T}_o \end{pmatrix}$$

The motivation for, and the development of, the above cost function is exactly the same as that given for the equivalent \mathcal{H}_∞ problem and so will not be repeated here. In the sequel, detailed comments are made on certain aspects of \mathcal{L}_1 control theory. For the moment, we confine ourselves to the following observations.

1. \mathcal{L}_1 control theory can rightly be considered a time domain theory, as specifications on both the input and output signals are given in the time domain.
2. \mathcal{L}_1 optimisation procedures for discrete time systems differ significantly from those used with continuous time systems. In particular, \mathcal{L}_1 optimal controllers for continuous time systems are irrational, even when the problem data are rational and even in the SISO case. Approaches for calculating rational sub-optimal \mathcal{L}_1 controllers have been suggested [46, 47], but in general the most significant application of the continuous time theory seems to be in furnishing bounds for the achievable performance of discrete time controllers. \mathcal{L}_1 controller design is therefore generally applied directly to discrete time systems.
3. \mathcal{L}_1 control theory is a very recent theory, and many results are still very new. Many important open questions still remain to be answered in connection with \mathcal{L}_1 optimisation. As pointed out in [48], from a theoretical point of view, stronger results regarding the support structure of the optimal solution to the general multi-block problem are needed. The existence in general of optimal rational solutions is another open question. In practice, it has been noted that even one-block problems may have high order optimal controllers, and thus the absence of a formal model reduction theory in the context of \mathcal{L}_1 optimisation is a significant drawback.
4. Commercial software packages which can be used to design \mathcal{L}_1 optimal controllers are not yet widely available in the control community.

2.9 Solutions to the Mixed Sensitivity \mathcal{L}_1 Control Problem

As with our treatment of \mathcal{H}_∞ control theory, we pass over the details of the mathematical techniques involved in \mathcal{L}_1 optimisation in favour of concentrating on the underlying engineering motivation for the problem. A common feature of all \mathcal{L}_1 optimisation is the use of vector space duality theory together with linear programming based techniques for which standard references are [20, 49]. A comprehensive overview of the field is given in [44]. To date the \mathcal{L}_1 optimisation problems which have been solved are as follows.

1. \mathcal{L}_1 optimal controllers for SISO discrete time systems [50]
2. \mathcal{L}_1 optimal controllers for MIMO discrete time systems [51]
3. The general multi-block \mathcal{L}_1 optimisation problem for discrete time systems [48]
4. \mathcal{L}_1 optimal controllers for SISO continuous time systems [42]
5. Rational suboptimal controllers for SISO continuous time systems [46, 47]

2.10 A Critique of \mathcal{L}_1 Control Theory

Having previously described some basic limitations of standard \mathcal{H}_∞ control theory, we now outline briefly some of the main strengths and weaknesses of \mathcal{L}_1 control theory. A comprehensive treatment is not intended, and we deal only with those aspects which have a bearing on this thesis.

2.10.1 (a) The Output Norm: Non Conservative Minimisation of Maximum Tracking Errors in The Time Domain

Perhaps the most important attraction of \mathcal{L}_1 control theory is that it optimally and non-conservatively minimizes maximum tracking errors in the time domain.

“The $\| \cdot \|_A$ norm is very interesting since the assumptions which lead to it, that both w and z are in $\mathcal{BL}_\infty^n(t)$, are very appealing. It is often the case in practice that the critical issue is the magnitude of signals and not their power or energy. Superficially, it could be argued that this would be the obvious norm of choice for most engineering problems, were it not for the mathematical difficulties associated with $\| \cdot \|_A$.”¹ - [Doyle,9].

It can be argued that the essential purpose of a control system is to ensure that the actual value of the plant's output vector, call it $y(t)$, remains close to given desired or target values which are described by the reference input, say $r(t)$, so that the tracking error $e(t) = y(t) - r(t)$ remains consistently small over time. In most applications it is essential or desirable that the tracking error $e(t)$ never exceeds a certain level at any time. Only by using the \mathcal{L}_∞ norm to measure the size of signals can this objective be rigorously captured. Standard \mathcal{H}_∞ control theory is centered on the \mathcal{L}_2 norm for signals. This norm involves averaging over time and over vector elements. So a small value of $\| e(t) \|_2$ does *not* mean that $e(t)$ will be reasonably small at every time t . Indeed, $e(t)$ can be extremely large at some t and still have a very small \mathcal{L}_2 norm, as in Lemma 2.1. The crucial implication of Lemmas 2.1 and 2.2 is that the \mathcal{L}_2 norm is a very poor mathematical model of the purpose of a control system, while the \mathcal{L}_∞ norm gives a far better and more meaningful measure of the quality of control. This is, perhaps, the most attractive feature of \mathcal{L}_1 control theory.

By way of example, consider the problem of controlling the trajectory of a flexible robot arm in an enclosed environment. Ideally, the tracking error $e(t)$ should be zero at all times t . In reality, perfect control is not possible and one must settle for minimising the deviation from the desired trajectory. But in what sense should this deviation be minimized? Clearly, the “real” objective and purpose of the control system is to ensure that this deviation is as small as possible *in the time domain and at each and every point in time*. Indeed, depending on the proximity of other devices

¹The mathematical symbols have been changed to the notation in use in this thesis

in the robot's operating environment it may be absolutely essential that this deviation never exceeds a certain limit at any time. This means therefore that achieving the condition

$$|e(t)| \leq 1\text{cm} \quad \forall t$$

constitutes much better control than, for instance,

$$\|e(t)\|_2 \leq 1$$

In fact, the latter condition allows no firm conclusion to be made about the quality of control in any 'real' or meaningful way. This consideration makes the \mathcal{L}_∞ norm very attractive indeed.

Using the \mathcal{L}_∞ norm on the output side has other important advantages too. It is useful if any device in the control loop has a maximum input rating which should not be exceeded, such as a plant with a saturation at its input. It is useful too if it is necessary to keep the system's state close to an equilibrium point for a linearized plant model, or if the system's state must be confined to a specified region of state space. The only way to handle precisely hard constraints on the time amplitude of signals in the system is by using the \mathcal{L}_∞ norm on the output side. In particular, the \mathcal{L}_1 approach then avoids the 'spike' problem, because it minimizes the worst case \mathcal{L}_∞ norm of the output $z(t)$ in the time domain. Indeed, this approach *optimally* avoids large 'spikes' in the time domain.

2.10.2 (b) Signal Set and Specification Lumping

\mathcal{L}_1 control theory does not suffer from signal set or specification lumping.

The difficulty with signal set lumping in the \mathcal{L}_2 norm comes ultimately from the inequality in

$$\mathcal{BL}_2^n(j\omega) \neq \mathcal{BL}_2(j\omega) \times \dots \times \mathcal{BL}_2(j\omega)$$

In contrast, when the signal norm employs the \mathcal{L}_∞ vector norm, signal set lumping is avoided. Indeed, \mathcal{L}_1 control theory uses the signal set $\mathcal{D}_w^{(m)}$, where

$$\begin{aligned} \mathcal{D}_w^{(m)} &= \{w(t) \mid w(t)^T = (w_1(t), \dots, w_n(t)), \quad \|w_i(t)\|_\infty \leq 1, \quad i = 1, \dots, n\} \\ &= \{w(t) \mid w(t)^T = (w_1(t), \dots, w_n(t)), \quad \|w(t)\|_\infty \leq 1\} \\ &= \mathcal{BL}_\infty^n(t) = \mathcal{BL}_\infty(t) \times \dots \times \mathcal{BL}_\infty(t) \end{aligned}$$

Chapter 3

A New Paradigm for Optimal Robust Controller Synthesis in the Frequency Domain

In the previous chapter a detailed description of some of the relative strengths and limitations of \mathcal{H}_∞ and \mathcal{L}_1 control theories was given. Based on this analysis, this chapter presents a new paradigm for optimal robust controller synthesis in the frequency domain. It is shown that by introducing new models of uncertainty, slight modifications to standard \mathcal{H}_∞ and \mathcal{H}_2 control theories result in an approach to controller design which overcomes some of the limitations of \mathcal{H}_∞ control theory and captures some of the most attractive features of \mathcal{L}_1 control. In particular we explore the potential of using frequency domain design techniques to optimally satisfy time domain specifications.

3.1 SISO Nominal Performance in \mathcal{H}_∞ : Non Conservative Minimisation of Maximum Tracking Errors in the Time Domain

Two commonly held perceptions with regard to \mathcal{H}_∞ control theory are that (a) \mathcal{H}_∞ deals with finite energy signals only [60], and (b) \mathcal{H}_∞ cannot be used to design controllers which meet time domain specifications exactly [63]. While passing reference has been made in the literature to the fact that \mathcal{H}_∞ control theory can be used to deal with sinusoidal signals, no attempt has been made to explore the potential for surmounting (a) and (b) above which arises from this fact. This may be in part due to the fact that a signal set consisting of sinusoidal signals only would seem to be too small for the purpose of modelling uncertain input signals in a realistic system. In this section, it is shown that uncertain signal sets based on sinusoidal signals can be constructed which seem ‘rich’ enough for most practical purposes. It is effectively demonstrated that with these new signal sets (a) and (b) above do not apply to \mathcal{H}_∞ control theory in the SISO case.

3.1.1 A Sinusoidal Signal Set $\mathcal{D}_w^{(s)}$

Consider the following signal set. Define $\mathcal{D}_w^{(s)}$ to be the following set of scalar exogenous inputs

$$\mathcal{D}_w^{(s)} = \{w(t) \mid w(t) = A \exp(j\omega t), \omega \text{ arbitrary}, |A| \leq 1\} \quad (3.1)$$

(with “s” for sinusoidal). This signal set consists of all sinusoidal signals with amplitude less than or equal to one. To see the main advantage of using this model, it will now be shown that for any w in this signal set, the standard \mathcal{H}_∞ system norm provides a non-conservative upper bound on the amplitude of the output $z(t)$ in the time domain. This result should be contrasted with Lemma 2.1.

Lemma 3.1 *Suppose that $z(j\omega) = T_{zw}(j\omega)w(j\omega)$, that $T_{zw}(s)$ is the transfer function of a stable LTI system which is SISO, and that $T_{zw}(j\omega)$ is a continuous function of ω . Then*

$$\sup_{w \in \mathcal{D}_w^{(s)}} \|z(t)\|_\infty = \|T_{zw}(s)\|_\infty$$

where $\mathcal{D}_w^{(s)}$ is defined in eqn. (3.1). Equivalently,

$$\| z(t) \|_\infty \leq \alpha \quad \forall w \in \mathcal{D}_w^{(s)} \Leftrightarrow \| T_{zw}(s) \|_\infty \leq \alpha$$

where α is any non-negative real scalar.

Proof

Consider an arbitrary exogenous input in $\mathcal{D}_w^{(s)}$, say

$$w(t) = A \exp(j\omega_0 t)$$

The output due to this input is then

$$z(t) = T_{zw}(j\omega_0) A \exp(j\omega_0 t) \tag{3.2}$$

$$\begin{aligned} \Rightarrow |z(t)| &= |AT_{zw}(j\omega_0) \exp(j\omega_0 t)| \\ \Rightarrow \sup_t |z(t)| &= |AT_{zw}(j\omega_0)| \\ \Rightarrow \| z(t) \|_\infty &= |AT_{zw}(j\omega_0)| \end{aligned}$$

Now since $T_{zw}(j\omega)$ is continuous, there is an $\omega_0 \in \mathcal{R} \cup \{\infty\}$ which achieves equality in

$$\| T_{zw}(j\omega) \|_\infty = \max_\omega |T_{zw}(j\omega)| = |T_{zw}(j\omega_0)|$$

and thus it follows from the definition of $\mathcal{D}_w^{(s)}$ that

$$\sup_{w \in \mathcal{D}_w^{(s)}} \| z(t) \|_\infty = \| T_{zw}(j\omega) \|_\infty$$

which completes the proof.

Two points about this proof may be worth commenting on. A transfer function represents a certain differential equation. In the above, differential equations are solved in the sense of the Fourier transform, rather than in the sense of the Laplace transform, which is why the system's transient response doesn't appear in eq. (3.2). The mathematical techniques being used in the proof as well as in the remainder of this paper are best described as a mixture of Fourier and Laplace transform techniques.

Note that this proof involves evaluating the transfer function $T_{zw}(s)$ at the isolated point $s = j\omega_0$. So this proof seems to require that $T_{zw}(j\omega)$ be a continuous function of ω . The case of discontinuous T_{zw} 's would not seem to be of practical importance. However, for certain theoretical purposes, $T_{zw}(s)$ is viewed as being a member of

the Hardy space \mathcal{H}_∞ , and this space contains discontinuous elements (Rudin 1987). When discussing discontinuous T_{zw} 's, one must work with the definition

$$\|T_{zw}(s)\|_\infty = \text{ess-sup}_{-\infty < \omega < +\infty} |T_{zw}(j\omega)|$$

When $T_{zw}(j\omega)$ is continuous in ω , the concepts of supremum (sup) and essential supremum (ess-sup) coincide, and the proof as stated above does the job. This technical difficulty will be circumvented shortly. \square

The above result is well known (see for instance Section 5.2.6 of [6], Section 3.4.1 of [44], Table 1 in [9], and Table 2.1 in [74]). However, its consequences, as described in the remainder of this section, are believed to be new. The proof has been included to draw attention to the necessity of using Fourier rather than Laplace transforms and to the difficulty with discontinuous $T_{zw}(j\omega)$'s. Of course, one can just as easily work with the signal set

$$\text{Re } \mathcal{D}_w^{(s)} = \{w(t) \mid w(t) = A \sin(\omega t + \phi), \omega, \phi \text{ arbitrary}, -1 \leq A \leq 1\}$$

Note carefully that this lemma involves the \mathcal{L}_∞ norm of $z(t)$, and a set of signals which is clearly very close to classical frequency response thinking. However, as noted above the set of signals involved may seem to be an unreasonably small set. For practical purposes, a much richer set is needed.

3.1.2 The Convex Hull is Free

We now show that the above observation holds not just for any signal in the set $\mathcal{D}_w^{(s)}$ but for any signal in the closure of its convex hull, to be denoted by $\overline{\text{Co}} \mathcal{D}_w^{(s)}$. Consider the convex hull of $\mathcal{D}_w^{(s)}$ which consists of all (finite) convex linear combinations of elements of $\mathcal{D}_w^{(s)}$, viz.

$$\text{Co } \mathcal{D}_w^{(s)} = \{w(t) \mid w(t) = \sum_{i=1}^k A_i \exp(j\omega_i t), \omega_i \text{ arbitrary}, \sum_{i=1}^k |A_i| \leq 1\}$$

The closure of the convex hull is given by

$$\overline{\text{Co}} \mathcal{D}_w^{(s)} = \{w(t) \mid w(t) = \sum_{i=1}^{\infty} A_i \exp(j\omega_i t), \omega_i \text{ arbitrary}, \sum_{i=1}^{\infty} |A_i| \leq 1\}$$

and we have the following lemma.

Lemma 3.2

$$\| z(t) \|_{\infty} \leq \alpha \quad \forall \quad w \in \mathcal{D}_w^{(s)} \Leftrightarrow \| z(t) \|_{\infty} \leq \alpha \quad \forall \quad w \in \overline{\text{Co}} \mathcal{D}_w^{(s)}$$

Proof

Consider any arbitrary signal in the closure of the convex hull of $\mathcal{D}_w^{(s)}$

$$w(t) = \sum_{i=1}^{\infty} A_i \exp(j\omega_i t), \quad \left(\sum_{i=1}^{\infty} |A_i| \leq 1 \right)$$

The output due to this input is then

$$\begin{aligned} z(t) &= \sum_{i=1}^{\infty} T_{zw}(j\omega_i) A_i \exp(j\omega_i t) \\ \Rightarrow |z(t)| &\leq \sum_{i=1}^{\infty} |T_{zw}(j\omega_i) A_i \exp(j\omega_i t)| \\ \Rightarrow |z(t)| &\leq \sum_{i=1}^{\infty} |T_{zw}(j\omega_i)| |A_i| |\exp(j\omega_i t)| \\ \Rightarrow |z(t)| &\leq \sup_{\omega} |T_{zw}(j\omega)| \sum_{i=1}^{\infty} |A_i| |\exp(j\omega_i t)| \\ \Rightarrow \sup_t |z(t)| &\leq \| T_{zw}(j\omega) \|_{\infty} \sum_{i=1}^{\infty} |A_i| \\ \Rightarrow \sup_{w \in \overline{\text{Co}} \mathcal{D}_w^{(s)}} \| z(t) \|_{\infty} &= \| T_{zw}(j\omega) \|_{\infty} \end{aligned}$$

where equality is achieved in the above expression by suitably choosing $w(t)$. \square

The above observation is true much more generally. Indeed, for *any* class of signals, \mathcal{D}_w say, it is clear that

$$\| z(t) \|_{\infty} \leq \alpha \quad \forall \quad w \in \mathcal{D}_w \Leftrightarrow \| z(t) \|_{\infty} \leq \alpha \quad \forall \quad w \in \overline{\text{Co}} \mathcal{D}_w$$

In other words, the convex hull is free. This is significant because it substantially increases the range of exogenous signals for which Lemma 3.1 applies.

3.1.3 A Frequency Domain \mathcal{L}_1 Norm Signal Set

The above result can be further exploited as follows. The convex hull of the set $\mathcal{D}_w^{(s)}$ may be written just as easily in the frequency domain,

$$\text{Co } \mathcal{D}_w^{(s)} = \{w(j\omega) \mid w(j\omega) = 2\pi \sum_{i=1}^k A_i \delta(\omega - \omega_i), \omega_i \text{ arbitrary}, \sum_{i=1}^k |A_i| \leq 1\}$$

which is more convenient for our purposes. (The Fourier transform of elements of $\mathcal{D}_w^{(s)}$ are impulse functions times 2π .) The closure of the convex hull is then

$$\overline{\text{Co } \mathcal{D}_w^{(s)}} = \{w(j\omega) \mid w(j\omega) = 2\pi \sum_{i=1}^{\infty} A_i \delta(\omega - \omega_i), \omega_i \text{ arbitrary}, \sum_{i=1}^{\infty} |A_i| \leq 1\}$$

This set consists of (finite or countably infinite) sequences of impulse functions in the frequency domain. This process can be taken a step further. Impulses are so-called generalized functions, and ‘ordinary’ functions can be viewed as a weighted sum of (uncountably infinitely many) impulses via the well known sifting property,

$$v(j\omega) = \int_{-\infty}^{+\infty} v(j\hat{\omega}) \delta(\omega - \hat{\omega}) d\hat{\omega}$$

Exploiting this observation, define

$$\begin{aligned} \widehat{\mathcal{D}}_w^{(1)} &= \{w(j\omega) \mid w(j\omega) = \alpha 2\pi \sum_{i=1}^{\infty} A_i \delta(\omega - \omega_i) + (1 - \alpha) 2\pi v(j\omega), \dots \\ &\quad \alpha \in [-1, +1], \omega_i \text{ arbitrary}, \sum_{i=1}^{\infty} |A_i| \leq 1, v(j\omega) \in \mathcal{BL}_1(j\omega)\} \end{aligned} \quad (3.3)$$

Another possible model for uncertain signals is then the signal set $\mathcal{D}_w^{(1)}$, where

$$\mathcal{D}_w^{(1)} = \{w(j\omega) \mid \|w(j\omega)\|_1 \leq 1\} = \mathcal{BL}_1(j\omega) \quad (3.4)$$

This is the signal set which we will work with subsequently. It consists of all signals whose \mathcal{L}_1 norm is less than or equal to unity *in the frequency domain*. It is essentially $\widehat{\mathcal{D}}_w^{(1)}$ times a constant, but with the use of generalized functions avoided. Note that

$$\mathcal{D}_w^{(s)} \subset \widehat{\mathcal{D}}_w^{(1)} \quad \text{and} \quad 2\pi \mathcal{D}_w^{(1)} \subset \widehat{\mathcal{D}}_w^{(1)}$$

It will now be shown that for any w in $\mathcal{D}_w^{(1)}$, the standard \mathcal{H}_{∞} norm provides a non-conservative upper bound on the amplitude of the system’s output $z(t)$ in the *time domain*, for the SISO case.

Lemma 3.3 Suppose that $z(j\omega) = T_{zw}(j\omega)w(j\omega)$, and that $T_{zw}(s)$ is the transfer function of a stable LTI system which is SISO. Then

$$\frac{1}{2\pi} \|T_{zw}(s)\|_{\infty} = \sup_{w \neq 0} \frac{\|z(t)\|_{\infty}}{\|w(j\omega)\|_1} = \sup_{w \in \mathcal{D}_w^{(1)}} \|z(t)\|_{\infty} \quad (3.5)$$

where $\mathcal{D}_w^{(1)}$ is defined in eqn. (3.4). Equivalently,

$$\|z(t)\|_{\infty} \leq \alpha \quad \forall w \in \mathcal{D}_w^{(1)} \Leftrightarrow \|T_{zw}(s)\|_{\infty} \leq 2\pi\alpha$$

where α is any non-negative real scalar.

Proof

Consider an arbitrary $w \in \mathcal{D}_w^{(1)}$. Using the inverse Fourier transform,

$$\begin{aligned} |z(t)| &= \frac{1}{2\pi} \left| \int_{-\infty}^{+\infty} z(j\omega) e^{j\omega t} d\omega \right| \\ &= \frac{1}{2\pi} \left| \int_{-\infty}^{+\infty} T_{zw}(j\omega) w(j\omega) e^{j\omega t} d\omega \right| \\ &\leq \frac{1}{2\pi} \int_{-\infty}^{+\infty} |T_{zw}(j\omega) w(j\omega)| d\omega \end{aligned}$$

Holder's inequality then shows that

$$\begin{aligned} \Rightarrow |z(t)| &\leq \frac{1}{2\pi} \sup_{\omega} |T_{zw}(j\omega)| \int_{-\infty}^{+\infty} |w(j\omega)| d\omega \\ &= \frac{1}{2\pi} \|T_{zw}(j\omega)\|_{\infty} \|w(j\omega)\|_1 \end{aligned}$$

Since $w \in \mathcal{D}_w^{(1)}$ and t were arbitrary,

$$\sup_{w \in \mathcal{D}_w^{(1)}} \|z(t)\|_{\infty} \leq \frac{1}{2\pi} \|T_{zw}(j\omega)\|_{\infty}$$

To show that equality holds in the above inequality, suppose that

$$\|T_{zw}(s)\|_{\infty} > \lambda_1$$

Then there is a subset $\Omega \subset \mathcal{R}$ such that

$$|T_{zw}(j\omega)| > \lambda_1 \quad \text{when } \omega \in \Omega$$

where

$$\int_{\Omega} d\omega = \mu_1$$

is strictly positive. Define

$$\widehat{w}(j\omega) = \begin{cases} \mu_1^{-1} \exp(-j\angle(T_{zw}(j\omega))) & \text{for } \omega \in \Omega \\ 0 & \text{otherwise} \end{cases}$$

Then, letting \widehat{z} be the output resulting from the input \widehat{w} ,

$$\begin{aligned} |\widehat{z}(t)|_{t=0} &= \frac{1}{2\pi} \int_{-\infty}^{+\infty} T_{zw}(j\omega) \widehat{w}(j\omega) \exp(j\omega t) d\omega \\ &= \frac{1}{2\pi \mu_1} \int_{\Omega} |T_{zw}(j\omega)| d\omega \\ &> \frac{\lambda_1}{2\pi \mu_1} \int_{\Omega} d\omega = \frac{\lambda_1}{2\pi} \end{aligned}$$

Since $\|\widehat{w}(j\omega)\|_1 = 1$, this shows that

$$\|T_{zw}(s)\|_{\infty} > \lambda_1 \Rightarrow \frac{\|\widehat{z}(t)\|_{\infty}}{\|\widehat{w}(j\omega)\|_1} > \frac{\lambda_1}{2\pi}$$

so that

$$\|T_{zw}(s)\|_{\infty} > \lambda_1 \Rightarrow \sup_{w \neq 0} \frac{\|z(t)\|_{\infty}}{\|w(j\omega)\|_1} > \frac{\lambda_1}{2\pi}$$

and

$$\|T_{zw}(s)\|_{\infty} \geq \frac{1}{2\pi} \sup_{w \neq 0} \frac{\|z(t)\|_{\infty}}{\|w(j\omega)\|_1}$$

completing the proof.

Loosely speaking, the essential idea behind this proof is that $\widehat{w}(j\omega)$ approximates the impulse function $\delta(\omega - \omega_0)$ where ω_0 approaches or attains the supremum in

$$\sup_{\omega} |T_{zw}(j\omega)| = \|T_{zw}(s)\|_{\infty}$$

Readers unfamiliar with the mathematical formalism of Lebesgue integration [53] should view $T_{zw}(j\omega)$ as a continuous function of ω . In this case, Ω may be taken to be an interval of strictly positive length. The more general case of possibly discontinuous $T_{zw}(j\omega)$'s requires the use of measure theory. Here, Ω is a set of strictly positive measure. In either case, an Ω with the required properties always exists. So this proof does not require $T_{zw}(j\omega)$ to be continuous in ω and it applies to any $T_{zw}(s) \in \mathcal{H}_{\infty}$.

□

3.2 SISO Robust Stability in \mathcal{H}_∞

In this section we return to the issue of system uncertainty. As discussed in Chapter 1, the principal tool used for investigating the effects of system uncertainty on closed loop stability is the Small Gain Theorem. Recall however that the SGT applies equally well to any induced norm, but not directly to semi-induced norms. The lemma given above for the new uncertain signal set $\mathcal{D}_w^{(1)}$ says that the \mathcal{H}_∞ norm can be viewed as a certain semi-induced norm, since different norms appear on the numerator and the denominator of eqn. (3.5). In this section we show that for the new signal set $\mathcal{D}_w^{(1)}$ the \mathcal{H}_∞ norm can also be interpreted as a certain induced norm – thus the SGT applies and the issue of designing for robust stability can be addressed.

Lemma 3.4 *Suppose that $z(j\omega) = T_{zw}(j\omega)w(j\omega)$, and that $T_{zw}(s)$ is the transfer function of a stable LTI system which is SISO. Then*

$$\|T_{zw}(s)\|_\infty = \sup_{w \neq 0} \frac{\|z(j\omega)\|_1}{\|w(j\omega)\|_1}$$

Equivalently,

$$\|z(j\omega)\|_1 \leq \alpha \quad \forall w(j\omega) \in \mathcal{BL}_1(j\omega) \Leftrightarrow \|T_{zw}(s)\|_\infty \leq \alpha$$

where α is any non-negative real scalar.

Proof

The proof is an easy application of Holder's inequality, which immediately yields

$$\begin{aligned} \|z(j\omega)\|_1 &= \int_{-\infty}^{+\infty} |z(j\omega)| d\omega \\ &= \int_{-\infty}^{+\infty} |T_{zw}(j\omega)w(j\omega)| d\omega \\ &\leq \sup_{\omega} |T_{zw}(j\omega)| \int_{-\infty}^{+\infty} |w(j\omega)| d\omega \\ &= \|T_{zw}(s)\|_\infty \|w(j\omega)\|_1 \end{aligned}$$

and when $w(j\omega) \in \mathcal{BL}_1(j\omega)$, so that $\|w(j\omega)\|_1 \leq 1$, we have that

$$\|z(j\omega)\|_1 \leq \|T_{zw}(s)\|_\infty$$

To show that this inequality is in fact an equality, suppose again that

$$\|T_{zw}(s)\|_{\infty} > \lambda_1$$

As before, there is then a subset $\Omega \subset \mathcal{R}$ such that

$$|T_{zw}(j\omega)| > \lambda_1 \quad \text{when } \omega \in \Omega$$

where

$$\int_{\Omega} d\omega = \mu_1$$

is strictly positive. Define

$$\hat{w}(j\omega) = \begin{cases} 1/\mu_1 & \text{for } \omega \in \Omega \\ 0 & \text{otherwise} \end{cases}$$

Then

$$\begin{aligned} \|\hat{z}(j\omega)\|_1 &= \int_{-\infty}^{+\infty} |T_{zw}(j\omega)\hat{w}(j\omega)| d\omega \\ &= \frac{1}{\mu_1} \int_{\Omega} |T_{zw}(j\omega)| d\omega \\ &> \frac{\lambda_1}{\mu_1} \int_{\Omega} d\omega = \lambda_1 \end{aligned}$$

Since $\|\hat{w}(j\omega)\|_1 = 1$, this shows that

$$\|T_{zw}(s)\|_{\infty} > \lambda_1 \Rightarrow \frac{\|\hat{z}(j\omega)\|_1}{\|\hat{w}(j\omega)\|_1} > \lambda_1$$

so that

$$\|T_{zw}(s)\|_{\infty} > \lambda_1 \Rightarrow \sup_{w \neq 0} \frac{\|z(j\omega)\|_1}{\|w(j\omega)\|_1} > \lambda_1$$

and

$$\|T_{zw}(s)\|_{\infty} \geq \sup_{w \neq 0} \frac{\|z(j\omega)\|_1}{\|w(j\omega)\|_1}$$

completing the proof.

Again, this proof does not require $T_{zw}(j\omega)$ to be continuous. \square

The above lemma says that the usual \mathcal{H}_{∞} norm may be viewed as an induced norm, being induced by the \mathcal{L}_1 norm in the frequency domain in the SISO case. This permits the application of the SGT to obtain sufficient conditions for robust stability. It is noteworthy that the \mathcal{H}_{∞} norm is also an induced norm in another distinct sense, as in Theorem 2.1 above. However, the above lemma is more suited to the needs of our modified theory, as will become clear shortly.

3.3 Interpretations of the \mathcal{H}_∞ Norm

Our results so far in this chapter may be summarised as follows.

Theorem 3.1 *Suppose that $z(j\omega) = T_{zw}(j\omega)w(j\omega)$, that $T_{zw}(s)$ is the transfer function of a stable LTI system which is SISO, and that $T_{zw}(j\omega)$ is continuous in ω . Then*

$$(1) \quad \|T_{zw}(s)\|_\infty$$

$$(2) \quad = \sup_{w \in \mathcal{D}_w^{(e)}} \|z(j\omega)\|_2$$

$$(3) \quad = \sup_{w \in \mathcal{D}_w^{(s)}} \|z(t)\|_\infty$$

$$(4) \quad = 2\pi \sup_{w \in \mathcal{D}_w^{(1)}} \|z(t)\|_\infty$$

$$(5) \quad = \sup_{w \in \mathcal{D}_w^{(1)}} \|z(j\omega)\|_1$$

where $\mathcal{D}_w^{(e)}$, $\mathcal{D}_w^{(s)}$ and $\mathcal{D}_w^{(1)}$ are given by equations (2.1), (3.1) and (3.4) respectively.

This theorem says that the optimal and sub-optimal solutions of several SISO problems coincide. So SISO \mathcal{H}_∞ controllers are optimal in several senses. Each of items (2) to (5) above points to a distinct motivation for the optimal controller synthesis problem of minimizing the quantity in item (1). Item (2) is the basis of the energy paradigm for \mathcal{H}_∞ control. It has been argued above that this approach is seriously flawed from a control engineering point of view. On the other hand, items (3) and (4) show that \mathcal{H}_∞ minimizes the worst case \mathcal{L}_∞ norm of the output for certain input signal sets. So in the SISO case, standard \mathcal{H}_∞ control theory already optimally and non-conservatively minimizes maximum tracking errors in the time domain. In particular, time domain ‘spikes’ are avoided, indeed optimally avoided. Items (2) and (5) are useful because they show that the system norm in item (1) is an induced norm. Finally, in [54] it is shown that the \mathcal{H}_∞ norm also has an interpretation in terms of the output power of a system subject to input signals of bounded power. In this approach however the functions used to measure the power of the input and

output signals are not strictly speaking norms, and thus we have not included this interpretation in the above theorem.

It seems remarkable that several different perspectives regarding the underlying engineering motivation for controller design lead to the \mathcal{H}_∞ norm, and correspond to the same optimal controller, in the SISO case. Things are only a little different in the MIMO case, as will be shown next.

3.4 MIMO Nominal Performance in \mathcal{H}_∞ : Non-Conservative Minimisation of Maximum Tracking Errors in the Time Domain

In this section we extend our results to deal with multivariable systems. It is shown that the modified theory leads to a new \mathcal{H}_∞ optimisation problem in the MIMO case. Our first task is to extend our new signal sets to deal with *vectors* of uncertain input signals.

3.4.1 Vector Extensions of the Signal Sets $\mathcal{D}_w^{(s)}$ and $\mathcal{D}_w^{(1)}$

The proposed signal sets are generalised to the MIMO case as follows. Specifically, consider the problem of choosing a controller K to minimize the effect of the input w on the output z when there are several *unrelated, independent* exogenous inputs, and in the absence of system uncertainty. Note that $T_{zw}(s)$ is now a transfer function matrix, say of dimension $m \times n$.

We define the following two classes of vector signals. Let

$$\mathcal{D}_w^{(s)} = \{w(t) = (w_1(t), \dots, w_n(t))^T \mid w_i(t) = A_i \exp(j\omega_i t), \omega_i \text{ arb.}, |A_i| \leq 1, i = 1, \dots, n\} \quad (3.6)$$

and

$$\mathcal{D}_w^{(1)} = \{w(j\omega) = (w_1(j\omega), \dots, w_n(j\omega))^T \mid \|w_i(j\omega)\|_1 \leq 1, i = 1, \dots, n\} \quad (3.7)$$

Each vector element $w_i(t)$ of $w(t) \in \mathcal{D}_w^{(s)}$ is a sinusoid whose phase and frequency is arbitrary, and whose amplitude is less than or equal to one. Each vector element $w_i(j\omega)$ of $w(j\omega) \in \mathcal{D}_w^{(1)}$ belongs to the unit ball in $\mathcal{L}_1(j\omega)$ in the frequency domain.

It will be convenient to define the signal norm

$$\| w(j\omega) \|'_1 = \max_i \| w_i(j\omega) \|_1 \quad (3.8)$$

Clearly $\mathcal{D}_w^{(1)}$ is the unit ball in this norm, and

$$\mathcal{D}_w^{(1)} = \mathcal{BL}_1(j\omega) \times \dots \times \mathcal{BL}_1(j\omega)$$

3.4.2 A New \mathcal{H}_∞ Optimisation Problem

We show now that for both of the uncertain vector signal sets $\mathcal{D}_w^{(s)}$ and $\mathcal{D}_w^{(1)}$, the problem of minimising the \mathcal{L}_∞ norm in the time domain of the output due to the worst case input signal leads to a new \mathcal{H}_∞ optimisation problem. Define first of all the following system norm

$$\| T_{zw}(j\omega) \|_B = \max_i \sum_{j=1}^n \| (T_{zw}(j\omega))_{ij} \|_\infty \quad (3.9)$$

This system norm is obtained by taking the usual \mathcal{H}_∞ norm of each *element* of the transfer function matrix $T_{zw}(s)$, and *then* applying the max-row-sum matrix norm. It will be referred to as the **B norm**. The main theorem for handling uncertain signals in the proposed approach may now be stated.

Theorem 3.2 *Suppose that $z(j\omega) = T_{zw}(j\omega)w(j\omega)$, that $T_{zw}(s)$ is the transfer function matrix of a stable $m \times n$ LTI system, and that $T_{zw}(j\omega)$ is continuous in ω . Then*

$$\begin{aligned} (1) \quad & \| T_{zw}(s) \|_B \\ (2) \quad & = \sup_{w(t) \in \mathcal{D}_w^{(s)}} \| z(t) \|_\infty \\ (3) \quad & = \frac{1}{2\pi} \sup_{w(j\omega) \neq 0} \frac{\| z(t) \|_\infty}{\| w(j\omega) \|'_1} = \frac{1}{2\pi} \sup_{w(j\omega) \in \mathcal{D}_w^{(1)}} \| z(t) \|_\infty \\ (4) \quad & = \sup_{w(j\omega) \neq 0} \frac{\| z(j\omega) \|'_1}{\| w(j\omega) \|'_1} = \sup_{w(j\omega) \in \mathcal{D}_w^{(1)}} \| z(j\omega) \|'_1 \end{aligned}$$

where $\mathcal{D}_w^{(s)}$, $\mathcal{D}_w^{(1)}$, $\| \cdot \|'_1$ and $\| \cdot \|_B$, are defined in eqns. (3.6), (3.7), (3.8) and (3.9) respectively.

Proof

Consider an arbitrary $w(t)$ in $\mathcal{D}_w^{(s)}$, say

$$w(t) = \begin{pmatrix} w_1(t) \\ \vdots \\ w_n(t) \end{pmatrix} = \begin{pmatrix} A_1 \exp(j\omega_1 t) \\ \vdots \\ A_n \exp(j\omega_n t) \end{pmatrix}$$

The output which results from this input is

$$z_i(t) = \sum_{j=1}^n (T_{zw}(j\omega_j))_{ij} A_j \exp(j\omega_j t), \quad i = 1, \dots, m$$

Clearly,

$$\begin{aligned} \Rightarrow |z_i(t)| &\leq \left| \sum_{j=1}^n (T_{zw}(j\omega_j))_{ij} A_j \exp(j\omega_j t) \right| \\ &\leq \sum_{j=1}^n |(T_{zw}(j\omega_j))_{ij}| |A_j| \\ &\leq \sum_{j=1}^n \|T_{zw}(j\omega_j)\|_{ij} \|A_j\|_{\infty} \end{aligned}$$

and since i, t and $w(t) \in \mathcal{D}_w^{(s)}$ are arbitrary,

$$\Rightarrow \sup_{w \in \mathcal{D}_w^{(s)}} \|z(t)\|_{\infty} \leq \max_i \sum_{j=1}^n \|(T_{zw}(s))_{ij}\|_{\infty} = \|T_{zw}(s)\|_B$$

and equality can be attained by suitably choosing the ω_j 's and the A_j 's, establishing part (2). The crucial point is that the frequencies ω_j and the (complex valued) amplitudes A_j , $j = 1, \dots, n$ are independent of each other. So to attain equality, sinusoids with distinct frequencies need to be applied to distinct inputs w_j , $j = 1, \dots, n$.

Consider next a $w(t)$ in $\mathcal{D}_w^{(l)}$. The resulting output is

$$z(j\omega) = T_{zw}(j\omega)w(j\omega)$$

Inverse Fourier transforming gives

$$\Rightarrow z_i(t) = \frac{1}{2\pi} \sum_{j=1}^n \int_{-\infty}^{+\infty} (T_{zw}(j\omega))_{ij} w_j(j\omega) e^{j\omega t} d\omega$$

Clearly,

$$\Rightarrow |z_i(t)| \leq \frac{1}{2\pi} \sum_{j=1}^n \int_{-\infty}^{+\infty} |(T_{zw}(j\omega))_{ij} w_j(j\omega)| d\omega$$

Holder's inequality gives

$$\leq \frac{1}{2\pi} \sum_{j=1}^n \| (T_{zw}(j\omega))_{ij} \|_{\infty} \| w_j(j\omega) \|_1$$

Since this holds for all t and all i ,

$$\Rightarrow \| z(t) \|_{\infty} \leq \frac{1}{2\pi} \| T_{zw}(j\omega) \|_B \| w(j\omega) \|'_1$$

and when $\| w(j\omega) \|'_1 \leq 1$,

$$\leq \frac{1}{2\pi} \| T_{zw}(j\omega) \|_B$$

so that

$$\begin{aligned} \| z(t) \|_{\infty} &\leq \frac{1}{2\pi} \| T_{zw}(j\omega) \|_B \quad \forall w \in \mathcal{D}_w^{(1)} \\ \Rightarrow \sup_{w \in \mathcal{D}_w^{(1)}} \| z(t) \|_{\infty} &\leq \frac{1}{2\pi} \| T_{zw}(j\omega) \|_B \end{aligned}$$

To show that equality holds in the above inequality, suppose that

$$\| (T_{zw}(s))_{ij} \|_{\infty} > \lambda_{ij}$$

which clearly implies that

$$\| T_{zw}(s) \|_B > \max_i \sum_{j=1}^n \lambda_{ij}$$

Then there are subsets $\Omega_{ij} \subset \mathcal{R}$ such that

$$|(T_{zw}(j\omega))_{ij}| > \lambda_{ij} \quad \text{when } \omega \in \Omega_{ij}$$

where

$$\int_{\Omega_{ij}} d\omega = \mu_{ij}$$

are strictly positive. Fix i for the moment. Define

$$\hat{w}_j(j\omega) = \begin{cases} \mu_{ij}^{-1} \exp(-j\angle(T_{zw}(j\omega))_{ij}) & \text{for } \omega \in \Omega_{ij} \\ 0 & \text{otherwise} \end{cases}$$

Then, letting \widehat{z} be the output resulting from the input \widehat{w} ,

$$\begin{aligned} |\widehat{z}_i(t)|_{t=0} &= \frac{1}{2\pi} \sum_{j=1}^n \int_{-\infty}^{+\infty} (T_{zw}(j\omega))_{ij} \widehat{w}_j(j\omega) \exp(j\omega t) d\omega \\ &= \frac{1}{2\pi} \sum_{j=1}^n \frac{1}{\mu_{ij}} \int_{\Omega_{ij}} |(T_{zw}(j\omega))_{ij}| d\omega \\ &> \frac{1}{2\pi} \sum_{j=1}^n \frac{\lambda_{ij}}{\mu_{ij}} \int_{\Omega_{ij}} d\omega = \frac{1}{2\pi} \sum_{j=1}^n \lambda_{ij} \end{aligned}$$

Since i was arbitrary, whenever

$$\|T_{zw}(s)\|_B > \max_i \sum_{j=1}^n \lambda_{ij}$$

one has

$$\sup_{w \in \mathcal{D}_w^{(1)}} \|z(t)\|_\infty \geq \|\widehat{z}(t)\|_\infty \geq \max_i |\widehat{z}(t)|_{t=0} > \frac{1}{2\pi} \max_i \sum_{j=1}^n \lambda_{ij}$$

This shows that

$$\Rightarrow \sup_{w \in \mathcal{D}_w^{(1)}} \|z(t)\|_\infty \geq \frac{1}{2\pi} \|T_{zw}(s)\|_B$$

completing the proof.

Loosely speaking, the essential idea behind this proof is that by allowing each $w_j(j\omega)$ to approach an impulse function in the frequency domain, equality can be approached arbitrarily closely, establishing part (3). Again, the crucial point is that different frequencies may be required for each j in $w_j(j\omega) \rightarrow \delta(\omega - \omega_{0j})$.

To verify part (4), consider again a $w(t)$ in $\mathcal{D}_w^{(1)}$. This input gives rise to the output

$$z_i(j\omega) = \sum_{j=1}^n (T_{zw}(j\omega))_{ij} w_j(j\omega), \quad i = 1, \dots, m$$

so that

$$\begin{aligned} \max_i \|z_i(j\omega)\|_1 &= \max_i \int_{-\infty}^{+\infty} \left| \sum_{j=1}^n (T_{zw}(j\omega))_{ij} w_j(j\omega) \right| d\omega \\ &\leq \max_i \sum_{j=1}^n \int_{-\infty}^{+\infty} |(T_{zw}(j\omega))_{ij} w_j(j\omega)| d\omega \\ &\leq \max_i \sum_{j=1}^n \| (T_{zw}(j\omega))_{ij} \|_\infty \|w_j(j\omega)\|_1 \end{aligned}$$

$$\leq \max_i \sum_{j=1}^n \| (T_{zw}(j\omega))_{ij} \|_{\infty} \max_j \| w_j(j\omega) \|_1$$

$$\Rightarrow \| z(j\omega) \|'_1 \leq \| T_{zw}(j\omega) \|_B \| w(j\omega) \|'_1$$

and when $w(j\omega) \in \mathcal{D}_w^{(1)}$,

$$\leq \| T_{zw}(j\omega) \|_B \quad \forall w(j\omega) \in \mathcal{D}_w^{(1)}$$

$$\Rightarrow \sup_{w \in \mathcal{D}_w^{(1)}} \| z(j\omega) \|'_1 \leq \| T_{zw}(j\omega) \|_B$$

To show that this inequality is in fact an equality, suppose again that

$$\| (T_{zw}(s))_{ij} \|_{\infty} > \lambda_{ij}$$

As before, there are then subsets $\Omega_{ij} \subset \mathcal{R}$ such that

$$|(T_{zw}(j\omega))_{ij}| > \lambda_{ij} \quad \text{when } \omega \in \Omega_{ij}$$

where

$$\int_{\Omega_{ij}} d\omega = \mu_{ij}$$

are strictly positive. Fix i for the moment. Define

$$\widehat{w}_j(j\omega) = \begin{cases} \exp(-j\angle(T_{zw}(j\omega))_{ij})/\mu_{ij} & \text{for } \omega \in \Omega_{ij} \\ 0 & \text{otherwise} \end{cases}$$

and let \widehat{z} be the output resulting from this input. Then

$$\| \widehat{z}_i(j\omega) \|_1 = \int_{-\infty}^{+\infty} \left| \sum_{j=1}^n (T_{zw}(j\omega))_{ij} \widehat{w}_j(j\omega) \right| d\omega$$

$$= \int_{-\infty}^{+\infty} \sum_{j=1}^n |(T_{zw}(j\omega))_{ij} \widehat{w}_j(j\omega)| d\omega$$

$$= \sum_{j=1}^n \frac{1}{\mu_{ij}} \int_{\Omega_{ij}} |(T_{zw}(j\omega))_{ij}| d\omega$$

$$> \sum_{j=1}^n \frac{\lambda_{ij}}{\mu_{ij}} \int_{\Omega_{ij}} d\omega = \sum_{j=1}^n \lambda_{ij}$$

Since i was arbitrary,

$$\| \widehat{z}(j\omega) \|'_1 > \max_i \sum_{j=1}^n \lambda_{ij}$$

Hence, whenever

$$\|T_{zw}(s)\|_B > \max_i \sum_{j=1}^n \lambda_{ij}$$

we have

$$\sup_{w \in \mathcal{D}_w^{(1)}} \|z(j\omega)\|_1' \geq \|\hat{z}(j\omega)\|_1' > \max_i \sum_{j=1}^n \lambda_{ij}$$

so that

$$\sup_{w \in \mathcal{D}_w^{(1)}} \|z(j\omega)\|_1' \geq \|T_{zw}(s)\|_B$$

which completes the proof.

Note that as before only item (2) requires $T_{zw}(j\omega)$ to be continuous in ω . \square

Item (3) in this theorem shows that the B norm may be viewed as a semi-induced norm. As such, it uses the max-amplitude norm on the output side, so that time domain ‘spikes’ are avoided, and the B norm non-conservatively treats maximum tracking errors in the time domain. Both signal set lumping and specification lumping are avoided by the use of the \mathcal{L}_∞ vector norm. Item (4) shows that the B norm can just as well be viewed as an induced norm, thus permitting the application of the SGT to system uncertainty issues. Note that the quantity to be minimized is exactly the usual \mathcal{H}_∞ norm of $T_{zw}(s)$ in the SISO case, but is different in the MIMO case. So the expression of eqn. (3.9) defines a new \mathcal{H}_∞ type minimization problem for MIMO systems.

The observations in this theorem motivate the optimal controller synthesis problem of choosing K to minimize the closed loop system’s B norm. To the author’s knowledge, this synthesis problem has not been tackled at an analytical level – various methods are available for obtaining sub-optimal solutions however. In Chapter 4 a decoupling design procedure is presented which is used with \mathcal{H}_∞ loopshaping techniques in Chapter 5 to minimise the B norm for a realistic design example. Alternatively the convex optimization approach of Boyd *et al.* [55, 56, 6] would seem to be an attractive option for obtaining (nearly) optimal solutions numerically. Since the problem is a convex problem (after appealing to the Youla parameterization [68]), it can be tackled numerically. Indeed, combinations of specifications drawn from all the approaches discussed in this paper can be effectively tackled in such a numerical paradigm. Nonetheless, the optimal synthesis problem of minimizing the B norm is an important open problem. Some potentially useful progress has been made in

this direction at an analytical level in the case of SISO plants [57], while numerical approaches to the problem are being pursued in [58].

3.5 MIMO Robust Stability in \mathcal{H}_∞

Item (4) of the above theorem says that the proposed norm may be viewed as an induced norm, with the same norm in the numerator and denominator. It follows that the SGT may be used to obtain sufficient conditions for robust stability. As usual, we restrict our attention to unstructured uncertainty. Thus, define

$$\mathcal{D}_{\Delta_P}^{(1)} = \{\Delta_P(j\omega) \mid \Delta_P(j\omega) \text{ is B-stable, LTI, and } \|\Delta_P(j\omega)\|_B \leq 1\}$$

In this uncertainty set, Δ_P is constrained only by a single induced norm bound. Applying the SGT to the set-up of Figure 1.5, and specializing to the signal norm $\|\cdot\|_1'$, establishes the following.

Theorem 3.3 *Suppose that the system of Figure 1.5 is nominally stable. If*

$$\|T_{ri}(s)\|_B < \alpha$$

then the system of Figure 1.5 is BIBO stable for every LTI $\Delta_P(j\omega)$ which obeys

$$\|\Delta_P(j\omega)\|_B = \sup_{a \neq 0} \frac{\|\Delta_P(j\omega)a(j\omega)\|_1'}{\|a(j\omega)\|_1'} \leq \alpha^{-1}$$

This theorem guarantees robust stability for uncertainty sets of the form $\mathcal{D}_{\Delta_P}^{(1)}$ above. It is unclear at present if the condition $\|T_{ri}(s)\|_B < 1$ is necessary as well as sufficient for robust stability with this uncertainty set. So the converse is an open problem. To prove necessity, one would need to exhibit a destabilizing Δ_P when $\|T_{ri}(s)\|_B \geq 1$. It seems likely that the converse is true, but only if NL and/or TV Δ_P 's are considered, as in

$$\hat{\mathcal{D}}_{\Delta_P}^{(1)} = \{\Delta_P \mid \Delta_P \text{ is stable, and } \|\Delta_P\|_B \leq 1\}$$

The observation in this theorem also motivates the optimal controller synthesis problem of minimizing the system norm $\|T_{zw}(s)\|_B$.

3.6 A New Approach to \mathcal{H}_∞ Weighting Function Selection

The issue of weighting function selection in standard \mathcal{H}_∞ control theory was discussed at length in Chapter 2. In this section we examine the implications of the modified \mathcal{H}_∞ control theory presented above for weighting function selection. In particular we focus on the distinct roles played by weighting functions on the ‘input’ and ‘output’ sides of the system.

One of the most fundamental ideas in robust control theory is to formulate the controller design problem as a mathematical optimization problem. In order to obtain optimization problems for controller design, i.e. problems which are sufficiently precise to lead to well-defined mathematical optimization problems, two basic issues need to be settled. Firstly, the intuitive notion of the ‘size’ of the signal to be minimized must be formalized, and secondly the set of possible uncertain inputs must be formally stated. The combination of a signal norm plus a weighting transfer function can be used for both of these purposes, and these two roles for norms and weights are then quite distinct. This distinction becomes more explicit, if we consider Figure 3.1 below.

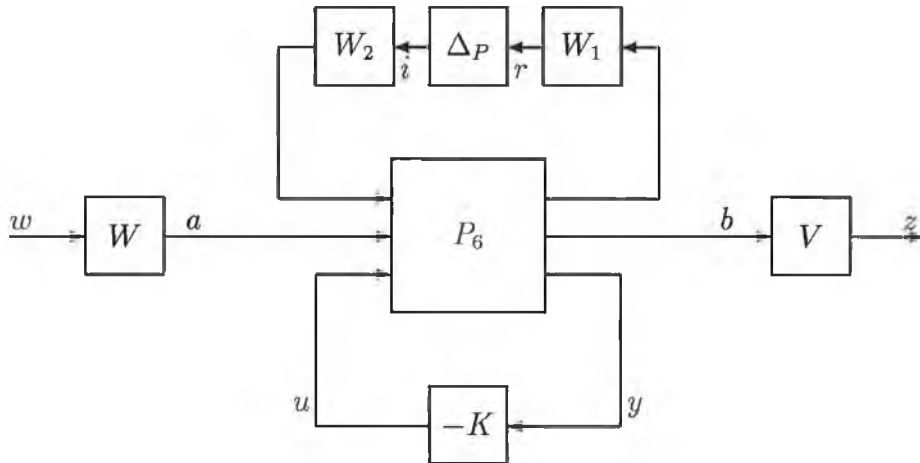


Figure 3.1: The Canonical Form with extracted weights

The figure shows the canonical form for linear controller design given in Figure 1.3 of Chapter 1 – in this representation however, weighting functions are extracted from the augmented plant. It is important to distinguish between the physical interpretation

of the signals w and a in the above representation. In applications, uncertain input signals generally correspond to sensor or measurement noise and to external disturbances acting on the plant. It is the signal a in Figure 3.1 which represents such signals. So it is the set \mathcal{D}_a , and not \mathcal{D}_w , which represents the engineer's judgement on what the sensor noise, external disturbance and command inputs are likely to be, or which class of them s/he wants the system to be optimized for. These inputs then give rise to non-zero tracking errors, non-zero actuator inputs, etc., and the objective of the controller is to keep the size of this output signal as small as possible. Again, it is important to distinguish between the physical interpretation of the signals z and b . It is the signal b which represents such output signals, i.e. the signals in the system which the controller seeks to minimize. The weighting transfer function V allows for extra flexibility in quantifying the size of b . As is well known, keeping the size of different signals small are often conflicting requirements, and V allows different signals to be differentially emphasized. Also, keeping the low and high frequency components of a signal small necessarily involves tradeoffs, and V may be used to place a different degree of emphasis on distinct frequency ranges. The transfer function from a to b will be denoted by T_{ba} . Then clearly,

$$T_{zw} = VT_{ba}W$$

The distinction between the roles of norms and weighting functions on the input and output sides now becomes more apparent. The output side norm together with the weight V is used to quantify the size of b , and so to formalize the precise sense in which the signal b is to be minimized. This raises the questions of which norm is best applied to the signal z and how to choose the weight V . The issue here is that of modelling the objectives and purpose of the control system.

On the other hand, the combination of the input side norm and input side weight W is used to formally specify the signal set \mathcal{D}_a . Again, this raises the question of how to choose this norm and weight. The issue here is that of modelling the uncertain input signals to the system w . In the presence of unstructured system uncertainty, norms and weights play a third role, that of modelling the uncertainty present in the plant model, or of quantifying the level of validity of the plant model.

Two important issues are now apparent. The first is how to choose which norms to use, and it is here that the fundamental differences between the \mathcal{H}_∞ and the \mathcal{L}_1 theories arise, and between other alternatives. This issue has been discussed in detail in the prequel. Indeed the results presented already in this chapter demonstrate that

the use of different norms can give theories with remarkably different properties. The second is the problem of weight selection. This issue will be discussed in the following paragraphs.

Note that, in particular, the weights W and V play very different roles, a point which perhaps deserves to be more widely appreciated. As compared with Figure 1.3, Figure 3.1 makes this distinction much clearer. A particularly important difference between input and output side weights is that for MIMO systems with diagonal weighting function matrices each element of the output weight V_{ii} affects only the corresponding element of the output signal. In contrast, each element of the input weight W_{ii} affects every element in the output signal. A fundamental implication of the above discussion is that the current practice in \mathcal{H}^∞ design of placing a single weighting function on the output side only is flawed, since it unnecessarily gives up design freedom. If the weights are to be regarded as models of exogenous inputs, only weights on the input side can capture this physical reality.

Consider therefore the following approach. Let the weighting function W be viewed as a fixed model of possible disturbance and noise inputs. The output weighting function V may then be used to examine and tune the relative quality of control of each individual element of the output, and to manage the tradeoffs between them. So V enables each output signal z_i to be weighted separately, allowing the relative importance of each to be traded off by tuning the appropriate diagonal element of V . Note that this approach is much more practical under the modified \mathcal{H}_∞ control theory presented in this chapter, since the proposed manipulation of V is made simpler by the absence of specification lumping. The relationship between the elements of a diagonal V and each element of z is more transparent, and thus the ‘gap’ between the design parameters and specifications is narrowed.

Similarly, the use of both input and output weighting functions W_1 and W_2 in our model of plant uncertainty allows extra design flexibility, especially in the MIMO case. This approach to weighting function selection in the modified \mathcal{H}_∞ control theory would then naturally lead to mixed sensitivity \mathcal{H}_∞ optimisation problems of the form

$$\inf_K \| J(s) \|_B$$

where the infimum is over all LTI stabilizing controllers, and J is a matrix cost function given by

$$J = \begin{pmatrix} V_S(s)S_o(s)W_S(s) & V_T(s)T_o(s)W_T(s) \end{pmatrix}$$

The proposed approach provides a physical basis for the selection/manipulation of weighting functions. It has been shown that this cannot be sensibly done with the energy paradigm for standard \mathcal{H}^∞ control theory. It is felt that future progress in this area should allow the accomodation of (a) a more accurate statement of the ‘real’ objectives of the control system, (b) more refined models of plant uncertainty (i.e. structured system uncertainty), and, (c) more accurate models of classes of input disturbance/noise signals (i.e. more structured signal uncertainty). In other words, an improved theory should cope with improved models on both the input side and the output side.

3.7 Robust Performance and Relations with Standard \mathcal{H}_∞ Theory

It is too early to comment on the issue of robust performance in the modified \mathcal{H}_∞ theory proposed. Even the most obvious questions concerning robust performance in the presence of system uncertainty, whether structured or unstructured, are entirely open, in both analysis and synthesis.

It is however interesting to note that the standard \mathcal{H}_∞ norm and the B norm are closely related, and cannot be very far apart. This fact may be formally stated as follows.

Theorem 3.4 *Suppose that $z(j\omega) = T_{zw}(j\omega)w(j\omega)$, and that $T_{zw}(s)$ is the transfer function matrix of a stable $m \times n$ LTI system. Then*

$$\frac{1}{m} \| T_{zw}(s) \|_\infty \leq \| T_{zw}(s) \|_B \leq n \| T_{zw}(s) \|_\infty \quad (3.10)$$

Proof

It is well known [71], that

$$\begin{aligned} \max_i \max_j \sup_\omega | (T_{zw})_{ij}(j\omega) | &\leq \sup_\omega \bar{\sigma}(T_{zw}(j\omega)) \leq n \times \max_i \max_j \sup_\omega | (T_{zw})_{ij}(j\omega) | \\ \Rightarrow \frac{1}{m} \max_i \sum_{j=1}^m \| (T_{zw})_{ij}(j\omega) \|_\infty &\leq \| T_{zw}(j\omega) \|_\infty \leq n \times \max_i \sum_{j=1}^m \| (T_{zw})_{ij}(j\omega) \|_\infty \\ \Rightarrow \frac{1}{m} \| T_{zw}(j\omega) \|_B &\leq \| T_{zw}(j\omega) \|_\infty \leq n \| T_{zw}(j\omega) \|_B \end{aligned}$$

□

The above bounds are the best possible for an arbitrary $T_{zw}(s)$ in \mathcal{H}^∞ . When these bounds are used to show that standard \mathcal{H}_∞ optimal controllers do not suffer from ‘spikes’, eqn. (3.10) does much better than eqn. (2.6).

3.8 Nominal Performance in \mathcal{H}_2 : Non-Conservative Minimisation of Maximum Tracking Errors in the Time Domain

In previous sections, it was shown that by choosing novel signal sets to model uncertain input signals, a slightly modified \mathcal{H}_∞ control theory can be used to non-conservatively minimize maximum tracking errors in the time domain. It was seen that the resulting optimization problem is the standard \mathcal{H}_∞ control problem in the SISO case, and a slight variation on the standard problem in the MIMO case. In this section, it is shown that analogous observations apply to signal uncertainty in \mathcal{H}_2 control theory. However, the situation with system uncertainty in \mathcal{H}_2 is fundamentally different.

3.8.1 The SISO Case: A Solved Problem

The system norm used in standard \mathcal{H}_2 control theory is

$$\|T_{zw}(s)\|_2 = \sqrt{\frac{1}{2\pi} \int_{-\infty}^{+\infty} |T_{zw}(j\omega)|^2 d\omega} \quad (\text{SISO}) \quad (3.11)$$

$$\begin{aligned} \|T_{zw}(s)\|_2 &= \sqrt{\frac{1}{2\pi} \int_{-\infty}^{+\infty} \text{Trace}(T_{zw}^*(j\omega)T_{zw}(j\omega))d\omega} \quad (\text{MIMO}) \quad (3.12) \\ &= \sqrt{\frac{1}{2\pi} \int_{-\infty}^{+\infty} \sum_{i=1}^n \sum_{j=1}^n |(T_{zw}(j\omega))_{ij}|^2 d\omega} \quad (\text{MIMO}) \end{aligned}$$

With reference to Figure 1.4, the problem treated by standard \mathcal{H}_2 -control theory is then

$$\inf_K \|T_{zw}(s)\|_2$$

where the infimum is over all LTI stabilizing controllers, and this is a solved problem [13, 44]. The engineering motivation for this problem is generally given in terms of a signal input class which is viewed as a stochastic process [59]. Although deterministic justifications can be provided, they are unconvincing in the MIMO case.

Consider the following lemma [60, 74], which is valid for the SISO case only.

Lemma 3.5 *Suppose that $z(j\omega) = T_{zw}(j\omega)w(j\omega)$, and that $T_{zw}(s)$ is the transfer function of a stable LTI system which is SISO. Then*

$$\|T_{zw}(s)\|_2 = \sup_{w \neq 0} \frac{\|z(t)\|_\infty}{\|w(j\omega)\|_2} = \sup_{w \in \mathcal{BL}_2(j\omega)} \|z(t)\|_\infty$$

This lemma says that the \mathcal{H}_2 system norm is a semi-induced norm, with the \mathcal{L}_∞ signal norm on the numerator or output side. Thus, in the SISO case \mathcal{H}_2 control theory already non-conservatively minimizes maximum errors in the time domain, provided the exogenous input $w(j\omega)$ is viewed as ranging through the signal set $\mathcal{D}_w^{(e)} = \mathcal{BL}_2(j\omega)$. This lemma is described in [60, 74] for the SISO case only, and it does not seem to have a natural extension to the MIMO case which corresponds to the standard \mathcal{H}_2 norm of eqn. (3.12).

3.8.2 An Extension to the MIMO Case

In keeping with the philosophy of this thesis, we now show that an alternative class of signal sets overcomes the above difficulty with \mathcal{H}_2 control theory. Specifically, we extend the above lemma to the MIMO case in a manner which avoids specification and signal set lumping, and which non-conservatively handles maximum tracking errors in the time domain, as follows. Define $\mathcal{D}_w^{(3)}$ to be the signal set

$$\mathcal{D}_w^{(3)} = \{w(j\omega) = (w_1(j\omega), \dots, w_n(j\omega))^T \mid \|w_i(j\omega)\|_2 \leq 1, i = 1, \dots, n\} \quad (3.13)$$

It is convenient to define the following norm for vector signals

$$\|w(j\omega)\|_2' = \max_i \|w_i(j\omega)\|_2 \quad (3.14)$$

This norm is obtained by taking the \mathcal{L}_2 norm of each element of the vector signal, and then the \mathcal{L}_∞ norm with respect to vector elements. The signal set $\mathcal{D}_w^{(3)}$ is the unit ball with respect to this norm. Define the following system norm

$$\|T_{zw}(j\omega)\|_C = \max_i \sum_{j=1}^n \|(T_{zw}(j\omega))_{ij}\|_2 \quad (3.15)$$

which will be referred to as the **C norm**. This norm involves taking the \mathcal{L}_2 norm of each element of $T_{zw}(s)$ before applying the max-row-sum matrix norm. The appropriate MIMO extension of the above lemma is then as follows.

Theorem 3.5 *Suppose that $z(j\omega) = T_{zw}(j\omega)w(j\omega)$, and that $T_{zw}(s)$ is the transfer function matrix of a stable $m \times n$ LTI system. Then*

$$\|T_{zw}(s)\|_C = \sup_{w \neq 0} \frac{\|z(t)\|_\infty}{\|w(j\omega)\|_2'} = \sup_{w \in \mathcal{D}_w^{(3)}} \|z(t)\|_\infty$$

where $\mathcal{D}_w^{(3)}$, $\|\cdot\|_2'$ and $\|\cdot\|_C$ are defined in eqns. (3.13), (3.14) and (3.15) respectively.

Proof

The output vector z is given by

$$z_i(j\omega) = \sum_{j=1}^n (T_{zw}(j\omega))_{ij} w_j(j\omega), \quad i = 1, \dots, m$$

Inverse Fourier transforming gives

$$\Rightarrow |z_i(t)| = \frac{1}{2\pi} \left| \sum_{j=1}^n \int_{-\infty}^{+\infty} (T_{zw}(j\omega))_{ij} w_j(j\omega) e^{j\omega t} d\omega \right|$$

and using well known inequalities,

$$\begin{aligned} &\leq \frac{1}{2\pi} \sum_{j=1}^n \int_{-\infty}^{+\infty} |(T_{zw}(j\omega))_{ij} w_j(j\omega) e^{j\omega t}| d\omega \\ &\leq \sum_{j=1}^n \|(T_{zw}(j\omega))_{ij}\|_2 \|w_j(j\omega)\|_2 \end{aligned}$$

Since this holds for all i and all t ,

$$\Rightarrow \|z(t)\|_\infty \leq \max_i \sum_{j=1}^n \|(T_{zw}(j\omega))_{ij}\|_2 \max_j \|w_j(j\omega)\|_2$$

When $w(j\omega) \in \mathcal{D}_w^{(3)}$,

$$\leq \max_i \sum_{j=1}^n \|(T_{zw}(j\omega))_{ij}\|_2 = \|T_{zw}(s)\|_C$$

so that

$$\|z(t)\|_\infty \leq \|T_{zw}(j\omega)\|_C \quad \forall w \in \mathcal{D}_w^{(3)}$$

$$\Rightarrow \sup_{w \in \mathcal{D}_w^{(3)}} \|z(t)\|_\infty \leq \|T_{zw}(j\omega)\|_C$$

To show that equality in the above expression can be attained, fix i for the moment and define $\hat{w}(j\omega)$ by

$$\hat{w}_j(j\omega) = (T_{zw}(j\omega))_{ij}^* / \|(T_{zw}(j\omega))_{ij}\|_2, \quad j = 1, \dots, n$$

which is clearly in $\mathcal{D}_w^{(3)}$. Then, letting $\hat{z}(t)$ be the output resulting from this input,

$$\begin{aligned} \hat{z}_i(t) &= \frac{1}{2\pi} \sum_{j=1}^n \int_{-\infty}^{+\infty} (T_{zw}(j\omega))_{ij} \hat{w}_j(j\omega) \exp(j\omega t) d\omega \\ &= \frac{1}{2\pi} \sum_{j=1}^n \int_{-\infty}^{+\infty} (T_{zw}(j\omega))_{ij} \frac{(T_{zw}(j\omega))_{ij}^*}{\|(T_{zw}(j\omega))_{ij}\|_2} \exp(j\omega t) d\omega \\ &\Rightarrow |\hat{z}_i(t)|_{t=0} = \sum_{j=1}^n \|(T_{zw}(j\omega))_{ij}\|_2 \end{aligned}$$

Since i was arbitrary,

$$\begin{aligned} \sup_{w \in \mathcal{D}_w^{(3)}} \|z(t)\|_\infty &\geq \|\hat{z}(t)\|_\infty = \max_i \sum_{j=1}^n \|(T_{zw}(j\omega))_{ij}\|_2 \\ &= \|T_{zw}(s)\|_C \end{aligned}$$

completing the proof. \square

As with the earlier modified formulation of the MIMO \mathcal{H}_∞ problem, one is led to an optimization problem which is a slight variation on the standard or classical \mathcal{H}_2 control problem in the MIMO case, and which is identical to the standard problem in the SISO case.

This theorem shows that a slight modification to the standard \mathcal{H}_2 norm leads to a quite attractive approach to controller design. Minimizing the C norm corresponds to optimally and non-conservatively minimizing maximum tracking errors in the time domain. Specification and signal set lumping are avoided. The approach can be viewed as a frequency domain theory. It can reasonably be called ‘max-row-sum \mathcal{H}_2 control theory’.

3.9 Robust Specifications in \mathcal{H}_2

A significant limitation of the \mathcal{H}_2 system norm, whether the standard one or the above modified one, is that it is not an induced norm. The C norm is merely a semi-induced norm, and the standard \mathcal{H}_2 norm is not even a semi-induced norm in the MIMO case. This means that the SGT does not apply. The important consequence of this is that robust stability and robust performance issues cannot be treated in this norm.

Consequently, to handle robust stability and robust performance specifications, it is necessary to use mixed norms. In other words, using norms which are a mixture of the \mathcal{H}_2 norm and some other distinct norm or norms becomes unavoidable. This is a large part of the motivation behind the study of mixed $\mathcal{H}_2/\mathcal{H}_\infty$ optimal synthesis problems, and there is a literature on such problems. With reference to Figure 1.3, one approach is to attempt to minimize the nominal \mathcal{H}_2 norm of $T_{zw}(s)$ subject to a constraint on the infinity norm of $T_{ri}(s)$. This approach is studied in [61]. In [62], this approach is extended to robust performance. In both references, the results are sub-optimal. The optimal synthesis of mixed $\mathcal{H}_2/\mathcal{H}_\infty$ problems which avoid signal set lumping, i.e. involving the above C norm, is a family of open problems.

One can consider mixed norm problems much more generally. Mixed $\mathcal{H}_\infty/\mathcal{L}_1$ problems are considered in [63], but the \mathcal{H}_∞ norm used is the standard one. The observations of this paper suggest that it may be worthwhile to extend this line of development ([61, 62, 63], and references therein) by considering combinations of A norm and/or B norm and/or C norm specifications. Of course, finding analytical solutions to such problems is likely to be extremely difficult.

Chapter 4

A Decoupling Design Method for Super-Optimal Robust Control

This chapter presents a decoupling design method for optimal robust multivariable controller synthesis. It is shown that for square, stable plants which are minimum-phase, the solutions of n independent SISO problems yield one of many optimal solutions to the $n \times n$ MIMO controller synthesis problem. The proposed approach to the multivariable design problem fully decouples the system, significantly improves design transparency, and results in controllers which can rightly be considered super-optimal. The above result holds for the standard \mathcal{H}_∞ and \mathcal{L}_1 control problems, as well as for the modified \mathcal{H}_∞ problem presented in Chapter 3. For square, stable plants which are non-minimum-phase, the solutions of n independent MISO problems yield one of many optimal solutions to the $n \times n$ MIMO problem, under the \mathcal{L}_1 and modified \mathcal{H}_∞ problem formulations. The resulting controller half decouples the system and is super-optimal. It is shown that for the standard \mathcal{H}_∞ control problem the resulting controller is sub-optimal.

4.1 Motivation for Decoupling the Design Process

Ever since the multivariable control problem has been studied, designers have sought ways of avoiding its inherent complexities by seeking to decouple or diagonalise the system, thus allowing the calculation of SISO controllers on a loop by loop basis. This goal has led to the development and widespread use of formalised design procedures such as the Inverse Nyquist Array and Characteristic Loci [72]. As is well known however, limitations of these techniques include their somewhat heuristic nature, and the underlying assumption that the plant in question has an inherent degree of diagonal dominance. The advent of robust control theory in the early 1980's revealed an even more serious problem, namely the absence of an explicit and satisfactory acknowledgement of the importance of plant uncertainty and other robustness issues. Recognition of the fundamental importance of these issues led to the development of robust controller design techniques such as \mathcal{H}_∞ control theory and \mathcal{L}_1 control theory. One of the greatest benefits of these design procedures is that they are truly multivariable in nature. Thus, in the context of robust control theory it is certainly no longer *necessary* to decouple the system in order to achieve satisfactory designs. In this section it is argued however, that compelling reasons still exist for decoupling multivariable robust control problems (when and if this is possible), so that design can be undertaken on a SISO loop by loop basis.

Firstly, consider the problem of weighting function selection. Current multivariable design techniques require the selection and subsequent manipulation of transfer function weighting matrices. As argued in Chapter 2 however, the relation between these matrices and the resulting 'optimal' design is far from transparent. Various design issues, such as those due to right half plane poles and zeros, impose some fairly complicated tradeoff limitations. From the viewpoint of the engineer the prospect of choosing, let alone iteratively manipulating a 7×7 matrix of interdependent transfer functions for example, is certainly a daunting one. Thus an obvious advantage of decoupling the design process is that it simplifies this task, since independent weighting transfer functions can be chosen one at a time for each loop of the system.

Secondly there is the problem of signal set and specification lumping. As observed in Chapter 2, this problem occurs in multivariable \mathcal{H}_∞ control theory due to the fact that specifications relating to both the exogenous inputs to the system w , and

the regulated variables z , are given in terms of the vector \mathcal{L}_2 norm. Consider for instance a plant with several outputs. Information on the value of each output is produced via measurements from *independent* sensors or transducers - imperfections in these measurements are then generally modelled as additive noise and included in the vector of exogenous inputs w . Other elements of the vector w may be due to unknown external disturbances acting on each plant input or output, and again these disturbances may be totally independent of each other. Lumping each of these signals into a single vector w with $\|w(j\omega)\|_2 \leq 1$ creates an artificial interdependence between each element of w which is conservative and highly undesirable. Similar remarks apply to the output side. In practice, different regulated variables may need to be controlled to different levels of precision. Minimising $\|z(j\omega)\|_2$ involves averaging over distinct plant outputs, over frequency and over vector directions, and thus obscures which loops of the system are or are not being effectively controlled. One way of avoiding signal set and specification lumping is to formulate the new \mathcal{H}_∞ control problem presented in Chapter 3. Alternatively, in certain limited cases the design process can be decoupled and solved one loop at a time.

A third advantage of decoupling the design process is that the focus of attention is not fixed exclusively on the ‘worst’ loop of the system. In standard \mathcal{H}_∞ control for example, the objective is to minimise the maximum singular value of some matrix cost function J . In general however this objective may be achieved by a set of controllers, and thus a certain amount of design freedom is wasted if we simply select one of these controllers at random. This ‘extra’ design freedom has been studied in the literature on super-optimal \mathcal{H}_∞ control [64, 65, 66, 67] in order to calculate a controller which minimises *all* of the singular values of J . Since this chapter considers three different robust control problem formulations, we will use the following definition of super-optimality in terms of the output vector of regulated variables z , this being appropriate in the present context. *A super-optimal robust controller must minimise (according to the appropriate norm) not just the largest z_i but also the second largest, the third largest, etc.* This chapter will show that under certain assumptions robust control theory naturally allows the development of decoupling design techniques which result in super-optimal controllers.

Finally, the ability to design for robustness on a loop by loop basis means that the designer can subsequently apply classical frequency or time domain design techniques to further shape any individual loop of the system.

4.2 Three Robust Control Problem Formulations

In this section we define the three problem formulations addressed in this chapter. We first of all define the mixed sensitivity matrix cost function J , given by

$$J(s) = \begin{pmatrix} W_S(s)S_o(s) & W_T(s)T_o(s) \end{pmatrix}$$

where S_o and T_o are the sensitivity and complementary sensitivity function matrices respectively. With respect to this cost function the three optimal controller synthesis problems considered in this chapter are as follows.

1. The Mixed Sensitivity \mathcal{H}_∞ Control Problem given by

$$\inf_K \|J(s)\|_\infty$$

where the infimum is over all LTI stabilizing controllers.

2. The Mixed Sensitivity Modified \mathcal{H}_∞ Control Problem given by

$$\inf_K \|J(s)\|_B$$

where the infimum is over all LTI stabilizing controllers, and the B norm is as defined in Chapter 3.

3. The Mixed Sensitivity \mathcal{L}_1 Control Problem given by

$$\inf_K \|\hat{J}\|_A$$

where the infimum is over all LTI stabilizing controllers.

4.3 Full Decoupling and Super-Optimality: the Minimum-Phase Case

In this section the framework of the Youla parameterisation of all stabilising controllers [68] is used to show that for a square stable plant P which is also minimum-phase, the three multivariable controller design problems defined above decouple completely into n independent SISO optimisation problems. The solutions to these n optimisation problems yield super-optimal controllers for each of the three problem formulations. We will need the following lemma.

Lemma 4.1 Let $A_1 = (a^{(1)} \dots a^{(p)})$ be a block partitioned matrix, and let $A_2 = (\text{diag}(a^{(1)}) \dots \text{diag}(a^{(p)}))$ be its block diagonal equivalent. Thus

$$A_1 = \begin{pmatrix} a_{11}^{(1)} & \dots & a_{1n}^{(1)} & \dots & a_{11}^{(p)} & \dots & a_{1n}^{(p)} \\ a_{21}^{(1)} & \dots & a_{2n}^{(1)} & \dots & a_{21}^{(p)} & \dots & a_{2n}^{(p)} \\ \vdots & \vdots & \vdots & \dots & \vdots & \vdots & \vdots \\ a_{n1}^{(1)} & \dots & a_{nn}^{(1)} & \dots & a_{n1}^{(p)} & \dots & a_{nn}^{(p)} \end{pmatrix}$$

and

$$A_2 = \begin{pmatrix} a_{11}^{(1)} & 0 & \dots & 0 & \dots & a_{11}^{(p)} & 0 & \dots & 0 \\ 0 & a_{22}^{(1)} & \dots & 0 & \dots & 0 & a_{22}^{(p)} & \dots & 0 \\ \vdots & \vdots & \vdots & \dots & \vdots & \vdots & \vdots & \vdots & \vdots \\ 0 & 0 & \dots & a_{nn}^{(1)} & \dots & 0 & 0 & \dots & a_{nn}^{(p)} \end{pmatrix}$$

Then

$$\|A_1(j\omega)\|_\infty \geq \|A_2(j\omega)\|_\infty$$

Proof:

For any matrix A ,

$$\bar{\sigma}(A) = \max_{x \in \mathbb{C}^n, x \neq 0} \frac{\|x^* A\|_2}{\|x^*\|_2}$$

Thus

$$\bar{\sigma}(A_1) = \max_{x \in \mathbb{C}^n, x \neq 0} \frac{\|x^* A_1\|_2}{\|x^*\|_2}$$

so that

$$\bar{\sigma}(A_1) \geq \frac{\|x_i^* A_1\|_2}{\|x_i^*\|_2}$$

where x_i is any particular x . Let

$$x_i = \begin{pmatrix} 1 & 0 & 0 & 0 & \dots \end{pmatrix}^T$$

Then

$$\bar{\sigma}(A_1) \geq \frac{\left\| \begin{pmatrix} a_{11}^{(1)} & \dots & a_{1n}^{(1)} & \dots & a_{11}^{(p)} & \dots & a_{1n}^{(p)} \end{pmatrix} \right\|_2}{1}$$

$$\begin{aligned} \bar{\sigma}(A_1) &\geq \sqrt{\sum_{i=1}^p \sum_{j=1}^n |a_{1j}^{(i)}|^2} \\ &\geq \sqrt{|a_{11}^{(1)}|^2 + \dots + |a_{11}^{(p)}|^2} \end{aligned}$$

Now let

$$x_i = \begin{pmatrix} 0 & 1 & 0 & 0 & \dots \end{pmatrix}^T$$

Then

$$\bar{\sigma}(A_1) \geq \frac{\left\| \begin{pmatrix} a_{21}^{(1)} & \dots & a_{2n}^{(1)} & \dots & a_{21}^{(p)} & \dots & a_{2n}^{(p)} \end{pmatrix} \right\|_2}{1}$$

$$\begin{aligned} \bar{\sigma}(A_1) &\geq \sqrt{\sum_{i=1}^p \sum_{j=1}^n |a_{2j}^{(i)}|^2} \\ &\geq \sqrt{|a_{22}^{(1)}|^2 + \dots + |a_{22}^{(p)}|^2} \end{aligned}$$

and so on ...

Thus

$$\bar{\sigma}(A_1) \geq \max \begin{cases} \sqrt{|a_{11}^{(1)}|^2 + \dots + |a_{11}^{(p)}|^2} \\ \sqrt{|a_{22}^{(1)}|^2 + \dots + |a_{22}^{(p)}|^2} \\ \vdots \\ \vdots \end{cases}$$

Now since

$$\begin{aligned} \bar{\sigma}(A_2) &= \sqrt{\max \text{ eigenvalue of } A_2 A_2^*} \\ \bar{\sigma}(A_2) &= \max \begin{cases} \sqrt{|a_{11}^{(1)}|^2 + \dots + |a_{11}^{(p)}|^2} \\ \sqrt{|a_{22}^{(1)}|^2 + \dots + |a_{22}^{(p)}|^2} \\ \vdots \\ \vdots \end{cases} \end{aligned}$$

Thus

$$\begin{aligned} \bar{\sigma}(A_1) &\geq \bar{\sigma}(A_2) \\ \Rightarrow \sup_{\omega} \bar{\sigma}(A_1(j\omega)) &\geq \sup_{\omega} \bar{\sigma}(A_2(j\omega)) \\ \Rightarrow \|A_1(j\omega)\|_{\infty} &\geq \|A_2(j\omega)\|_{\infty} \end{aligned}$$

□

We can now state the main result of this section.

Theorem 4.1 *For a square, stable and minimum-phase multivariable plant P , the solutions of n independent SISO optimisation problems yield an optimal solution to the corresponding $n \times n$ MIMO problem, for each of the mixed sensitivity control problems defined above. In each case the resulting controller is super-optimal.*

Proof

Since the plant P is stable, the Youla parameter is given by

$$Q = (I + KP)^{-1}K \quad Q \in \mathcal{RH}^\infty$$

where

$$K = (I + QP)^{-1}Q$$

is any stabilising controller. Thus in terms of the Youla parameter, the mixed sensitivity matrix cost function J is given by

$$J = (W_S(I + QP) - W_TQP)$$

Now since the plant P is stable and minimum-phase, without loss of generality we can take P to be the identity matrix I , so that

$$J = (W_S(I + Q) - W_TQ) = \begin{pmatrix} (W_S)_{11}(1 + q_{11}) & (W_S)_{22}q_{12} & \dots & (W_S)_{nn}q_{1n} & -(W_T)_{11}q_{11} & \dots & -(W_T)_{nn}q_{1n} \\ (W_S)_{11}q_{21} & (W_S)_{22}(1 + q_{22}) & \dots & (W_S)_{nn}q_{2n} & -(W_T)_{11}q_{21} & \dots & -(W_T)_{nn}q_{2n} \\ \vdots & \vdots & \ddots & \vdots & \vdots & \ddots & \vdots \\ (W_S)_{11}q_{n1} & (W_S)_{22}q_{n2} & \dots & (W_S)_{nn}(1 + q_{nn}) & -(W_T)_{11}q_{n1} & \dots & -(W_T)_{nn}q_{nn} \end{pmatrix}$$

Now each q_{ij} is a free stable parameter. Thus observe that the structure of J above, allows us to choose a diagonal Youla parameter matrix Q , i.e. we can make the off diagonal elements q_{ij} $i \neq j$ equal to zero, leaving us with n independent SISO optimisation problems. The solutions to these n problems then form the diagonal of the Youla parameter matrix Q . We now show that this choice of Q yields an optimal controller for each of the three problems defined above.

In the case of the mixed sensitivity \mathcal{H}_∞ control problem the n independent optimisation problems become:

$$\inf_{q_{11}(j\omega) \in \mathcal{RH}^\infty} \| ((W_S)_{11}(j\omega)(1 + q_{11}(j\omega)) - (W_T)_{11}(j\omega)q_{11}(j\omega)) \|_\infty$$

$$\inf_{q_{22}(j\omega) \in \mathcal{RH}^\infty} \| ((W_S)_{22}(j\omega)(1 + q_{22}(j\omega)) - (W_T)_{22}(j\omega)q_{22}(j\omega)) \|_\infty$$

:

$$\inf_{q_{nn}(j\omega) \in \mathcal{RH}^\infty} \| ((W_S)_{nn}(j\omega)(1 + q_{nn}(j\omega)) - (W_T)_{nn}(j\omega)q_{nn}(j\omega)) \|_\infty$$

Now by Lemma 4.1, we have that the controller K corresponding to the above diagonal Youla parameter Q is an optimal solution of the mixed sensitivity \mathcal{H}_∞ control problem. It is also clear that this controller is super-optimal, according to our definition.

In the case of the mixed sensitivity modified \mathcal{H}_∞ control problem the n independent optimisation problems are:

$$\inf_{q_{11}(j\omega) \in \mathcal{RH}^\infty} \| (W_S)_{11}(j\omega)(1 + q_{11}(j\omega)) \|_\infty + \| (W_T)_{11}(j\omega)q_{11}(j\omega) \|_\infty$$

$$\inf_{q_{22}(j\omega) \in \mathcal{RH}^\infty} \| (W_S)_{22}(j\omega)(1 + q_{22}(j\omega)) \|_\infty + \| (W_T)_{22}(j\omega)q_{22}(j\omega) \|_\infty$$

:

$$\inf_{q_{nn}(j\omega) \in \mathcal{RH}^\infty} \| (W_S)_{nn}(j\omega)(1 + q_{nn}(j\omega)) \|_\infty + \| (W_T)_{nn}(j\omega)q_{nn}(j\omega) \|_\infty$$

It follows directly from the definition of the B norm that the corresponding controller K is an optimal solution of the mixed sensitivity modified \mathcal{H}_∞ control problem control problem, and that it is super-optimal, according to our definition.

In the case of the mixed sensitivity \mathcal{L}_1 Control Problem the optimisation problems are:

$$\inf_{\hat{q}_{11} \in \hat{A}} \| (\hat{W}_S)_{11}(1 + \hat{q}_{11}) \|_1 + \| (\hat{W}_T)_{11}\hat{q}_{11} \|_1$$

$$\inf_{\hat{q}_{22} \in \hat{A}} \| (\hat{W}_S)_{22}(1 + \hat{q}_{22}) \|_1 + \| (\hat{W}_T)_{22}\hat{q}_{22} \|_1$$

:

$$\inf_{\hat{q}_{nn} \in \hat{A}} \| (\hat{W}_S)_{nn}(1 + \hat{q}_{nn}) \|_1 + \| (\hat{W}_T)_{nn}\hat{q}_{nn} \|_1$$

Again optimality and super-optimality of the corresponding controller K follows directly from the definition of the A norm. \square

4.4 Half Decoupling: the Non-Minimum-Phase Case

In this section the Youla parameter and a version of a design method proposed in [69] are used to show that for square stable plants which are non-minimum-phase, the multivariable design problem decouples into n independent MISO optimisation problems. Optimal solutions to the $n \times n$ MIMO \mathcal{L}_1 and modified \mathcal{H}_∞ mixed sensitivity problems can be constructed from the solutions to these n MISO optimisation problems. It is shown that these optimal solutions are in fact super-optimal.

For the mixed sensitivity \mathcal{H}_∞ control problem however, the proposed decoupling design method yields a sub-optimal controller.

4.4.1 Super-Optimal Solutions to the \mathcal{L}_1 and Modified \mathcal{H}_∞ Mixed Sensitivity Problems

We first of all address the \mathcal{L}_1 and modified \mathcal{H}_∞ mixed sensitivity problems. Consider the following theorem.

Theorem 4.2 *Let P be a square, stable and non-minimum-phase plant. Then the solutions of n MISO optimisation problems yield one of many optimal solutions to the $n \times n$ mixed sensitivity problem, under both the \mathcal{L}_1 and modified \mathcal{H}_∞ formulations. For both problem formulations the resulting controller is super-optimal.*

Proof

Let the plant P be column partitioned as

$$P = (p_1 \ p_2 \ \dots \ p_n)$$

and let the $n \times n$ Youla parameter matrix Q be row partitioned as

$$Q = \begin{pmatrix} q_1 \\ q_2 \\ \vdots \\ q_n \end{pmatrix}$$

In terms of the Youla parameter, the mixed sensitivity matrix cost function is given by

$$J = ((I + QG)W_1 \quad -QGW_3)$$

which can be row partitioned as:

$$\begin{pmatrix} J_1 \\ J_2 \\ \vdots \\ J_n \end{pmatrix} = \begin{pmatrix} (W_S)_{11}(1 + q_1 p_1) & (W_S)_{22} q_1 p_2 & \dots & (W_S)_{nn} q_1 p_n & -(W_T)_{11} q_1 p_1 & \dots & -(W_T)_{nn} q_1 p_n \\ (W_S)_{11} q_2 p_1 & (W_S)_{22}(1 + q_2 p_2) & \dots & (W_S)_{nn} q_2 p_n & -(W_T)_{11} q_2 p_1 & \dots & -(W_T)_{nn} q_2 p_n \\ \vdots & \vdots & & \vdots & \vdots & & \vdots \\ (W_S)_{11} q_n p_1 & (W_S)_{22} q_n p_2 & \dots & (W_S)_{nn}(1 + q_n p_n) & -(W_T)_{11} q_n p_1 & \dots & -(W_T)_{nn} q_n p_n \end{pmatrix}$$

From the above equation it is clear that each row of the transfer function matrix J_i depends only on the corresponding row q_i of the Youla parameter matrix. Therefore since the q_i 's are free stable parameters, an internally stabilising controller K can be constructed one row or 'loop' at a time by choosing the q_i 's to be the solutions to n independent MISO optimisation problems.

In the case of the mixed sensitivity \mathcal{L}_1 Control Problem these are:

$$\begin{aligned} \inf q_1 & \| \hat{J}_1(z) \|_{\hat{A}} \\ \inf q_2 & \| \hat{J}_2(z) \|_{\hat{A}} \\ & \vdots \\ \inf q_n & \| \hat{J}_n(z) \|_{\hat{A}} \end{aligned}$$

It follows directly from the definition of the A norm that the corresponding controller K is an optimal solution of the mixed sensitivity \mathcal{L}_1 control problem, and that it is super-optimal, according to our definition.

In the case of the mixed sensitivity modified \mathcal{H}_∞ control problem the n independent MISO optimisation problems are:

$$\begin{aligned} \inf_{q_1(j\omega) \in \mathcal{RH}^\infty} & \| J_1(j\omega) \|_B \\ \inf_{q_2(j\omega) \in \mathcal{RH}^\infty} & \| J_2(j\omega) \|_B \\ & \vdots \\ \inf_{q_n(j\omega) \in \mathcal{RH}^\infty} & \| J_n(j\omega) \|_B \end{aligned}$$

Again optimality and super-optimality of the corresponding controller K follows directly from the definition of the B norm.

4.4.2 A Sub-Optimal Solution to the Mixed Sensitivity \mathcal{H}_∞ Control Problem

We now turn to the mixed sensitivity \mathcal{H}_∞ control problem. We will need the following lemma.

Lemma 4.2 *Let $T_{zw}(j\omega)$ be any $n \times m$ transfer function matrix with input $w(j\omega)$ and output $z(j\omega)$. Define the system norm*

$$\|T_{zw}(j\omega)\|_D = \sup_i \sup_{w \neq 0} \frac{\|z_i(j\omega)\|_2}{\|w(j\omega)\|_2}$$

Then we have the following relation

$$\|T_{zw}(j\omega)\|_D \leq \|T_{zw}(j\omega)\|_\infty \leq \sqrt{n} \times \|T_{zw}(j\omega)\|_D$$

Proof

First of all note that

$$\begin{aligned} \|T_{zw}(j\omega)\|_\infty^2 &= \sup_{w \neq 0} \frac{\|z(j\omega)\|_2^2}{\|w(j\omega)\|_2^2} \\ &= \sup_{w \neq 0} \frac{\sum_i^n \|z_i(j\omega)\|_2^2}{\|w(j\omega)\|_2^2} \\ &\leq \sup_{w \neq 0} \frac{(\sum_i^n \|z_i(j\omega)\|_2)^2}{\|w(j\omega)\|_2^2} \\ &\leq \sup_{w \neq 0} \frac{(n \times \sup_i \|z_i(j\omega)\|_2)^2}{\|w(j\omega)\|_2^2} \\ &\leq \left(\sup_{w \neq 0} \frac{n \times \sup_i \|z_i(j\omega)\|_2}{\|w(j\omega)\|_2} \right)^2 \\ &\leq \left(n \times \sup_i \sup_{w \neq 0} \frac{\|z_i(j\omega)\|_2}{\|w(j\omega)\|_2} \right)^2 \\ \Rightarrow \|T_{zw}(j\omega)\|_\infty &\leq \sqrt{n} \times \|T_{zw}(j\omega)\|_D \end{aligned}$$

Now we also have that

$$\begin{aligned} \|T_{zw}(j\omega)\|_D^2 &= \left(\sup_{w \neq 0} \sup_i \frac{\|z_i(j\omega)\|_2}{\|w(j\omega)\|_2} \right)^2 \\ &= \sup_{w \neq 0} \frac{\sup_i \|z_i(j\omega)\|_2^2}{\|w(j\omega)\|_2^2} \\ &\leq \sup_{w \neq 0} \frac{\sum_i^n \|z_i(j\omega)\|_2^2}{\|w(j\omega)\|_2^2} \end{aligned}$$

$$\begin{aligned}
&\leq \sup_{w \neq 0} \frac{\|z(j\omega)\|_2^2}{\|w(j\omega)\|_2^2} \\
&\leq \|T_{zw}(j\omega)\|_\infty^2 \\
\Rightarrow \|T_{zw}(j\omega)\|_D &\leq \|T_{zw}(j\omega)\|_\infty
\end{aligned}$$

Therefore

$$\|T_{zw}(j\omega)\|_D \leq \|T_{zw}(j\omega)\|_\infty \leq \sqrt{n} \times \|T_{zw}(j\omega)\|_D$$

□

We can now prove the following theorem, which says that for a non-minimum phase plant, a controller constructed according to the proposed decoupling design method is sub-optimal.

Theorem 4.3 *Let P be a square, stable and non-minimum-phase plant. Then the solutions of n MISO optimisation problems yield an internally stabilising controller for the $n \times n$ mixed sensitivity \mathcal{H}_∞ control problem. The resulting controller is sub-optimal.*

Proof

Proceeding according to the method of Theorem 4.2 above, it is clear that an internally stabilising controller can be constructed from the solutions to the following n independent optimisation problems:

$$\begin{aligned}
&\inf_{q_1(j\omega) \in \mathcal{RH}^\infty} \|J_1(j\omega)\|_\infty \\
&\inf_{q_2(j\omega) \in \mathcal{RH}^\infty} \|J_2(j\omega)\|_\infty \\
&\vdots \\
&\inf_{q_n(j\omega) \in \mathcal{RH}^\infty} \|J_n(j\omega)\|_\infty
\end{aligned}$$

Now from the definition of the D norm, it follows that a controller constructed as described above optimally solves the problem

$$\inf_K \|J(s)\|_D$$

where the infimum is over all LTI stabilizing controllers. However from Lemma 4.2 above we have that

$$\|J(j\omega)\|_D \leq \|J(j\omega)\|_\infty \leq \sqrt{n} \times \|J(j\omega)\|_D$$

proving that this controller is merely a sub-optimal solution of the mixed sensitivity \mathcal{H}_∞ control problem. \square

The above result is again due to the fact that the \mathcal{H}_∞ system norm is defined in terms of the \mathcal{L}_2 signal norm, whereas the A, B and D norms are defined in terms of the \mathcal{L}_∞ signal norm.

4.5 Discussion

In the next chapter the proposed decoupling design method is applied to a realistic design example. We end this chapter however with a brief note on the issue of properness. All real world plants are strictly proper, i.e. at infinite frequency their gain is zero. As will be clear at this stage, the design procedure and example above are based on the assumption that the plant is proper. Although this might suggest some applications difficulties, we point out that it is not an uncommon approach to formulate the theory under slightly relaxed conditions, and then to make the necessary practical adjustments. See for example the approach adopted by Zames and Francis in [18], in order to solve the SISO \mathcal{H}_∞ control problem.

In this particular case consider the following. Suppose we have a strictly proper plant $G(s) = C(sI - A)^{-1}B$. This plant can be made proper by adding a ϵD so that $G(s) = C(sI - A)^{-1}B + \epsilon D$. Thus $G(\infty) = \epsilon D$. If we let $D = I$ then in the limit as $\epsilon \rightarrow 0$, $G(s)$ becomes strictly proper. Therefore if we take a small enough ϵ we can implement the design procedure while still having a strictly proper plant for all practical purposes. In frequency domain terms this is simply the same as adding very high frequency zeroes to a strictly proper plant in order to make it proper, without changing the behaviour of the plant over the frequency range of interest. The fact that these types of procedures are necessary seems to be due in large part to the lack of a complete understanding of the implications of $j\omega$ -axis zeros in \mathcal{H}_∞ theory, especially in the multivariable case. See [29] for details.

We have shown in this chapter that given a stable plant, three important multivariable robust control problems can be solved one loop at a time by calculating the solutions to n MISO (non-minimum-phase plants) or n SISO (minimum-phase plants) optimisation problems and then re-assembling these solutions into a multivariable controller, according to the proposed design procedure. This design procedure has

the following advantages:

1. All available design freedom is utilised resulting in controllers which can rightly be termed super-optimal.
2. The conservative and distortive step of signal set and specification lumping is avoided, allowing the designer to control and ‘shape’ each loop of the system individually.
3. The multivariable design problem is given greater transparency and the weighting functions a clearer physical interpretation, thus making their selection less of an ‘art than a science’ [55].
4. The adoption of a decoupling approach to multivariable robust controller design allows the subsequent application of classical SISO design techniques, such as that proposed in [75] for instance, to the problem.

The proposed design procedure clearly has some limitations. Unstable plants can only be dealt with by selecting at least one output for stabilisation purposes only, as proposed in [69], – the effect this would have on super-optimality is unclear. Even in the case of stable but non-minimum-phase plants, the proposed procedure yields only sub-optimal controllers for the standard \mathcal{H}_∞ control problem. As shown above however, \mathcal{H}_∞ control problems formulated under the paradigm proposed in Chapter 3 do not suffer from this problem. Finally it seems clear that controllers designed according to the proposed method will in general have higher order than standard multivariable optimal controllers.

Chapter 5

Multivariable \mathcal{H}_∞ Synthesis via Decoupling and Loopshaping: Some Design Examples

This chapter presents some design examples which illustrate how many of the ideas developed in previous chapters can be applied to realistic controller synthesis problems. The decoupling design method proposed in Chapter 4 is applied to the problem of pitch axis control in a highly manoeuvrable experimental aircraft. Loopshaping techniques are used to improve robust performance and optimise B-norm reduction for the same example. Finally, the problem of shape control in a Sendzimir steel mill is considered from a \mathcal{H}_∞ perspective. The advantages of a classical decoupling approach to the multivariable design problem are again clearly demonstrated.

5.1 Super-Optimal Pitch Axis Control of a Highly Manoeuvrable Experimental Aircraft

In this section the decoupling design procedure proposed in Chapter 4 is applied to the problem of pitch axis control in a highly manoeuvrable experimental aircraft. The proposed procedure completely decouples the closed loop system and allows the design to be undertaken on a loop by loop basis. This result simplifies the selection of \mathcal{H}_∞ weighting functions and also makes possible the subsequent application of classical controller design techniques. The decoupling \mathcal{H}_∞ optimal controller is shown to be super-optimal, i.e the controller is optimal for *each* loop of the system, and not simply for the *worst* loop. The main advantage of the proposed method is that super-optimality is achieved with very little extra design effort.

5.1.1 Plant Description

The model of the aircraft used in the design is taken from [70], and consists of data from the HIMAT highly manoeuvrable experimental aircraft. The simplified nominal model of the aircraft P_0 has four states: forward speed (v), angle of attack (α), pitch rate (q) and pitch angle (θ); two inputs: elevon command (δ_e), and canard command (δ_c); and two measured outputs: angle of attack (α), and pitch angle (θ). Denoting the state vector x , input vector u and output vector y by

$$x = \begin{pmatrix} v \\ \alpha \\ q \\ \theta \end{pmatrix} \quad u = \begin{pmatrix} \delta_e \\ \delta_c \end{pmatrix} \quad y = \begin{pmatrix} \alpha \\ \theta \end{pmatrix}$$

we have

$$\begin{aligned} \dot{x} &= Ax + Bu \\ y &= Cx + Du \end{aligned}$$

where

$$A = \begin{pmatrix} -2.3e-02 & -3.7e-01 & -1.9e+01 & -3.2e+01 \\ 0.0e+00 & -1.9e+00 & 9.8e-01 & 0.0e+00 \\ 1.2e-02 & -1.2e+01 & 2.6e+00 & 0.0e+00 \\ 0.0e+00 & 0.0e+00 & 1.0e+00 & 0.0e+00 \end{pmatrix}$$

$$B = \begin{pmatrix} 0.0e+00 & 0.0e+00 \\ -4.1e-01 & 0.0e+00 \\ -7.8e+01 & 2.2e+01 \\ 0.0e+00 & 0.0e+00 \end{pmatrix}$$

$$C = \begin{pmatrix} 0.0e+00 & 5.7e+01 & 0.0e+00 & 0.0e+00 \\ 0.0e+00 & 0.0e+00 & 0.0e+00 & 5.7e+01 \end{pmatrix}$$

$$D = \begin{pmatrix} 0.0e+00 & 0.0e+00 \\ 0.0e+00 & 0.0e+00 \end{pmatrix}$$

The nominal model is stable and minimum phase, and can also be realised as a multivariable transfer function matrix P_0 .

Significant uncertainty regarding the dynamic behaviour of the aircraft arises from four principal sources [70] :

1. Uncertainty in the canard and elevon actuators. Conversion of electrical control signals into actual mechanical deflections will always be subject to errors due to imperfections in the electronics and hydraulics of the actuators.

2. Uncertainty in the forces and moments generated on the aircraft due to specific deflections of the canard elevon. These effects are mainly a result of aerodynamic coefficients varying with flight conditions, as well as imperfect knowledge of the exact geometry of the airplane.

3. Uncertainty in the linear and angular accelerations produced by the aerodynamically generated forces and moments. This is due to inaccuracies in modelling various inertial parameters as well as neglecting certain dynamics such as fuel slosh and airframe flexibility.

4. Other unknown forms of uncertainty.

In this design we ignore the above knowledge of the structure of the uncertainty, and instead lump all these effects into an unstructured uncertainty block Δ_P , together with a weighting function W_3 . Δ_P is assumed stable with

$$\|\Delta_P\|_\infty \leq 1$$

but otherwise unknown. W_3 is chosen to reflect variations in the level of plant uncertainty as a function of frequency, and for this example is given by

$$W_3(s) = \frac{50(s+100)}{s+10000} \times I_2$$

This choice of weighting function allows a potential percentage modelling error of 50 percent at low frequencies, increasing up to a factor of 50 at high frequencies. Δ_P and W_3 are included as a multiplicative plant input uncertainty in the closed loop system, so that our actual system consists of a parameterised set of plants \mathcal{P} where

$$\mathcal{P} = \{P_0(I + \Delta_P W_3) : \Delta_P \text{ stable, } \|\Delta_P\|_\infty \leq 1\}$$

Then the closed loop system achieves robust stability iff

$$\|W_3 P_0 K (I + P_0 K)^{-1}\|_\infty = \|W_3 T\|_\infty < 1$$

where T is the complementary sensitivity function.

5.1.2 Closed Loop Design Objectives

The robustness and performance of the closed loop system will be measured in terms of the singular values of the (nominal) transfer function matrix

$$T_{zw} = \begin{pmatrix} W_1 S & W_3 T \end{pmatrix}$$

where S is the output sensitivity function $(I + P_0 K)^{-1}$ and

$$W_1(s) = \frac{0.5(s + 3)}{s + 0.03} \times I_2$$

The weighting function W_1 is chosen to ensure good disturbance rejection and command following at low frequencies - at high frequencies robustness to plant uncertainty becomes the dominant objective. Note that T_{zw} is the transfer function between the vector of all exogenous inputs to the system, w , and the output z . In [70] the framework of μ analysis and synthesis is used to design for robust performance, i.e. a certain level of disturbance rejection is guaranteed for every plant in the set \mathcal{P} . In this section however, we adopt the standard \mathcal{H}_∞ approach and design for nominal performance with robust stability. Our purpose is to show that with very little extra design effort a decoupling \mathcal{H}_∞ optimal controller can be found which is super-optimal.

5.1.3 A Standard \mathcal{H}_∞ Design

For comparative purposes, we present results for this plant with a standard \mathcal{H}_∞ design using the MATLAB Robust Control Toolbox [71]. Figure 5.1 shows the weighting

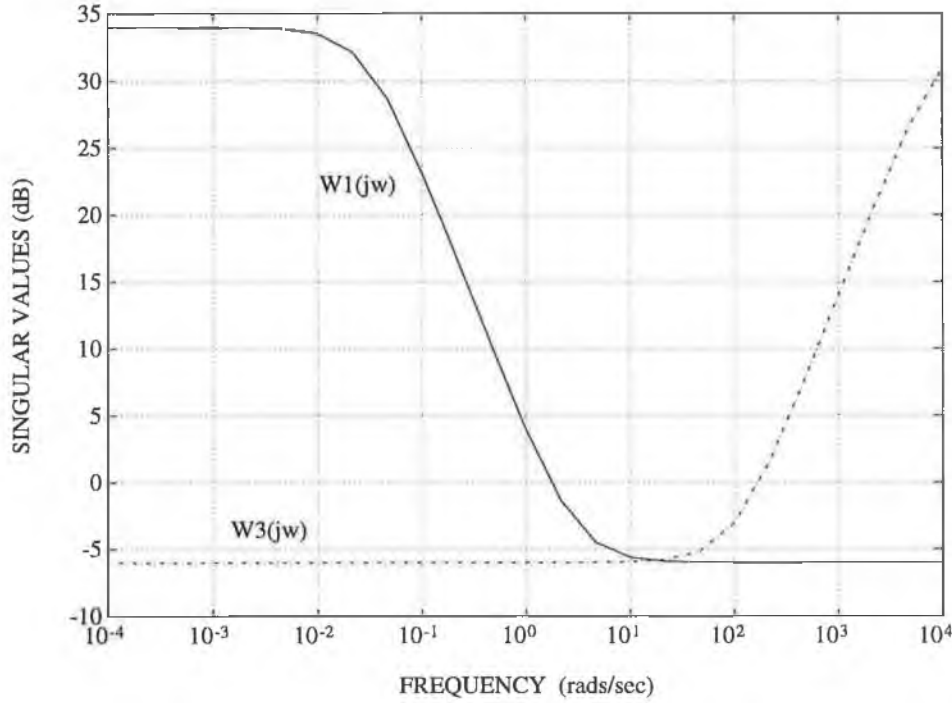


Figure 5.1: \mathcal{H}_∞ Weighting Functions

functions W_1 and W_3 used in the design. After some iterations, a \mathcal{H}_∞ optimal 9th order controller was found which satisfied the design specifications. The singular values of T_{zw} are shown in Figure 5.2 and the sensitivity and complementary sensitivity functions are plotted in Figure 5.3.

5.1.4 A Decoupling Controller

In this section we show that by using the design method proposed in Chapter 4, we can synthesise an MIMO controller which is also \mathcal{H}_∞ optimal, but which in addition completely decouples the closed loop system. The design proceeds according to the following steps:

1. Calculate the SISO controller K_1 where

$$K_1 = \inf_K \sup_{\omega} \bar{\sigma} \left(\begin{pmatrix} (W_1)_{11}(j\omega)S_{11}(j\omega) & (W_3)_{11}(j\omega)T_{11}(j\omega) \end{pmatrix} \right)$$

1. Calculate the SISO controller K_2 where

$$K_2 = \inf_K \sup_{\omega} \bar{\sigma} \left(\begin{pmatrix} (W_1)_{22}(j\omega)S_{22}(j\omega) & (W_3)_{22}(j\omega)T_{22}(j\omega) \end{pmatrix} \right)$$

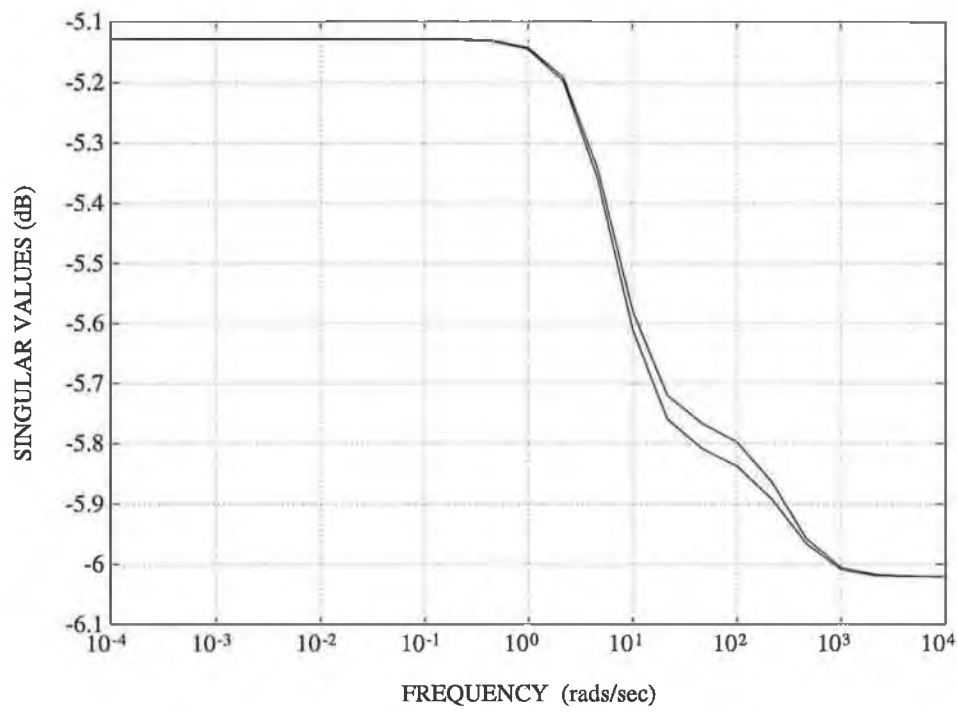


Figure 5.2: T_{zw} for Standard \mathcal{H}_∞ Controller

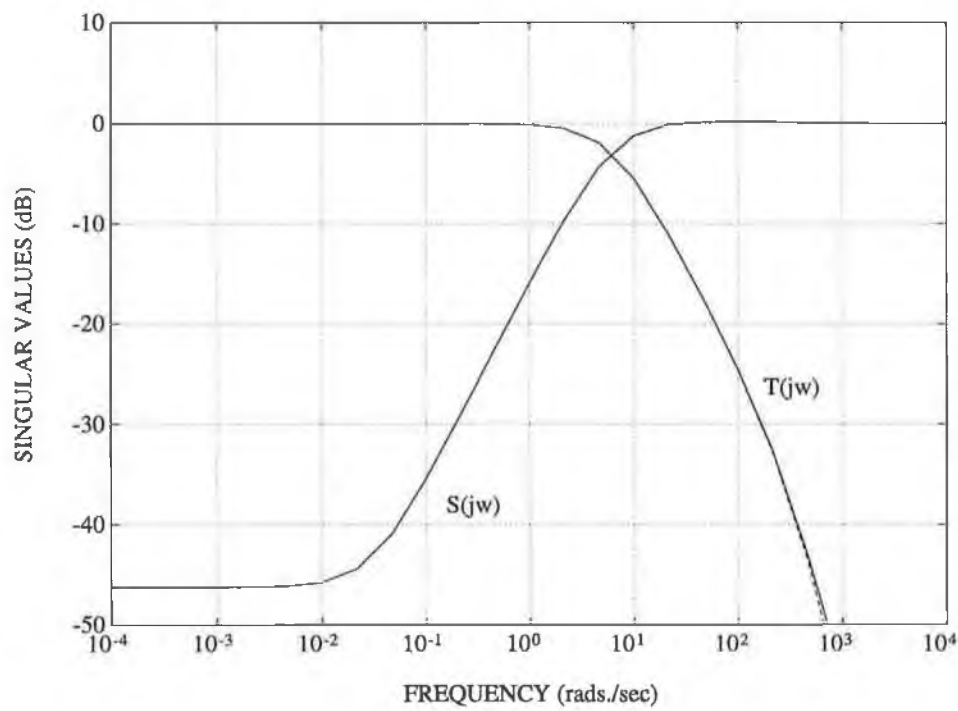


Figure 5.3: S and T for Standard \mathcal{H}_∞ Controller

3. Calculate the decoupling MIMO controller K_d where

$$K_d = \begin{pmatrix} K_1 & 0 \\ 0 & K_2 \end{pmatrix} \begin{pmatrix} (P_0)_{11} & 0 \\ 0 & (P_0)_{22} \end{pmatrix} (P_0^{-1})$$

Note that since P_0 in this case is strictly proper, it is necessary to augment it with some high frequency zeros prior to inversion. This practice is quite normal in \mathcal{H}_∞ design, see for example pp. 309 of [72].

4. Use model reduction techniques to reduce the order of the controller. In this case the state space description of K_d was converted to the Jordan form and the uncontrollable and unobservable states were then discarded. The MATLAB function `Schmr` based on the Schur decomposition method of [73] was then used to calculate a lower order approximation of K_d . This process reduced the order of the controller from 23 to 12, with no loss of performance.

The state space controller matrices are given below in Jordan form. Note that the very high frequency RHP pole in the controller is due to the fact that the original minimum-phase plant was augmented with some high frequency zeros in order to make it invertible. Since this pole is well outside our frequency range of interest it has a negligible effect on the overall design.

$$\begin{aligned}
\text{eig}(A) &= \begin{pmatrix} 2.34e+06 \\ -9.19e+01 - 1.12e+04i \\ -9.19e+01 + 1.12e+04i \\ -1.09e+03 + 2.63e-05i \\ -3.07e+02 \\ -2.86e+02 \\ -1.60e-03 + 4.50e-02i \\ -1.60e-03 - 4.50e-02i \\ -3.00e-02 \\ -3.00e-02 \\ -1.99e-03 \\ -2.00e-03 \end{pmatrix} \\
B &= \begin{pmatrix} 9.33e-02 & & 1.41e-04 & + & 7.08e-05i \\ 7.98e-04 & + & 4.50e-04i & - & 3.70e-03i \\ -4.50e-04 & - & 7.98e-04i & + & 1.18e-03i \\ 0 & & 1.27e+04 & - & 2.23e00i \\ 0 & & 1.94e+04 & - & 4.29e+02i \\ 1.79e+04 & - & 6.53e+01i & - & 3.09e+01 \\ -3.89e+02 & - & 1.08e+02i & - & 4.07e+01 \\ 2.39e+02 & + & 3.38e+02i & - & 4.43e+01 \\ 1.36e+04 & + & 1.72e+04i & - & 8.40e+06 \\ -8.62e+02 & + & 2.10e+01i & - & 3.88e+07 \\ 0 & & 1.28e+02 & + & 2.78e+01i \\ -8.67e-05 & & -7.48e-03 & & \end{pmatrix} \\
C^T &= \begin{pmatrix} 1.78e+05 & - & 2.03e+00i & 1.45e+01 & - & 1.65e-04i \\ 9.67e+02 & + & 2.00e+02i & 4.53e+04 & - & 2.05e+05i \\ 2.01e+02 & + & 9.67e+02i & -2.05e+05 & + & 4.54e+04i \\ -8.57e-03 & + & 3.00e-07i & 1.49e-01 & + & 3.25e-05i \\ 5.64e-03 & + & 1.21e-04i & -1.33e-02 & - & 3.07e-04i \\ -4.05e-03 & - & 1.48e-05i & -1.43e-02 & - & 5.23e-05i \\ 3.40e-09 & - & 1.04e-08i & 1.17e-08 & - & 3.56e-08i \\ -1.09e-08 & - & 3.90e-10i & -3.74e-08 & - & 1.30e-09i \\ -1.46e-05 & + & 1.79e-05i & -5.02e-05 & + & 6.14e-05i \\ -2.06e-05 & - & 1.06e-05i & -7.05e-05 & - & 3.64e-05i \\ 6.73e-08 & + & 1.83e-08i & 3.65e-07 & - & 2.55e-07i \\ -7.50e-09 & + & 2.99e-16i & -8.94e+00 & + & 3.42e-07i \end{pmatrix} \\
D &= \begin{pmatrix} 0 & 0 \\ 0 & 0 \end{pmatrix}
\end{aligned}$$

Results for this design are given in the figures below. Note that the reduced order controller does not make the closed loop system *perfectly* diagonal – see Figure 5.4. The level of decoupling is however more than adequate for the purposes of the design, as verified in Figures 5.5 and 5.6. It is seen that K_d decouples the system while performing just as well as the standard \mathcal{H}_∞ optimal controller.

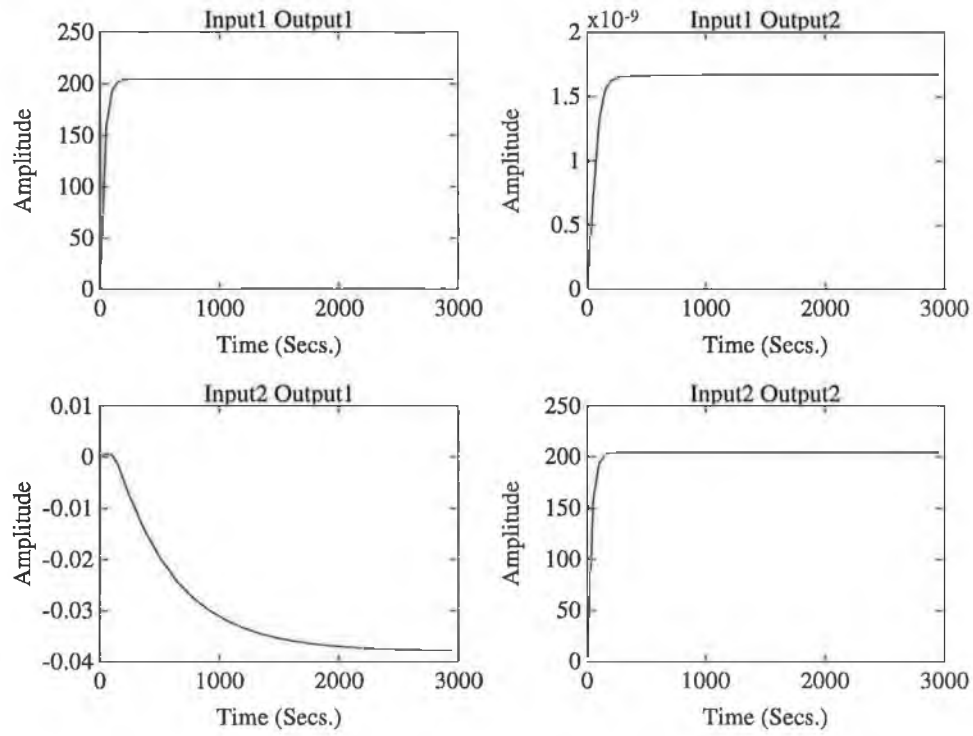


Figure 5.4: Step Response of Loop Gain $L = K_d P_0$

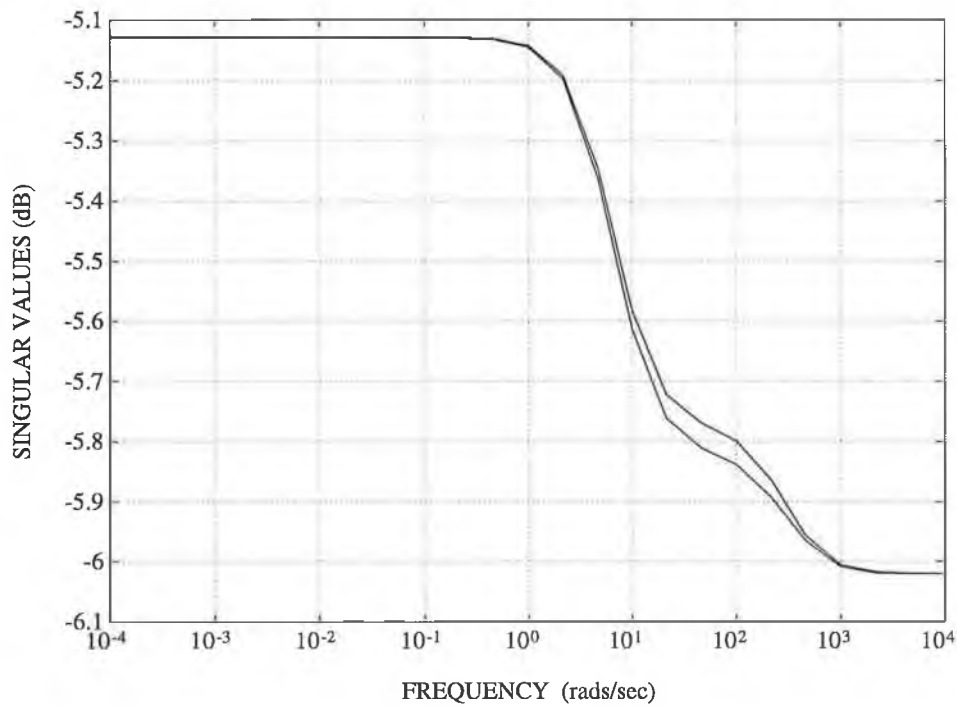


Figure 5.5: T_{zw} for Decoupling \mathcal{H}_∞ Controller K_d

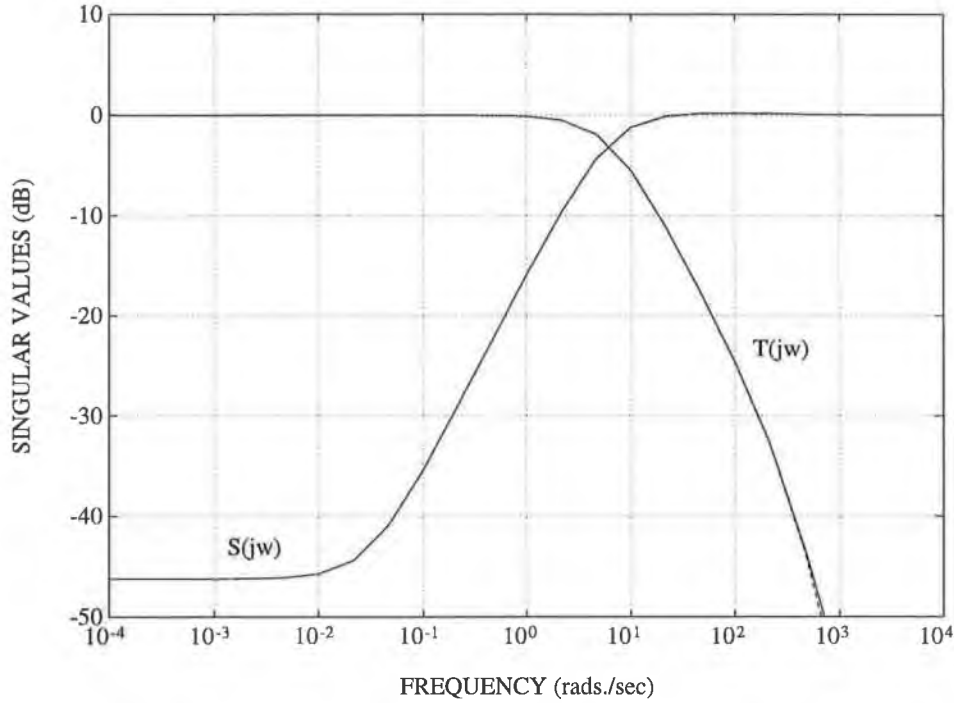


Figure 5.6: S and T for decoupling \mathcal{H}_∞ controller K_d

5.1.5 Super-Optimal Control

In the above example the two singular values of the closed loop system coincide almost exactly at all frequencies. To see that a \mathcal{H}_∞ optimal controller designed according to the above method is in fact super-optimal, consider the following situation. We assume that the level of uncertainty in the second loop of the system is reduced to 10 percent of that present in the first loop. In addition we assume that the level of disturbances acting on the second loop is decreased by the same amount. Our weighting functions therefore become

$$W_3(s) = \frac{50(s + 100)}{s + 10000} \times \begin{pmatrix} 1 & 0 \\ 0 & 0.1 \end{pmatrix} \quad W_1(s) = \frac{0.5(s + 3)}{s + 0.03} \times \begin{pmatrix} 1 & 0 \\ 0 & 0.1 \end{pmatrix}$$

A plot of the singular values of the matrix T_{zw} for a standard MIMO \mathcal{H}_∞ design using these new weighting functions is given in Figure 5.7. It seems clear from the plot that while the software has effectively minimised the maximum singular value of the matrix, less attention has been paid to the smaller singular value. By using the proposed decoupling design method however, a \mathcal{H}_∞ optimal controller can be found which minimises both singular values, resulting in a super-optimal design - see Figure 5.8

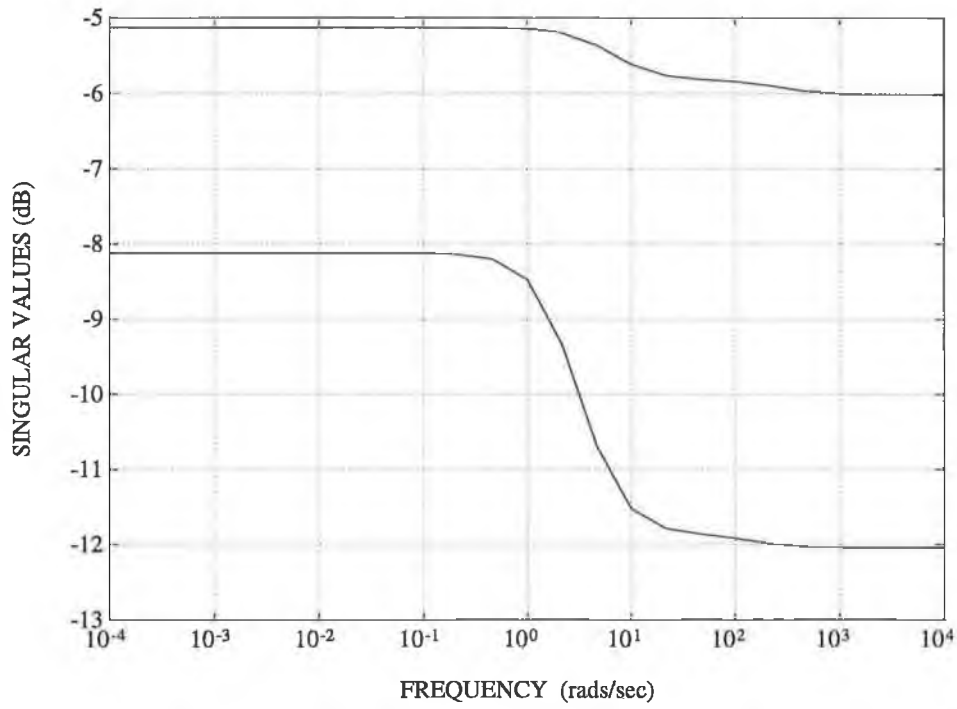


Figure 5.7: T_{zw} for Standard \mathcal{H}_∞ Controller

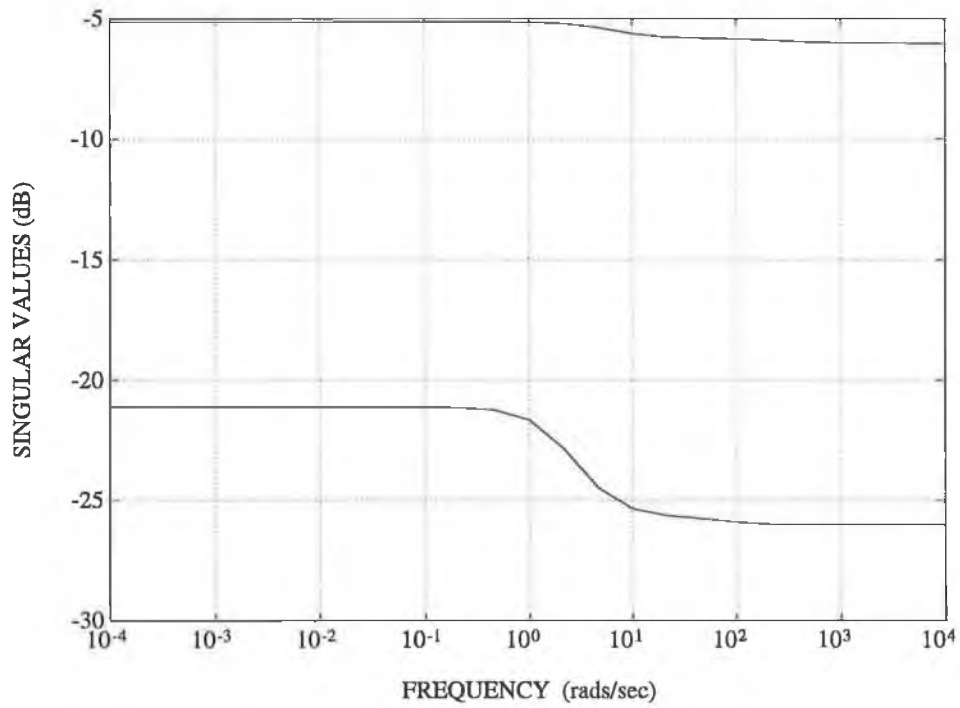


Figure 5.8: T_{zw} for Super-Optimal \mathcal{H}_∞ Controller

After controller order reduction techniques were applied, the super-optimal controller was found to be of order 12, two degrees higher than the standard \mathcal{H}_∞ controller. The state space controller matrices are in fact identical to those given in the previous section.

5.1.6 Discussion and Implications

The design method proposed in Chapter 4, is seen to be readily applicable to a realistic design example. The resulting controller completely decouples the system and is super-optimal. The decoupling result means that classical multivariable design methods such as the Inverse Nyquist Array and Characteristic Loci can easily be applied to the system after the initial \mathcal{H}_∞ design. This allows the designer extra freedom to meet other specifications, relating to response time, pole locations etc., presumably at the cost of some loss of robustness. The benefits of a super-optimal controller were revealed in this example by varying the levels of uncertainty and required performance in the second loop of the system. Indeed it seems clear that the assumption that every loop of a MIMO system is subject to uncertainty and disturbances of the same magnitude and spectral content will rarely be true in practice. As sensors become more accurate and our ability to model uncertainty and disturbances improves it clearly makes sense to try and achieve the best possible performance from each loop of the system. Quite apart from the issues of disturbances and uncertainty, many plants are themselves strongly directional, so that standard \mathcal{H}_∞ design will, as demonstrated above, fail to optimise performance in all except the ‘worst’ loop of the system.

Algorithms and techniques for the design of super-optimal \mathcal{H}_∞ controllers already exist [64, 67]. The main advantage of the method outlined above however is its simplicity and transparency in terms of engineering design. Super-optimal control is achieved with only a slight increase in the order of the controller, subject only to the requirement that the nominal model be stable and minimum phase. Finally it is noted that in [70], robust performance objectives are satisfied for the above example using μ synthesis. This technique involves repeatedly solving scaled \mathcal{H}_∞ optimisation problems, via so called ‘D-K iteration’. It seems likely therefore that applying the decoupling design approach detailed above to each of these \mathcal{H}_∞ optimisation problems could usefully improve the final μ synthesis design. This may be a fruitful avenue for future research.

5.2 Loopshaping for Robust Performance and B-Norm Reduction

In this section a loopshaping design procedure for SISO systems, detailed in [75], is extended to the multivariable case. The strategy proposed is to use the decoupling design method of Chapter 4 to diagonalise the closed loop system, and subsequently to shape each loop of the system individually. Loopshaping is used to improve the robust performance of the system (under the assumption that plant uncertainty is diagonal in structure) and also to minimise the B-norm (as described in Chapter 3) of the nominal system. The design procedure is applied to the HIMAT pitch axis controller problem outlined in the previous section.

5.2.1 Loopshaping for SISO systems

We begin by giving \mathcal{H}_∞ optimisation of SISO stable minimum phase systems an interpretation in terms of classical loopshaping ideas. For a comprehensive treatment see [74, 75]. Recall that the so-called mixed sensitivity problem in \mathcal{H}_∞ optimisation is given by

$$\inf_{K(s) \in \mathcal{RH}^\infty} \left\| \begin{pmatrix} W_1 S & W_3 T \end{pmatrix} \right\|_\infty = \inf_{K(s) \in \mathcal{RH}^\infty} \sup_\omega J(j\omega)$$

where

$$J(j\omega) = \sqrt{|W_1(j\omega)S(j\omega)|^2 + |W_3(j\omega)T(j\omega)|^2}$$

This optimisation problem basically involves finding the optimum trade-off between performance (command following and disturbance rejection) and robustness (insensitivity to plant uncertainty and measurement noise), over frequency. In terms of classical loopshaping, the above problem will be shown to be consistent with the following three requirements on the (open) loop gain of the system, L , with crossover frequency ω_c .

1. $|L(j\omega)| \gg 1$, for $\omega \ll \omega_c$
2. $|L(j\omega)| \ll 1$, for $\omega \gg \omega_c$
3. $L(j\omega) \in \mathcal{RH}^\infty$

We now show that requirement 3 above translates into a limit on the rate of roll off of $|L(j\omega)|$ at frequencies close to ω_c .

Since $L(0) > 0$ and $|L(j\omega)|$ is a monotonically decreasing function, the phase angle of L starts out at zero and decreases, i.e the Nyquist plot of L starts on the positive real axis and begins to move clockwise. By the Nyquist stability criterion, nominal internal stability holds if the angle of L at gain crossover has not yet gone down to -180 degrees, i.e crossover occurs in the third or fourth quadrants. Now by the phase formula for stable minimum phase systems [76], we have that for any frequency ω_0

$$\angle L(j\omega_0) = \frac{1}{\pi} \int_{-\infty}^{\infty} \frac{d \ln |L|}{dv} \ln \coth \frac{|v|}{2} dv$$

where the integration variable v is

$$v = \ln \left(\frac{\omega}{\omega_0} \right)$$

In the above formula, the function

$$\ln \coth \frac{|v|}{2} = \ln \left| \frac{\omega + \omega_0}{\omega - \omega_0} \right|$$

is strictly positive and peaks at ω_0 . Thus since

$$\frac{d \ln |L|}{dv}$$

will always be negative, the steeper the slope of L (strictly $\ln |L|$) near the frequency ω_0 , the more negative the value of $\angle L$. This means that internal instability is unavoidable if $|L|$ rolls off too rapidly near crossover, since the phase of L will reach -180 degrees before its gain is reduced to below unity. A standard rule of thumb is that the slope of $|L|$ should not be more than 20 dB per decade. Classical designers therefore aim to maximise the stability margin of the system by ‘flattening’ $|L|$ as much as possible in the frequencies near crossover.

To see that the above requirements are compatible with the mixed sensitivity \mathcal{H}_∞ optimisation problem described above, observe that

$$J(j\omega) \approx \begin{cases} |W_1/L| & \text{for } \omega \ll \omega_c \\ |W_3 L| & \text{for } \omega \gg \omega_c \\ \sqrt{|W_1|^2 + |W_3|^2} / 2 \cos \frac{\angle L(j\omega_c)}{2} & \text{for } \omega \approx \omega_c \end{cases}$$

Now since the optimal \mathcal{H}_∞ cost function $J(j\omega)$ is all pass, it is quite clear from the above expressions that the three requirements from classical loopshaping all serve to push $J(j\omega)$ down towards its optimal value.

It is useful to note that the problematic design conflict is not between the required values of S and T per se. It is between the *objective* of making S small and T large at low and high frequencies respectively, and the *necessity* of keeping the roll off rate of L sufficiently small. In classical Loopshaping the designer directly chooses L to satisfy this trade-off. In \mathcal{H}_∞ design it is the respective shapes and crossover frequencies of the weighting functions W_1 and W_3 that must be chosen. Since \mathcal{H}_∞ optimisation is performed over the set of all stabilising controllers (via the Youla parameterisation [68]), closed loop stability is guaranteed - if too ambitious a set of weighting functions are chosen, the software will simply report that it cannot compute a stabilising controller. This is often because the crossover gap, i.e. the difference between the crossover frequencies of W_1 and W_3 is too narrow, resulting in a required roll off rate which is too steep. If this gap is increased a stabilising controller may be found but the resulting J may still have a sharp peak near ω_c . This is due to the third term in the above expression for J being too large. Thus in \mathcal{H}_∞ optimisation, difficulty of design is closely related to the width of the crossover gap.

5.2.2 Loopshaping MIMO systems for Improved Robust Performance

With reference to Figure 1.3, the Robust Performance Problem or Robust Disturbance Attenuation Problem (RDAP), is

$$\inf_{K(s) \in \mathcal{RH}^\infty} \sup_{\Delta_P} \|T_{zw}\|_\infty$$

In the MIMO case, no useful closed form expression is available for controller synthesis. The best that can be done at present seems to be to recast the problem in the framework of the structured singular value [78], and compute a controller using μ synthesis techniques. This process is however computationally demanding and the resulting controller may not be globally optimal. However, in the SISO case the RDAP problem is exactly equivalent to

$$\inf_{K(s) \in \mathcal{RH}^\infty} \|J_{rdap}(j\omega)\|_\infty$$

where

$$J_{rdap}(j\omega) = |W_1(j\omega)S(j\omega)| + |W_3(j\omega)T(j\omega)|$$

This problem is solved to within a factor of $\sqrt{2}$ by the mixed sensitivity \mathcal{H}_∞ optimisation problem discussed in the last section. In [75], a design method is presented

which uses this fact together with classical loopshaping ideas, to design for robust performance without resorting to μ synthesis. In this section we propose a modest extension of this method to the multivariable case. We first of all give a brief description of the design method for SISO systems. The method relies on the following two lemmas [39, 75].

Lemma 5.1

$$J(j\omega) \leq J_{rdap}(j\omega) \leq \sqrt{2}J(j\omega)$$

Lemma 5.2 *If there exists an ω_0 such that*

$$|L(j\omega_0)| = \frac{|W_1(j\omega_0)|}{|W_3(j\omega_0)|}$$

then for a controller which optimally solves the \mathcal{H}_∞ mixed sensitivity problem,

$$\max_{\omega} J_{rdap}(j\omega) = J_{rdap}(j\omega_0) = \sqrt{2}J(j\omega_0)$$

Proof

$$\begin{aligned} |L(j\omega)| &= \frac{|T(j\omega)|}{|S(j\omega)|} \\ \Rightarrow |L(j\omega_0)| &= \frac{|W_1(j\omega_0)|}{|W_3(j\omega_0)|} = \frac{|T(j\omega_0)|}{|S(j\omega_0)|} \\ \Rightarrow |W_1S(j\omega_0)| &= |W_3T(j\omega_0)| \\ &= \sqrt{\frac{J(j\omega_0)^2}{2}} \\ \Rightarrow |W_1S(j\omega_0)| + |W_3T(j\omega_0)| &= 2\sqrt{\frac{J(j\omega_0)^2}{2}} \\ \Rightarrow J_{rdap}(j\omega_0) &= \sqrt{2}J(j\omega_0) \end{aligned}$$

□

The significance of Lemma 5.2 above is that for any ‘sensible’ design, there will be some frequency ω_0 at which

$$|W_1S(j\omega_0)| = |W_3T(j\omega_0)|$$

and therefore the upper bound in Lemma 5.1 will (almost) always be achieved. Solving the \mathcal{H}_∞ mixed sensitivity problem makes $J(j\omega)$ an all-pass function with magnitude

γ_0 . The corresponding J_{rdap} is typically a bell shaped curve which is always greater than J , with a peak value of $\leq \sqrt{2}\gamma_0$ at the frequency ω_0 . In [77], a theorem is given which suggests that the optimal J_{rdap} is also all-pass. The proposed approach is therefore to use standard \mathcal{H}_∞ optimisation to bring J_{rdap} down to within $\sqrt{2}$ of its optimal value, and then to use loopshaping techniques to ‘flatten’ J_{rdap} . The reason for the peak in the value of J_{rdap} is that since $J_{rdap}(\omega) \geq J(\omega)$ the crossover gap of J_{rdap} is always narrower than that of J . Thus J_{rdap} is flattened by using a cascade compensator to further reduce the slope of L near crossover. The easiest way to do this is of course simply to decrease L slightly at frequencies below crossover and increase it slightly at frequencies above crossover. The resulting increase in the value of J is of no consequence since robust and not nominal performance is the ‘real’ design objective.

The key to extending the above design method to the multivariable case is the fact that a completely decoupled $n \times n$ MIMO system can be treated as n independent SISO systems for the purposes of design. Let us return to the HIMAT pitch axis controller design example of the last section. Recall that the \mathcal{H}_∞ optimal controller K_d calculated according to the design method of Chapter 4, completely decouples the closed loop system. This means that the nominal open loop gain L , the nominal sensitivity function S , and the nominal complementary sensitivity function T , are all diagonal. Thus we are free to insert a diagonal cascade compensator which we can use to minimize the peak value of J_{rdap} for each loop of the system. A limitation of this approach is that MIMO robust performance will only be guaranteed for diagonal Δ_P ’s. This is due to the fact that

$$S = [I + KP_0(I + \Delta_P)]^{-1}$$

i.e. the actual (as opposed to nominal) sensitivity function S is only completely diagonal for diagonal Δ_P ’s. The assumption that Δ_P is diagonal in structure is however often well motivated from physical considerations. In [79] for example the modelling of an uncertainty matrix for a distillation column is considered. The authors note that non-zero off-diagonal terms in a multiplicative input uncertainty matrix imply that a change in one input may result in an undesired change in another one. Although conceding that this may be the case for some plants, for example if the actuators are located very close together, the authors conclude that for most plants, including the distillation column, it is more reasonable to assume that the actuators are *independent*, that is, Δ_I is diagonal. Obviously, similar arguments apply in many situations

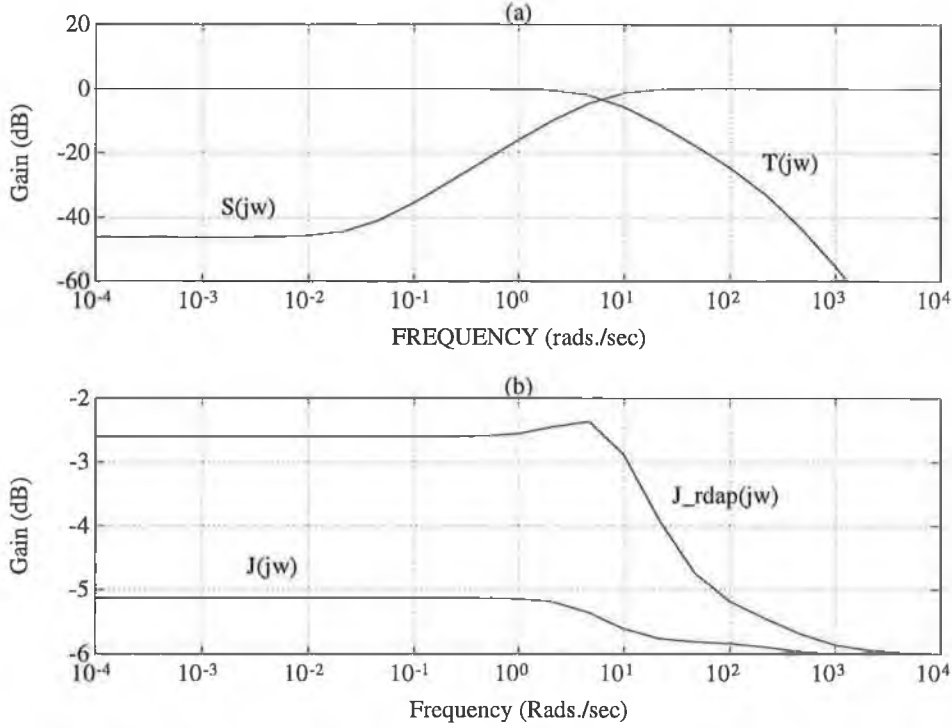


Figure 5.9: S , T , J , and J_{rdap} for loop 1, with K_d

for output multiplicative uncertainty. Figure 5.9 shows Bode plots of S , T , J , and J_{rdap} for loop 1 of the HIMAT design with decoupling controller K_d . As expected, J is essentially all-pass while J_{rdap} has a peak near the crossover frequency. We choose the (1,1) element of our cascade compensator to be

$$K_1 = \frac{(1.9s + 1.9)}{(2s + 1)} \times \frac{0.8(2s + 1.9)(0.05s + 0.8)}{(0.6s + 1)(0.04s + 1)}$$

Figure 5.10 shows the effect of K_1 on the loop gain L . The second term has the effect of flattening the loop gain at frequencies near ω_c by increasing L more at high frequencies than at low frequencies. The first term increases the loop gain slightly at low frequencies to compensate for the non-bell-like shape of J_{rdap} . As shown in Figure 5.11, this slight adjustment in the loop gain has a significant effect on the shape of J_{rdap} and $\|J_{rdap}\|_\infty$ is reduced from -2.36 dB (0.762) to -3.56 dB (0.663), an improvement of almost 10 percent. For the second loop of the system, the (2,2) element of our cascade compensator

$$K_2 = \frac{(1.9s + 1.9)}{(2s + 1)} \times \frac{0.7(2s + 1.9)(0.05s + 0.8)}{(0.6s + 1)(0.04s + 1)}$$

reduces $\|J_{rdap}\|_\infty$ from -2.35 dB (0.763) to -3.46 dB (0.671), again an improvement of just under 10 percent – see Figures 5.12, 5.13, and 5.14. The full MIMO closed

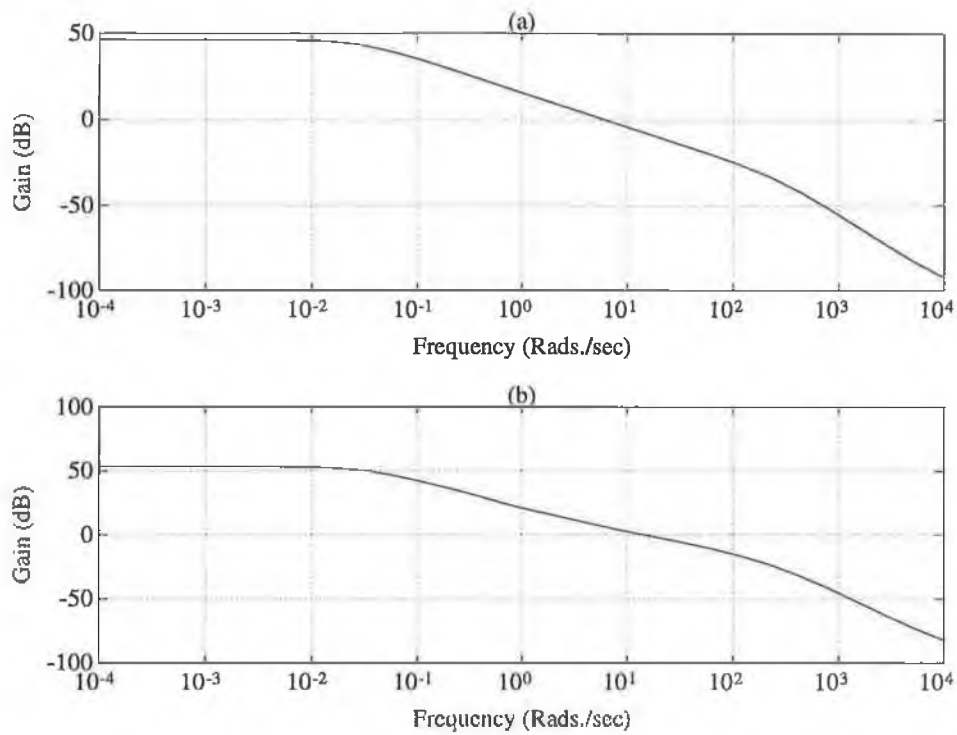


Figure 5.10: (a.) L without K_1 , (b.) L with K_1

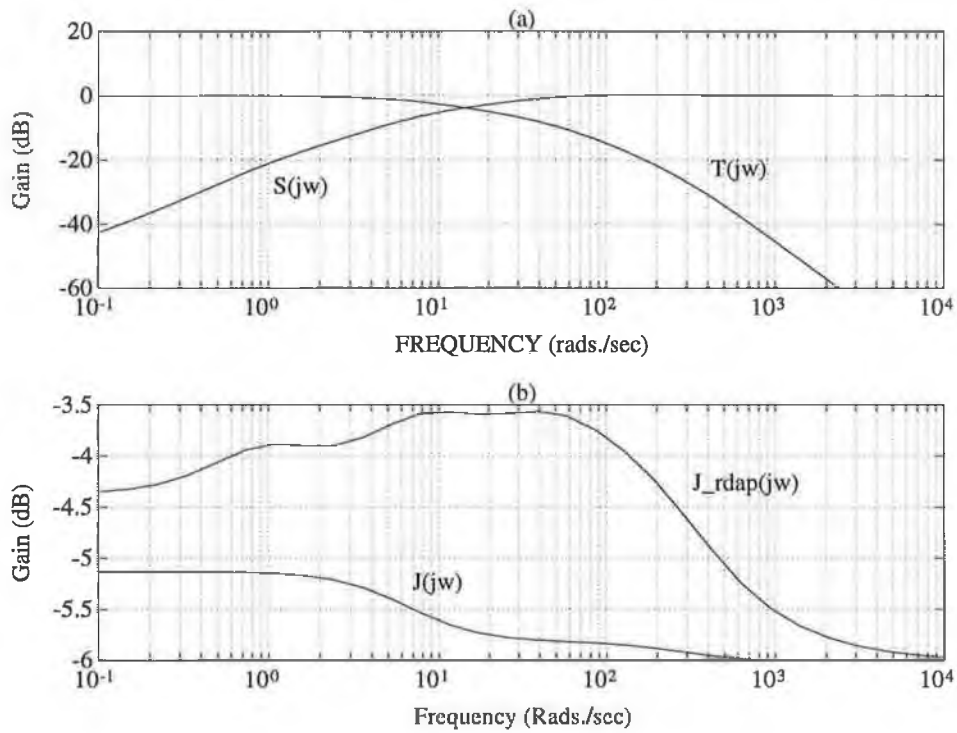


Figure 5.11: S , T , J , and J_{rdap} for loop 1, with K_d and K_1

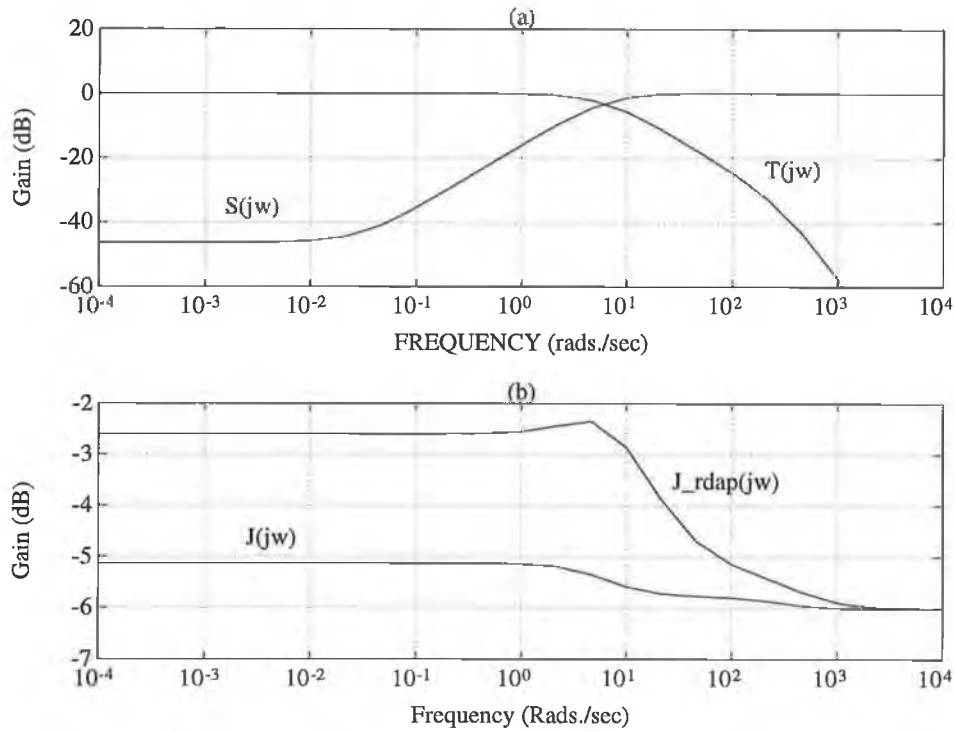


Figure 5.12: S , T , J , and J_{rdap} for loop 2, with K_d

loop compensator is thus given by

$$K(s) = \begin{pmatrix} K_1(s) & 0 \\ 0 & K_2(s) \end{pmatrix} K_d(s)$$

where $K_1(s)$ and $K_2(s)$ are given above. State space Jordan form matrices for $K_d(s)$ are given in Section 5.14.

The above results assume that Δ_P is diagonal, however it can reasonably be argued that as long as the uncertainty in the plant is at least diagonally dominant, the above approach will still produce useful designs. Indeed as noted above, for many plants this is a well motivated assumption. Improvement in robust performance for completely unstructured Δ_P 's is not guaranteed but can always be checked a posteriori by μ analysis.

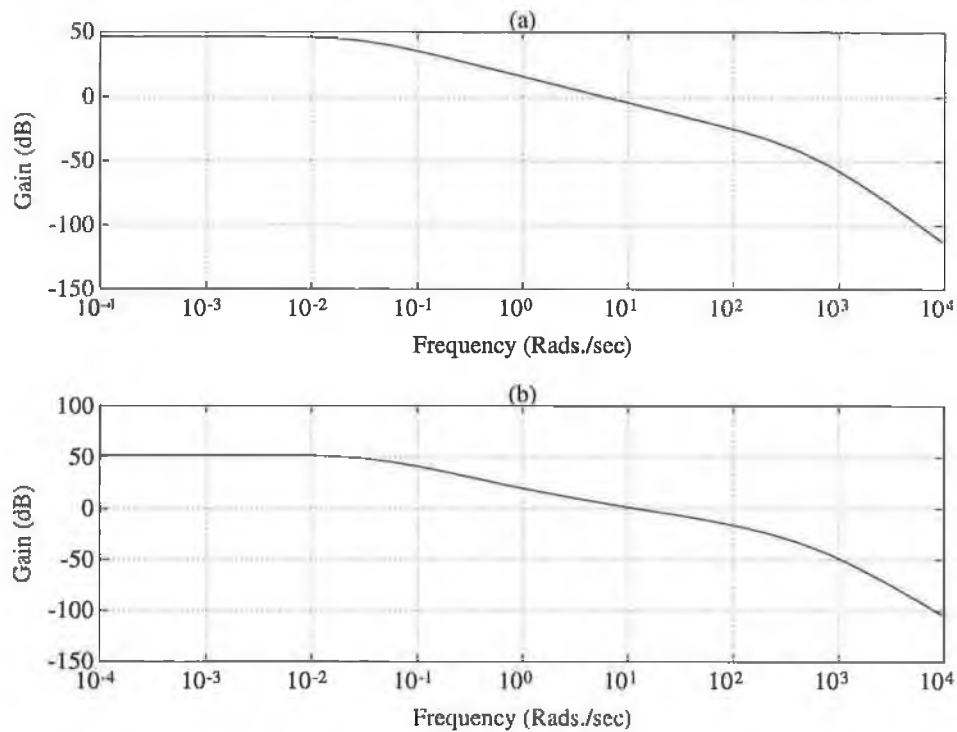


Figure 5.13: (a.) L without K_2 , (b.) L with K_2

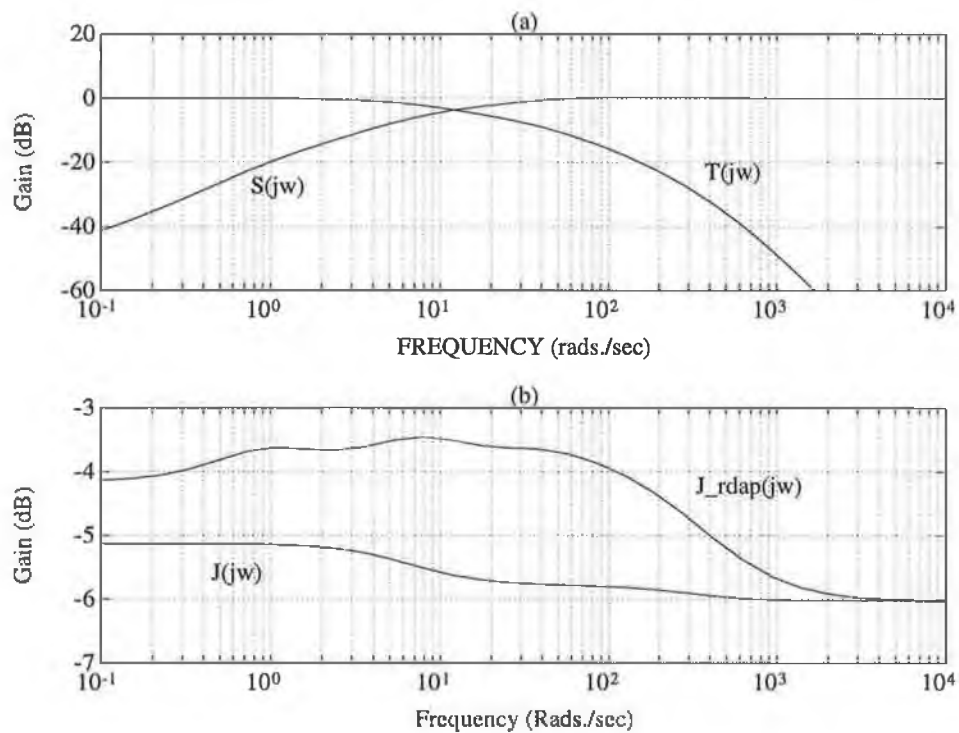


Figure 5.14: S , T , J , and J_{rdap} for loop 2, with K_d and K_2

5.2.3 Loopshaping MIMO systems for Time Domain Objectives

In this section we use the loopshaping procedure outlined above to reduce the B-norm of the closed loop system for the same HIMAT pitch axis controller example. Recall that in Chapter 3 we defined the B-norm for an $n \times n$ multivariable system as

$$\|T_{zw}(j\omega)\|_B = \max_i \sum_{j=1}^n \|(T_{zw}(j\omega))_{ij}\|_\infty$$

We have already seen that for the HIMAT example with decoupling controller K_d , S and T are diagonal, and thus T_{zw} is block diagonal. Thus the B-norm for this system can be rewritten as

$$\|T_{zw}(j\omega)\|_B = \max_i \|(W_1)_{ii}(j\omega)S_{ii}(j\omega)\|_\infty + \|(W_3)_{ii}(j\omega)T_{ii}(j\omega)\|_\infty$$

Thus minimizing the B-norm for this system is equivalent to solving 2 SISO optimisation problems of the form

$$\inf_{K(s) \in \mathcal{RH}^\infty} \|J_B(j\omega)\|_\infty \text{ where } J_B = \|W_1(j\omega)S(j\omega)\|_\infty + \|W_3(j\omega)T(j\omega)\|_\infty$$

It is interesting to consider the relationship between the cost functions, J , J_{rdap} , and J_B . We already have that

$$J(j\omega) \leq J_{rdap}(j\omega) \leq \sqrt{2}J(j\omega)$$

Futhermore, it is easy to show that

$$J_{rdap}(j\omega) \leq J_B(j\omega) \leq 2J_{rdap}(j\omega)$$

This gives

$$J(j\omega) \leq J_B(j\omega) \leq 2 \times \sqrt{2} J(j\omega)$$

Thus since an analytical solution to the B-norm minimisation problem is not available, we propose the following two-step procedure for sub-optimal synthesis:

1. Minimize J for each loop of the system by calculating the \mathcal{H}_∞ optimal decoupling controller K_d .
2. Use classical loopshaping techniques to design a cascade compensator to minimize J_B for each loop of the system.

Loopshaping in this case is done with the aim of ‘flattening’ W_1S and W_3T since it

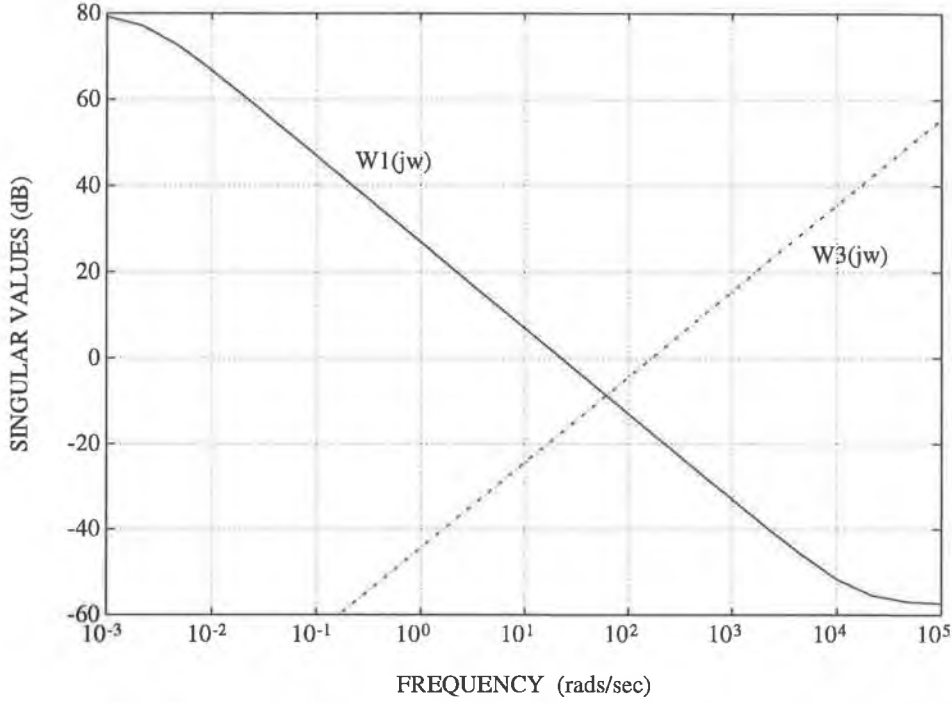


Figure 5.15: Weighting Functions W_1 and W_3

can be shown that the optimal value of J_B is also all-pass. Due to the relatively flat shape of the original weighting functions W_1 and W_3 in our HIMAT example, W_1S and W_3T for each loop of the system are already almost all-pass for our \mathcal{H}_∞ optimal controller. Thus in order to demonstrate our approach we change the weights to

$$W_1(s) = \frac{(0.6e - 4)s + 1}{(0.45e + 3)s + 1} \quad W_3(s) = \frac{(0.6e + 3)s + 1}{(0.6e - 1)s + 10^5}$$

As can be seen from Figure 5.15, these weights simply have the effect of penalising S and T more at very low and very high frequencies respectively. A \mathcal{H}_∞ optimal decoupling controller for these new weights was then calculated according to the proposed design procedure. The resulting W_1S and W_3T for loop 1 of the system are shown in Figure 5.16. The value of J_B for loop 1 of this design is -2.0194 dB. In order to reduce this figure, we introduce a cascade compensator

$$K_1(s) = \frac{(1.4e - 4)s + 1.2}{(2.3e - 4)s + 1}$$

The effect this compensator has on the loop gain of the system is shown in Figure 5.17. Note that the approach taken is simply to increase the loop gain slightly at those frequencies over which we want to reduce W_1S and to decrease it slightly at frequencies

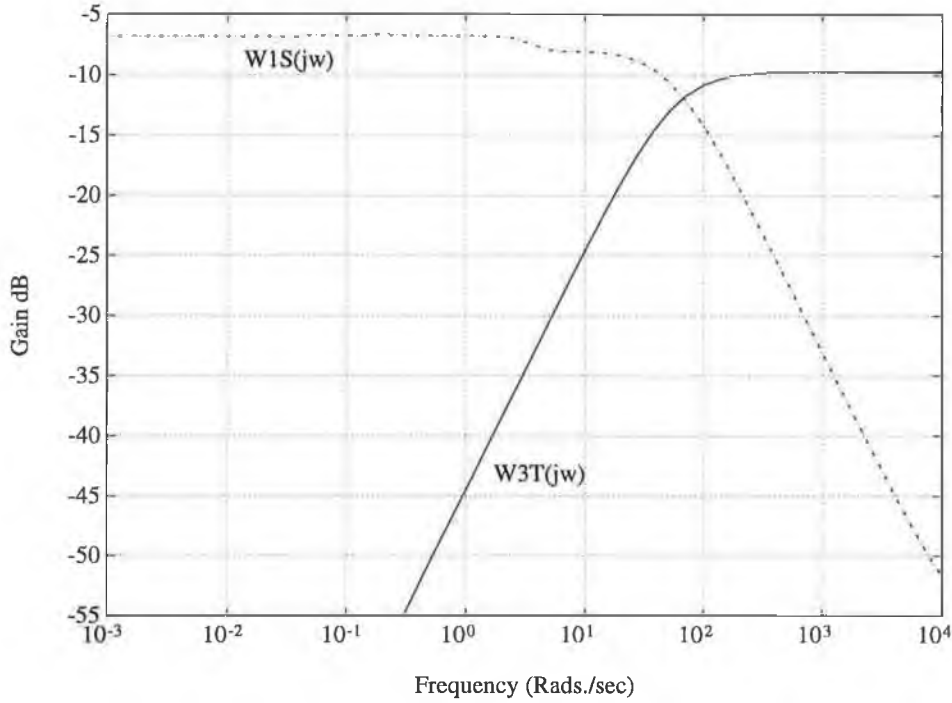


Figure 5.16: W_1S and W_3T for K_d (Loop 1)

where we want to reduce W_3T . With the compensator K_1 in the loop, W_1S and W_3T are as shown in Figure 5.18. Note that the value of J_B has been reduced to -3.5292 dB. Equivalent plots for loop 2 of the system are shown in Figures 5.19, 5.20, and 5.21. With the cascade compensator K_2 equal to K_1 , J_B for the second loop of the system is reduced from -1.2501 dB to -2.3865 dB. The full MIMO closed loop compensator is then given by

$$K(s) = \begin{pmatrix} K_1(s) & 0 \\ 0 & K_2(s) \end{pmatrix} K_d(s)$$

where $K_1(s)$ and $K_2(s)$ are given above and $K_d(s)$ is given below in state space Jordan form. Thus for this design, the implementation of classical loopshaping techniques has reduced the value of $\|T_{zw}(j\omega)\|_B$ from 0.866 to 0.759, an improvement of about 11 per cent. An interesting observation is that B-norm optimisation conflicts with the RDAP problem of minimising J_{rdap} for each loop of the system. This is shown clearly in Figure 5.22 where J_{rdap} before and after the addition of the compensator K_1 is plotted for loop 1 of the system. This trade off should come as no surprise however, since the B-norm is a *nominal* performance specification, and thus automatically conflicts with the *robust* performance specification of J_{rdap} .

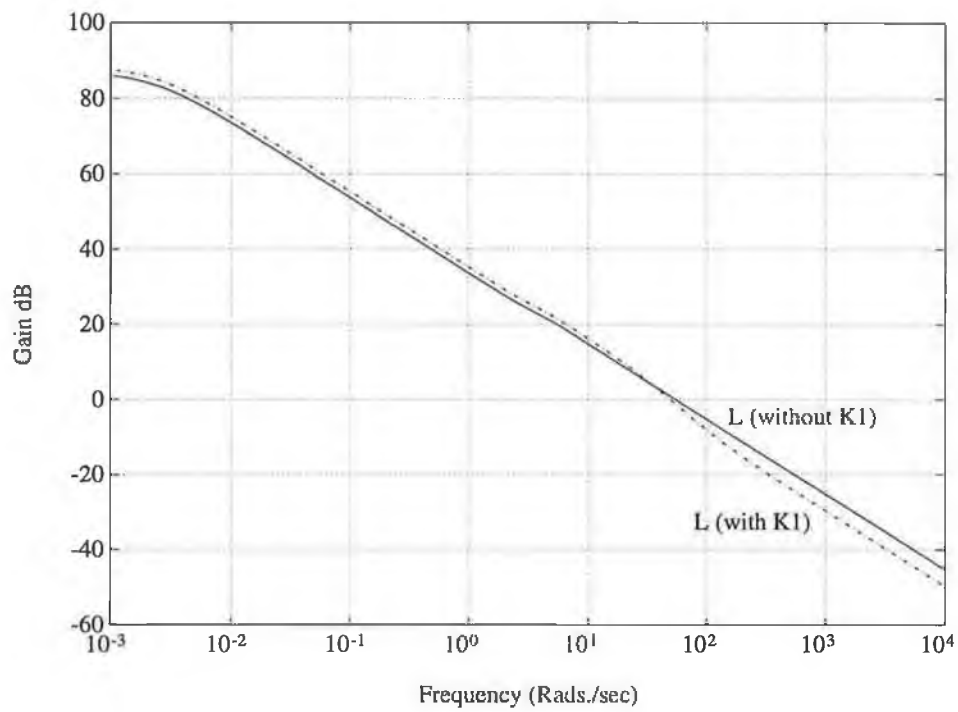


Figure 5.17: L with and without K_1 (Loop 1)

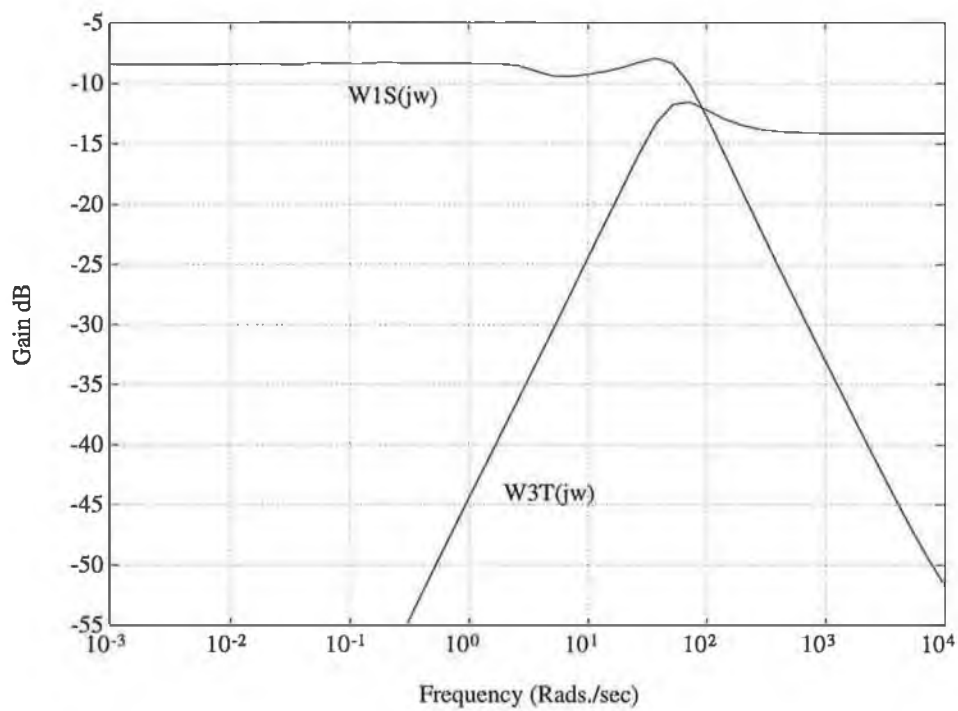


Figure 5.18: W_1S and W_3T for K_d and K_1

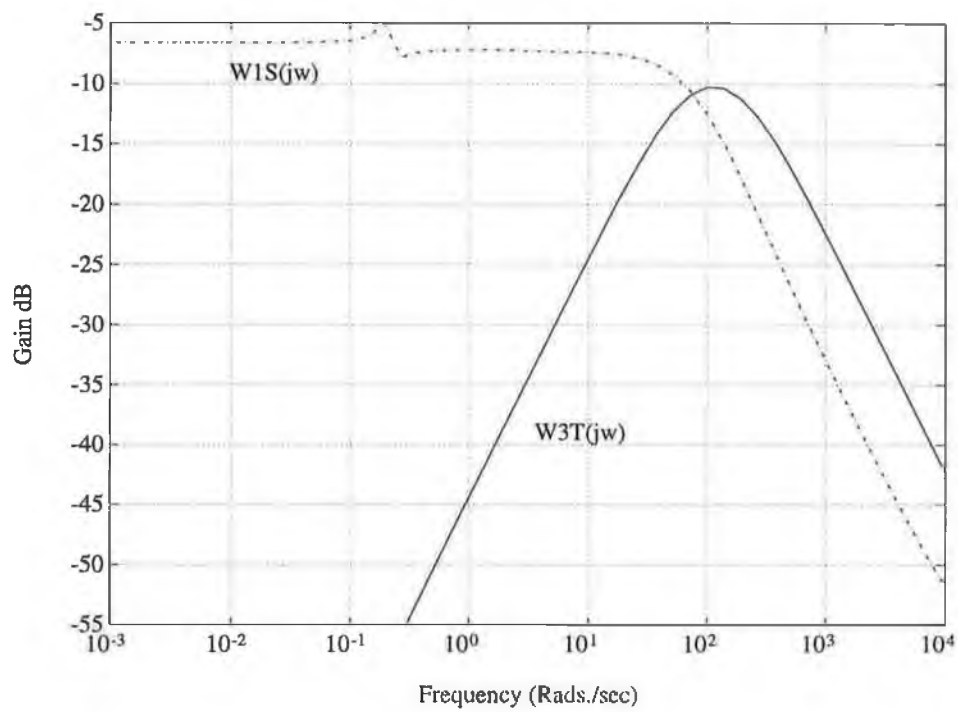


Figure 5.19: W_1S and W_3T for K_d (loop 2)

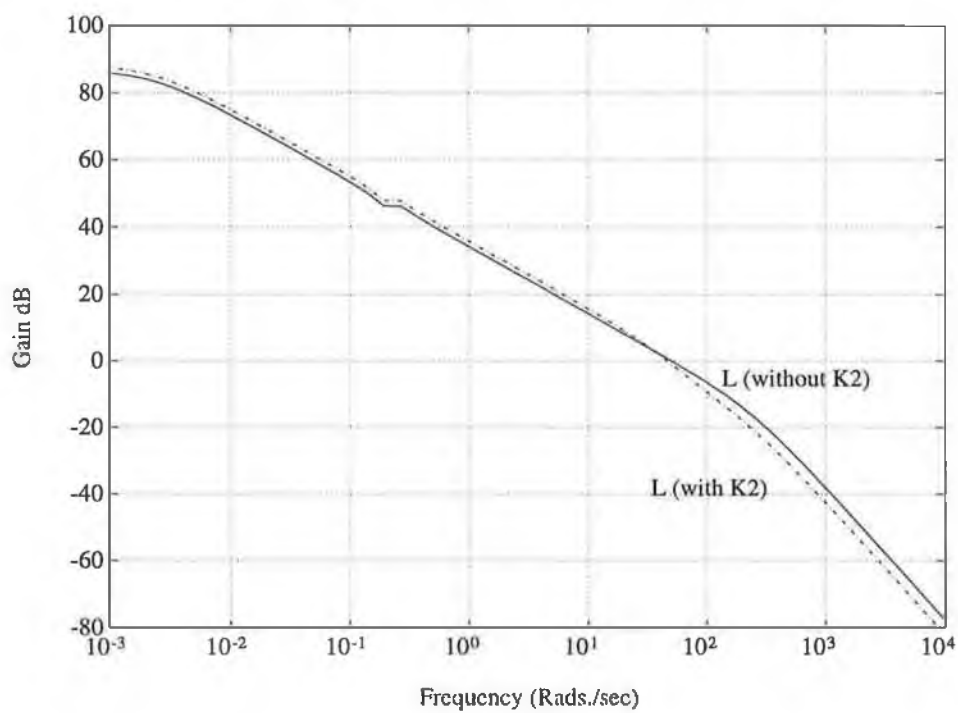


Figure 5.20: L with and without K_2 (Loop 2)

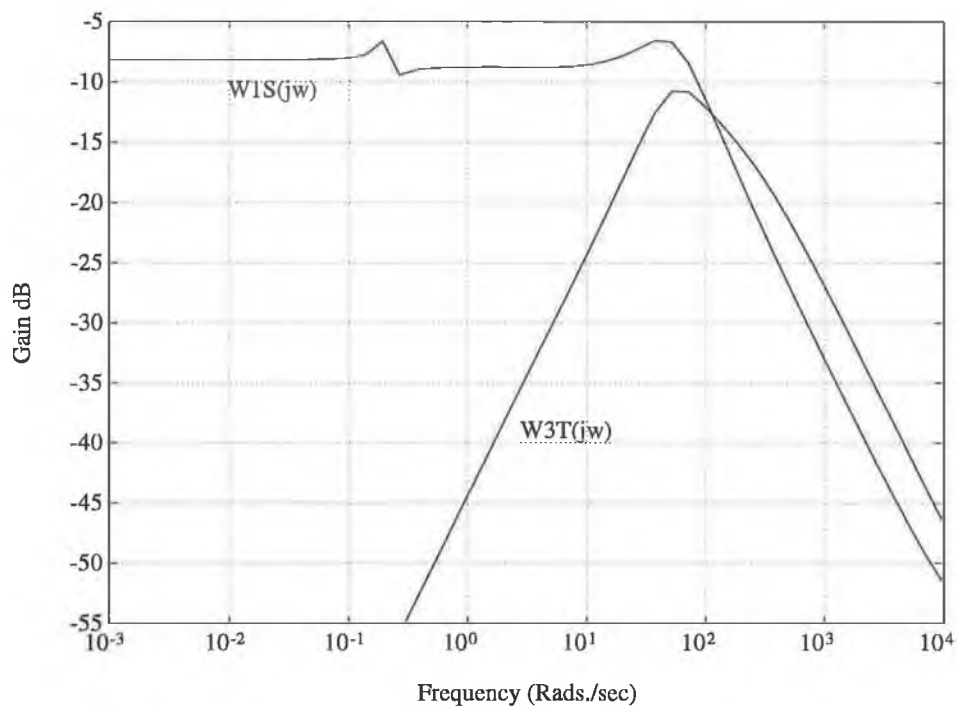


Figure 5.21: W_1S and W_3T for K_d and K_2

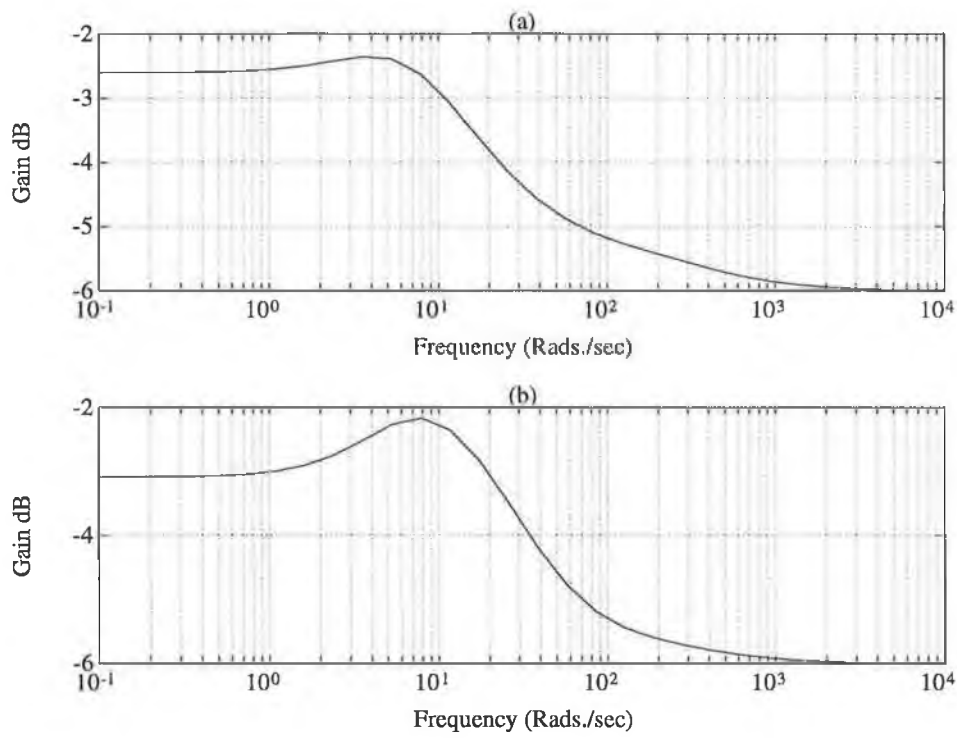


Figure 5.22: (a) J_{rdap} without K_1 , (b) J_{rdap} with K_1

$$\text{eig}(A) = \begin{pmatrix} 2.34e+00 \\ -9.45e+01 & - & 1.12e+04i \\ -9.45e+01 & + & 1.12e+04i \\ -2.49e+02 \\ -2.23e+00 & - & 3.43e+00i \\ -2.22e+00 & - & 3.43e+00i \\ -2.22e+00 & + & 3.43e+00i \\ -2.23e+00 & + & 3.43e+00i \\ -1.97e-02 & - & 2.08e-01i \\ -1.97e-02 & - & 2.08e-01i \\ -1.97e-02 & + & 2.08e-01i \\ -1.97e-02 & + & 2.08e-01i \\ -1.60e-03 & - & 4.50e-02i \\ -1.60e-03 & + & 4.50e-02i \\ -2.01e-03 \\ -2.22e-03 \\ -2.22e-03 \\ -2.00e-03 \end{pmatrix}$$

$$B = \begin{pmatrix} -1.53e+01 & + & 9.57e-01i & 0 & 1.11e-01 & + & 7.78e-02i \\ -9.02e-02 & - & 6.31e-02i & 1.11e-01 & - & 7.24e-02i \\ -9.31e-02 & + & 5.88e-02i & 1.15e-01 & - & 7.24e-02i \\ -1.87e-01 & - & 8.59e-02i & 2.20e+09 & + & 2.73e+09i \\ -3.88e+04 & - & 1.23e+05i & 3.47e+00 & - & 4.67e+00i \\ 2.67e-03 & - & 2.25e-03i & 4.64e+04 & + & 1.56e+05i \\ -2.77e-03 & - & 1.61e-03i & 1.16e+05 & + & 9.50e+04i \\ 6.92e+04 & + & 1.09e+05i & 4.21e+00 & - & 3.96e+00i \\ 1.29e+03 & - & 2.45e+03i & -1.98e+00 & - & 9.53e-01i \\ -5.36e-04 & + & 9.68e-04i & -2.14e+04 & - & 9.06e+02i \\ -2.02e+03 & + & 2.93e+03i & -2.98e+00 & + & 4.25e-01i \\ 1.63e-03 & + & 2.26e-03i & -1.12e+04 & - & 1.42e+04i \\ 4.69e+07 & + & 3.74e+07i & 3.98e-01 & - & 1.35e+00i \\ -2.90e+07 & + & 3.59e+07i & -1.06e+00 & - & 2.31e-01i \\ -5.27e-01 & - & 5.41e-01i & -1.35e+09 & + & 3.26e+08i \\ 6.59e+02 & + & 8.12e+02i & 1.76e+09 & - & 1.77e+09i \\ 8.81e+08 & - & 1.44e+08i & -3.48e+06 & + & 2.31e+06i \\ -4.35e-02 & & & -2.99e+00 & + & 9.34e-05i \end{pmatrix}$$

$$C^T = \begin{pmatrix} -3.56e+05 & - & 2.23e+04i & -2.90e+01 & - & 1.81e+00i \\ -1.60e+03 & + & 1.16e+03i & 2.43e+05 & + & 3.44e+05i \\ -1.65e+03 & - & 1.08e+03i & 2.26e+05 & - & 3.55e+05i \\ 0 & & & 0 & & \\ 0 & & & -1.12e-05 & & \\ 0 & & & 0 & & \\ 0 & & & 0 & & \\ 0 & & & -1.18e-05 & & \\ 0 & & & -1.14e-05 & + & 1.17e-05i \\ 0 & & & 0 & & \\ 0 & & & -1.22e-5 & & \\ 0 & & & 0 & & \\ 0 & & & 0 & & \\ 0 & & & 0 & & \\ 0 & & & 0 & & \\ 0 & & & 0 & & \\ 0 & & & -1.79e+01 & - & 1.09e-05i \end{pmatrix}$$

$$D = \begin{pmatrix} 0 & 0 \\ 0 & 0 \end{pmatrix}$$

5.3 Robust Shape Control in a Sendzimir Cold-Rolling Steel Mill - A Decoupling Approach

In this section the shape control problem for a Sendzimir 20-roll cold rolling steel mill is considered. The operation of the mill over a wide range of conditions arising from roll changes, changes in rolling schedules and changes in material gauge, width and hardness, poses significant design challenges. In addition, the linearised model of the multivariable plant is ill-conditioned. Previous approaches to the problem have been based on nominal designs with little a priori consideration of robustness issues. This resulted in the need for a large number of precompensator matrices to cater for the full range of operating conditions. In this section a single decoupling \mathcal{H}_∞ controller is designed, via the singular value decomposition, for one complete schedule. Robustness in the face of changing operating conditions is explicitly characterised a priori and validated a posteriori by nonlinear simulation. Design results suggest a systematic approach to controller scheduling via \mathcal{H}_∞ optimisation. Our treatment follows closely that of [5].

5.3.1 The Control Problem

The *shape* of a steel strip in the current context refers to the stress distribution in the strip. Perfect shape implies a uniform internal stress distribution, so that if cut into narrow strips, the steel will lie flat on a flat surface. Bad shape can cause the strip to buckle or even tear. The shape of the steel is measured by taking a differential tension profile across the strip at 8 (modelled) equally spaced points. The output of the system is thus a profile represented in vector form. Strip shape is controlled by bending the rolls of the mill, causing elongation of the strip at points where the rolls are closest. ‘Long’ or loose sections of the strip have associated compressive stress, while ‘short’ or tight sections suffer from tensile stress.

Accurate control of the shape of the steel strip in cold rolling is a difficult problem, due to the multi-pass, multi-schedule nature of the process. The approximately 2500 different passes and schedules required to achieve a required final gauge for different grades and widths of rolled strip involve variations in mill setup, such as roll diameters and strip speed as well as variations in material characteristics, such as input/output gauges for each pass, strip width, and material hardness. These factors can cause variations of up to 300 percent in the parameters of the mill model, thus the current

requirement for a large number of controllers comes as no surprise.

The sendzimir mill is a so-called reversing mill, and a separate schedule containing a number of passes is specified for each different material rolled. A schedule can contain from 4 to 15 passes through the rolling cluster. Each pass involves different entry and exit gauges, with minor changes in the material hardness from pass to pass.

To date, the approach has been to design controllers using traditional multivariable techniques for a set of nominal cases, i.e. every schedule, and then to check closed loop stability for schedules and passes outside this nominal set [80, 81]. Significant limitations of this approach are (a) no attempt is made to explicitly model plant uncertainty due to varying operating conditions, (b) no attempt is made to actively design for robustness to this uncertainty, resulting in wide variations in controller performance across operating conditions (although stability may be retained), and (c) no systematic method for scheduling different controllers across different passes and schedules is obvious.

In this section these limitations are overcome by formulating the problem in the framework of \mathcal{H}_∞ control theory.

5.3.2 The Sendzimir Mill: Nominal Model

The Sendzimir mill model used in the design is taken from [80, 81, 82]. The mill has an ASEA ‘Stressometer’ for measuring the differential tension (or stress) profile across the strip. This device is mounted 2.91m downstream of the roll gap and produces 8 (modelled) output measurements. Four pressure measurements per revolution of this device are provided, causing a four-period-per-revolution sinusoid to be superimposed on the output signal (40Hz at a speed of 10 m/sec.). Further noise on the output signal is introduced due to the 2kHz magnetising currents used with the pressure sensors. Shape actuation is effected via the ‘As-U-Rolls’, which provide the equivalent of 8 independent (but equally spaced) point loads. This generates roll bending, causing differential elongation of the strip, thus influencing the shape profile.

The mill model therefore has 8 inputs and 8 outputs. The rolling cluster is the most complex part of the system and accounts for all of the interaction between the 8 (unmodelled) paths in the system. A linearised gain matrix G_a relates changes in the roll-gap shape profile to changes in the positions of the AUR’s [82]. Diagonal dynamic blocks account for the actuators, strip dynamics (between roll-gap and shapemeter)

and the shapemeter filters. The mill model is therefore of the form

$$y(s) = p(s)G_a f_a(u_a) \quad G_a \in \mathcal{R}^{8 \times 8}$$

where $p(s)$ models dynamics due to the strip and shapemeter, and the nonlinear function $f_a(\cdot)$ represents the AUR actuators. An actuator linearisation technique [83] can be applied to the nonlinear actuators, resulting in an approximately first order linear response for each actuator with a time constant of 2 seconds. The resulting overall mill dynamics are therefore modelled as

$$P(s) = p(s)G_a, \quad G_a \in \mathcal{R}^{8 \times 8}$$

with $p(s)$ given by

$$p(s) = \frac{e^{-0.582s}}{(1.064s + 1)(0.74s + 1)(2s + 1)}$$

for a medium strip speed of approximately 10m/s. For each of the six passes of the schedule we have a different gain matrix $(G_a)_i$, therefore the nominal gain matrix $(G_a)_n$ for the selected schedule is given by

$$(G_a)_n = \begin{pmatrix} 4.3907 & 4.9866 & -0.0720 & -2.1837 & -2.3299 & -2.0186 & -1.7916 & -1.7943 \\ 0.6112 & 2.5487 & 2.5138 & 0.2207 & -1.5248 & -1.9372 & -1.7115 & -1.7027 \\ -0.7673 & 0.4553 & 2.7242 & 1.7667 & -0.5024 & -1.7515 & -1.7883 & -1.7682 \\ -1.0494 & -1.0781 & 1.1593 & 2.6865 & 1.5551 & -0.6776 & -1.7538 & -1.7282 \\ -0.9135 & -1.6900 & -0.7009 & 1.4843 & 2.7079 & 1.2133 & -1.1479 & -1.1449 \\ -0.7882 & -1.7710 & -1.6810 & -0.3389 & 1.9747 & 2.7206 & 0.4609 & 0.4541 \\ -0.7566 & -1.7308 & -1.9495 & -1.5653 & 0.0505 & 2.3465 & 2.6623 & 2.6831 \\ -0.8345 & -1.8083 & -1.9580 & -2.2416 & -1.9845 & -0.1392 & 4.9882 & 4.9173 \end{pmatrix}$$

where

$$(G_a)_n = \frac{\sum_{i=1}^6 (G_a)_i}{6}$$

5.3.3 Nominal Model Reduction and Decoupling

Examination of the gain matrices of the mill reveals that they are remarkably ill-conditioned - the difference between the smallest and largest singular values typically being approximately four orders of magnitude. In addition, an order of magnitude difference exists between the 4 largest and 4 smallest singular values. As an example, the singular value spectrum of the nominal mill gain matrix G_a is

$$\{12.3568 \ 9.1120 \ 4.9125 \ 1.5625 \ 0.3306 \ 0.2101 \ 0.0259 \ 0.0051\}$$

Ill-conditioned plants can be said to be characterised by ‘strong directionality’ because inputs in vector directions corresponding to high plant gains (large singular values)

are strongly amplified by the plant, while inputs corresponding to low plant gains (small singular values) are not. It is well known that ill-conditioned plants can cause serious problems for control system design [79]. The main reason for these problems is plant uncertainty. For accurate control of ill-conditioned plants the controller should attempt to counteract the strong directionality by applying large input signals where the plant gain is low; i.e. the controller should try to approximately invert the plant. However, because of uncertainty, the direction of the large input may not correspond exactly with that of the low plant gain, and the resulting output may as a result be much larger than expected! Since the phenomenon of directionality clearly only exists in multivariable systems, classical design methods based on extensions of SISO techniques are likely to be unreliable for ill-conditioned plants. This is not surprising since techniques such as LQG/LTR, Inverse Nyquist Array, and Characteristic Loci do not explicitly characterise plant uncertainty.

Thus the conditioning of the plant is yet another argument in favour of treating the design problem in the framework of robust control theory. From the point of view of \mathcal{H}_∞ optimisation however, there is a further complication. For a typical mixed sensitivity design, \mathcal{H}_∞ software will attempt to minimise the maximum singular value of S at low frequencies. The problem here is that the smallest singular value of $(G_a)_n$ is *so* small (0.0051), that the maximum singular value of S will be approximately equal to unity at all frequencies, unless the controller has a huge gain in this direction (something which is clearly undesirable from the above argument). The meaning of any singular value of S being equal to unity at all frequencies is that the corresponding loop of the system is essentially open - no feedback is being applied. Note however that since the problem at hand is basically a regulator problem, i.e. the desired shape (stress) profile is uniform i.e. zero at all points, leaving those loops of the system with very small gain open does not represent a serious problem. The real difficulty stems from the fact that, as noted in Section 5.1, \mathcal{H}_∞ optimisation concentrates *exclusively* on minimising the largest singular value of S , and in general does *not* effectively minimise the remaining singular values. Thus for this problem the singular values of S corresponding to the loops with significant gain will not be effectively minimised. This analysis was borne out in practice when a \mathcal{H}_∞ design for the full 8×8 system was attempted. One solution to this problem might seem to be to try to decouple the system and design on a loop-by-loop basis, but since this would involve inverting a matrix which is close to singular it is not a realistic option.

Instead, we adopt the following approach based on a reparameterisation of the

plant in terms of its four most significant singular values, via the singular value decomposition. Partition the plant as:

$$P(s) = p(s)(G_a)_n = p(s)(U_1 \ U_2) \begin{pmatrix} \Sigma_1 & 0 \\ 0 & \Sigma_2 \end{pmatrix} \begin{pmatrix} V_1^T \\ V_2^T \end{pmatrix}$$

where

$$U_1, U_2, V_1, V_2 \in \mathcal{R}^{8 \times 4}, \quad \Sigma_1, \Sigma_2 \in \mathcal{R}^{4 \times 4}$$

Note that Σ_1 and Σ_2 are diagonal matrices, containing the singular values of the gain matrix. A parameterisation U_1^T is now applied to the mill output shape profile, while the control input is parameterised by V_1 . The \mathcal{H}_∞ design is now concentrated on the reduced dimension 4×4 system

$$P_{red}(s) = p(s)U_1^T(G_a)_nV_1$$

It is interesting to note that such a parameterisation is consistent with previous approaches to the design problem, and is also motivated by rolling practice considerations. Notice also that the parameterised system is completely decoupled, and thus this strategy is in keeping with our general approach to \mathcal{H}_∞ design.

5.3.4 Uncertainty Modelling

In addition to the nominal model of the mill, an attempt is made to explicitly characterise the various sources of uncertainty in the system. Changes in strip shape profile are modelled as disturbances at the plant output of the form

$$d(s) = W_1(s)\bar{d}(s), \quad \bar{d}(s) \in \mathcal{BL}_n^2$$

where

$$W_1(s) = \frac{10(10^{-5}s + 1)}{10^2s + 1}I_4$$

This choice of W_1 ensures that the sensitivity function S is penalised heavily at low frequencies to ensure good d.c. attenuation of disturbances in the form of step changes in incoming strip shape profile due to welds. The major source of uncertainty in the system comes from the variation in the elements of the (real) gain matrix G_a over the six passes in the schedule. This uncertainty can be modelled using a multiplicative output uncertainty description of the form

$$G_a = (G_a)_n (I + \Delta_G)$$

where

$$\Delta_G = W_3(s)\overline{\Delta}, \quad \|\overline{\Delta}\|_\infty \leq 1$$

and

$$\overline{\sigma}(W_3(s)) = \frac{\max_i \overline{\sigma}((G_a)_i - (G_a)_n)}{\overline{\sigma}((G_a)_n)}$$

Since the elements of the matrix G_a are real the above analysis would suggest choosing a constant diagonal matrix for W_3 . However, in order to attenuate the effect of the shapemeter measurement noise present in the system we require the complementary sensitivity function T to roll off at high frequencies and thus choose W_3 to be

$$W_3(s) = \frac{0.2774(10^{-3}s + 1)}{10^{-6}s + 1} I_4$$

Note that the above level of plant uncertainty at low frequencies (due to variations in the gain matrices), is quite unusual in \mathcal{H}_∞ design. It is generally assumed that our knowledge of the plant dynamics is quite good at d.c. and at low frequencies, and deteriorates with increasing frequency. The large value of W_3 at low frequencies in this design makes the task of securing adequate performance characteristics quite difficult, and necessitates careful selection of the corresponding weighting function W_1 . Note that this choice of W_3 is also made with the aim of rolling off the closed loop transfer function before the phase effects of the time delay in the system become significant. This is necessary since this time delay must be omitted from the nominal plant for the purposes of \mathcal{H}_∞ design. The process of selecting the weighting functions W_1 and W_3 for this design illustrates clearly the two viewpoints regarding their role. On the one hand they may be viewed as models of the frequency content of likely disturbances, plant uncertainty and measurement noise. On the other they may also be regarded simply as ‘knobs’ with which to shape S and T .

5.3.5 \mathcal{H}_∞ Controller Synthesis and Performance Analysis

The software used to calculate the controller was based on the \mathcal{H}_∞ optimisation function `hinf.m` in the MATLAB Robust Control Toolbox [71]. The initial controller was of order 20, so controller order reduction techniques were used to compute the 16th order controller, given at the end of this subsection in Jordan form. Figure 5.23 shows the sensitivity and complementary sensitivity functions for this controller. Note that S drops to -30dB at low frequency, ensuring good d.c. disturbance rejection, while T rolls off at high frequency giving a closed loop bandwidth of approx. 0.1

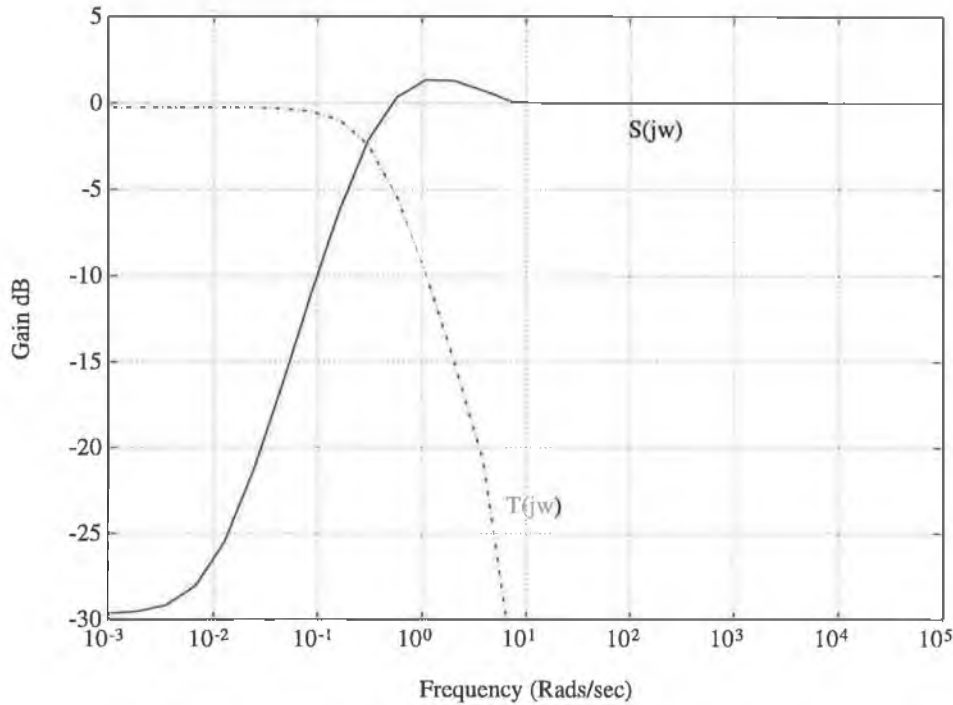


Figure 5.23: Sensitivity and Complementary Sensitivity Functions

rads/sec. and providing good attenuation of high frequency measurement noise. Note also that the closed loop transfer function rolls off before the effects of the time delay in the plant become significant.

To demonstrate the disturbance rejection properties of the design, the parameterised output response to a step disturbance in loop 2 of the idealised (i.e. linear, delay free) system is shown in Figure 5.24. Robustness to variations in the gain matrix G_a is clearly demonstrated by observing that disturbance attenuation is preserved for different G_a 's corresponding to different passes of the schedule. Also of note is the fact that disturbances are decoupled, i.e. the disturbance in loop 2 of the system produces a negligible effect on the outputs of the other loops of the system. These results indicate that a high level of *robust* performance is achieved by the design – this may appear a little surprising since \mathcal{H}_∞ design guarantees nominal performance only. A theoretical explanation for the above results can however be provided by referring to a result in [40], which we give below in the form of a lemma.

Lemma 5.3 *Define the Operating Band of a MIMO control system to be a finite frequency region $[-\omega_1, \omega_1]$ over which performance specifications are prescribed. Then define ϵ to be the \mathcal{L}_∞ norm of the nominal sensitivity matrix on this operating band,*

i.e.

$$\epsilon = \max_{-\omega_1 \leq \omega \leq \omega_1} \bar{\sigma}[S_0(j\omega)]$$

Finally define δ to be the \mathcal{L}_∞ norm of the multiplicative plant uncertainty matrix on this operating band, i.e.

$$\delta = \max_{-\omega_1 \leq \omega \leq \omega_1} \bar{\sigma}[\Delta(j\omega)]$$

Then for every plant $P_0(s)$ in the set of plants $P(s)$, the \mathcal{L}_∞ norm of the sensitivity matrix on the operating band is bounded above by

$$\frac{\epsilon}{(1 - \delta)(1 - \epsilon) - \epsilon} \quad \text{if} \quad (1 - \delta)(1 - \epsilon) > \epsilon$$

The essential meaning of this lemma is that if both the nominal sensitivity and the plant uncertainty are sufficiently small over the operating band, then the degradation in terms of robust performance over this band will not be very significant. We can apply this result to justify the level of robust performance obtained in our design as follows. Choose the frequency range $[-10^{-3}, 10^{-3}]$, as our operating band. Then from the design we have that $\delta = 0.2774$ and $\epsilon = 0.031$. Then the above lemma gives that

$$\max_{-10^{-3} \leq \omega \leq 10^{-3}} \bar{\sigma}[S(j\omega)] < 0.0447$$

since

$$(1 - \delta)(1 - \epsilon) = 0.7 > \epsilon$$

This result means that when the nominal sensitivity function has been ‘pushed down’ to approx. -30 dB over the operating band, the sensitivity function will stay below approx. -27 dB for every plant in the set $P(s)$. This explains the robustness of the performance characteristics seen in Figure 5.24.

The controller developed above was then simulated with a more detailed model of the mill, containing the transport delay (which was ignored in the design), nonlinear actuators together with their linearising precompensators, and a realistic incoming strip shape disturbance. The shape profile variations are shown in Figure 5.25 for the (nominal) controller used with $(G_a)_1$. Parameterised shape profile variations are shown in Figure 5.26 for pass 3. These results confirm the robustness and performance characteristics of the design. Finally, further attempts at controller order reduction based on the Schur decomposition method of [73], produced a 14th order controller with no significant deterioration in quality of control.

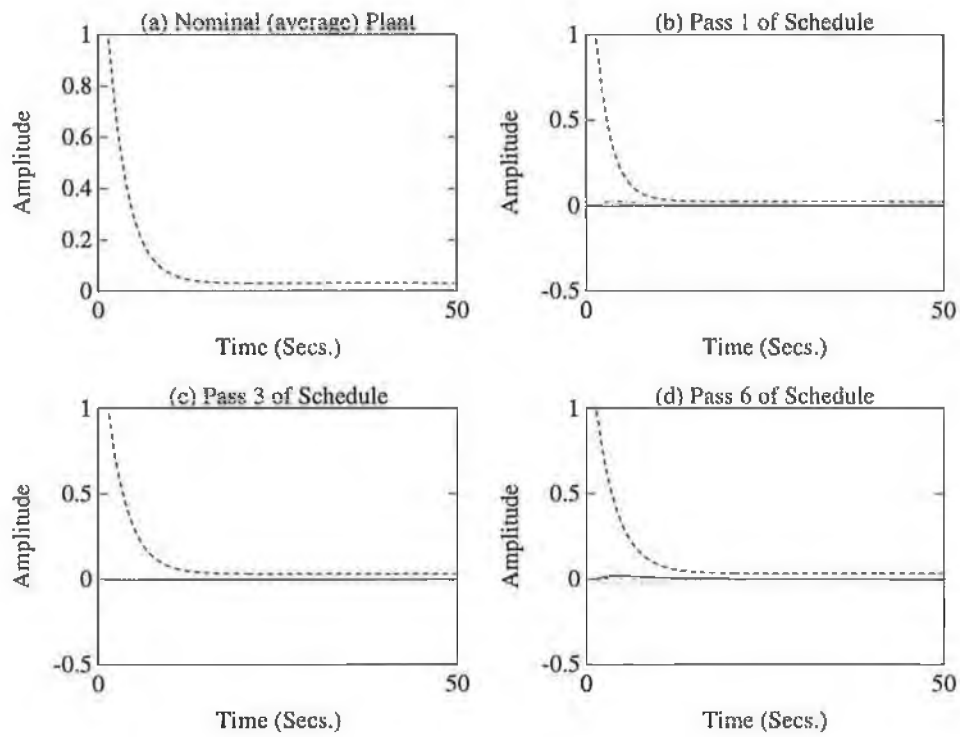


Figure 5.24: Disturbance Rejection properties of the system

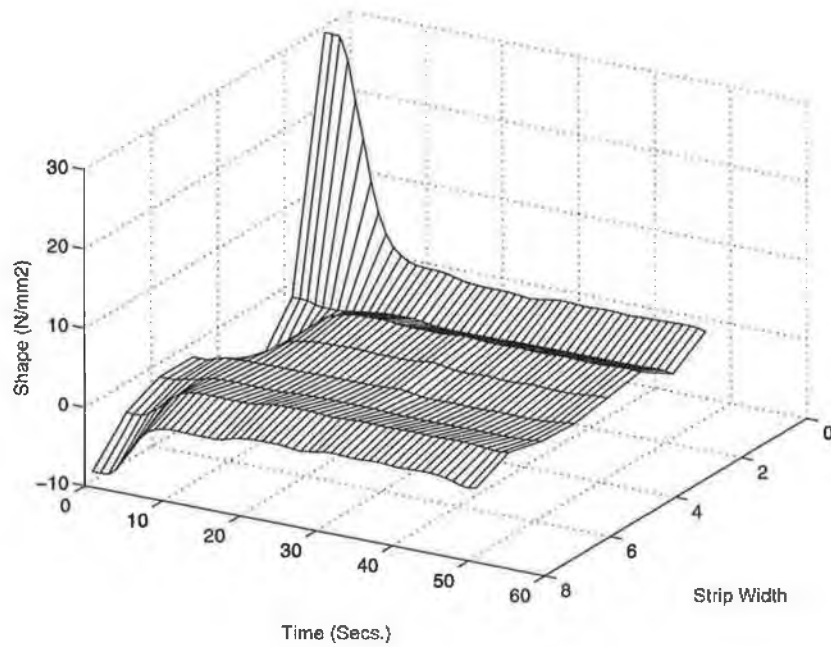


Figure 5.25: Shape Profile Variations (Pass 1.)

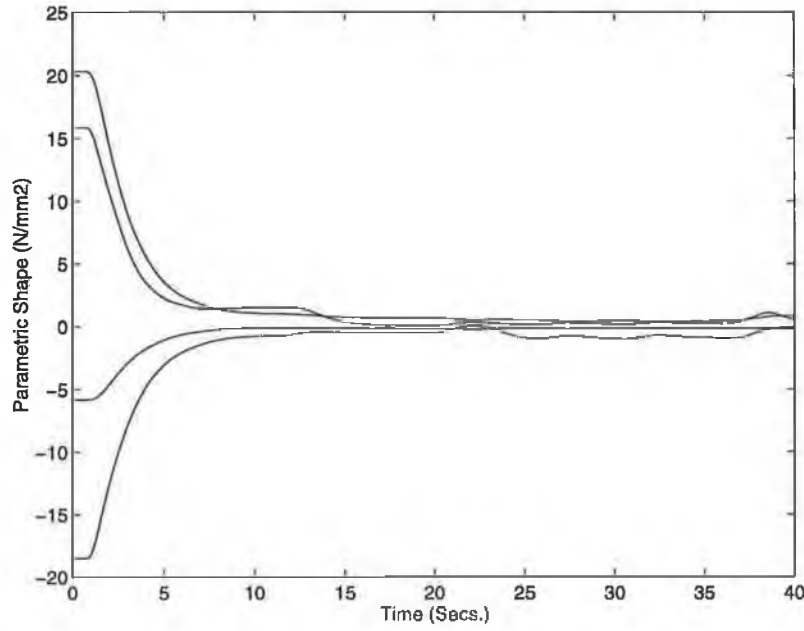


Figure 5.26: Parameterised Shape Profile Variations (Pass 3)

$$\text{eig}(A) = \begin{pmatrix} -1.6076 + 2.6923i \\ -1.6076 - 2.6923i \\ -3.5069 \\ -6.4409 \\ -5.8867 \\ -4.8711 \\ -3.0574 + 5.3484i \\ -3.0574 - 5.3484i \\ -2.2788 + 3.9461i \\ -2.2788 - 3.9461i \\ -2.7722 + 4.8383i \\ -2.7722 - 4.8383i \\ -0.0100 \\ -0.0100 \\ -0.0100 \\ -0.0100 \end{pmatrix}$$

$$B = \begin{pmatrix} 0 & 0.0004 & 0 & -5.1707 + 1.3296i \\ 0 & 0.0004 & 0 & -5.1707 - 1.3296i \\ 0 & 0.0005 & 0.0001 & -8.3054 \\ 5.6945 & 0 & 0 & 0 \\ 0 & 6.0045 & 0 & 0 \\ 0 & 0 & -6.7014 & 0 \\ -1.7091 - 3.0528i & 0 & 0 & 0 \\ -1.7091 + 3.0528i & 0 & 0 & 0 \\ 0 & 0 & 0.9755 - 4.0701i & 0 \\ 0 & 0 & 0.9755 + 4.0701i & 0 \\ 0 & -2.0329 + 3.1005i & 0 & 0 \\ 0 & -2.0329 - 3.1005i & 0 & 0 \\ -0.8599 & 1.7396 & -4.1888 & -3.9928 \\ 5.5923 & -6.5353 & 2.4728 & -2.8606 \\ -5.8928 + 2.3702i & 11.9527 + 0.4073i & 4.4220 - 2.0760i & 0.4375 + 0.7001i \\ -5.8928 - 2.3702i & 11.9527 - 0.4073i & 4.4220 + 2.0760i & 0.4375 - 0.7001i \end{pmatrix}$$

$$G^T = \begin{pmatrix} 0 & 0 & 0 & -0.3703 + 0.6589i \\ 0 & 0 & 0 & -0.3703 - 0.6589i \\ 0 & 0 & 0 & -0.5416 \\ 1.1543 & 0 & 0 & 0 \\ 0 & 1.0485 & 0 & 0 \\ 0 & 0 & -0.8501 & 0 \\ -1.3274 + 0.1567i & 0 & 0 & 0 \\ -1.3274 - 0.1567i & 0 & 0 & 0 \\ 0 & 0 & -0.7583 - 0.7282i & 0 \\ 0 & 0 & -0.7583 + 0.7282i & 0 \\ 0 & 0.6538 + 1.0507i & 0 & 0 \\ 0 & 0.6538 - 1.0507i & 0 & 0 \\ -0.0003 & 0.0008 & -0.0041 & -0.0306 \\ 0.0029 & 0.0009 & 0.0060 & -0.0213 \\ 0.0007 + 0.0036i & 0.0015 + 0.0029i & 0.0020 - 0.0028i & -0.0039 + 0.0098i \\ 0.0007 - 0.0036i & 0.0015 - 0.0029i & 0.0020 + 0.0028i & -0.0039 - 0.0098i \end{pmatrix}$$

$$D = \begin{pmatrix} 0 & 0 & 0 & 0 \\ 0 & 0 & 0 & 0 \\ 0 & 0 & 0 & 0 \\ 0 & 0 & 0 & 0 \end{pmatrix}$$

5.3.6 Discussion and Implications

The benefits of formulating the design problem under the framework of \mathcal{H}_∞ control theory have been clearly demonstrated. Controller synthesis is straightforward and automatic, with most of the design effort being expended, appropriately, on the modelling of uncertainty in the system. The ill-conditioned nature of the plant was dealt with by means of a SVD parameterisation, a procedure which also has the effect of decoupling the closed loop system. In contrast with previous approaches to the problem, robust stability of the design is guaranteed a priori, while analysis of the closed loop system confirms excellent robust performance. Some further benefits of the robustness characteristics of the design are also of note. In particular, it is known that the mill matrices, produced by a static model developed in [82], contain modelling inaccuracies as well as linearisation approximations. Further nonlinear effects are present in the real system due to the operation of the actuators. \mathcal{H}_∞ designs naturally provide a degree of immunity to such errors, as noted in [84]. Finally, the success of this design for a single plant schedule points to an automated design philosophy, which could provide a systematic means of developing a set of controllers for use across the full range of plant operating conditions.

Chapter 6

Conclusions

This chapter contains a discussion of the various observations made throughout the thesis. The main contributions of the thesis are the answers provided to the questions at the start of each section below. In particular some conclusions are drawn regarding the ways in which uncertainty and control specifications are modelled in robust control theory. We also consider the usefulness of a classical decoupling approach to MIMO design problems in the context of robust control.

6.1 \mathcal{H}_∞ Control Theory and Time Domain ‘Spikes’

I. Do \mathcal{H}_∞ optimal controllers suffer from time domain ‘spikes’?

One purpose of this thesis is to show that existing \mathcal{H}_∞ theory does not suffer from the ‘spike’ problem discussed in Chapter 2, provided that appropriate models are adopted for uncertain signal sets.

Previous work in the area of \mathcal{H}_∞ control theory has been based on the use of the \mathcal{L}_2 signal norm on both the input and the output sides. A consequence of using this conventional or energy paradigm for \mathcal{H}_∞ is that, as shown in Lemma 2.1, the output of the system can be subject to ‘spikes’ with arbitrarily large amplitude in the time domain. This is true even when the output signal has been effectively minimized in the usual \mathcal{H}_∞ sense. This result is a theoretical one, and heuristic arguments can be made that extremely large output spikes will not occur in practice. Certainly however, convincing and useful bounds on the time amplitude of $z(t)$ cannot always be guaranteed under the standard \mathcal{H}_∞ control framework. The problem therefore seems to be the ‘gap’ between what is theoretically possible, and what is seen to occur in real life applications. This gap is narrowed by the results presented in Chapter 3, where it is shown that in addition to minimizing the worst case output in the \mathcal{L}_2 norm sense, optimal \mathcal{H}_∞ controllers are also optimal or nearly optimal in other senses. The standard \mathcal{H}_∞ norm guarantees an upper bound on the time domain amplitude of the output signal at all times for the proposed signal sets $\mathcal{D}_w^{(s)}$, $\mathcal{D}_w^{(1)}$ and $\widehat{\mathcal{D}}_w^{(1)}$. It is demonstrated that these proposed signal sets are rich enough for many practical purposes. In the SISO case, optimal non-conservative bounds on $\|z(t)\|_\infty$ are obtained for these signal sets. In the MIMO case, there are still good bounds on $\|z(t)\|_\infty$ for these signal sets because the B norm and the standard \mathcal{H}_∞ norm can be related to each other by tight bounds, as in Theorem 3.4. However, the usual \mathcal{H}_∞ objective function must be modified a little if such bounds are to be non-conservative in the MIMO case.

The conclusion drawn is that the ‘spike’ difficulty is not with existing \mathcal{H}_∞ theory *per se*, it is with the control theoretic pedagogy (i.e. the energy paradigm) which is conventionally attached to it.

6.2 Specification Modelling in Robust Control Theory

II. *Which signal norm provides the best model of the objectives of feedback control systems?*

The \mathcal{L}_1 literature in general and Lemmas 2.1 and 2.2 in particular show that the use of the \mathcal{L}_2 norm to measure the size of output signals is inherently flawed and should be abandoned. The essential significance of Lemma 2.1 is that the \mathcal{L}_2 norm gives a very poor mathematical model of or statement of the ‘real’ objectives and purpose of control systems. It is argued in Chapter 3 that for the majority of applications, the \mathcal{L}_∞ norm provides a much better model of the control specifications than the \mathcal{L}_2 norm, mainly because it non-conservatively treats maximum tracking errors in the time domain. As is clear from the \mathcal{L}_1 literature, doing so requires the \mathcal{L}_∞ norm to be used on the output side. Thus it is significant that as shown in Chapter 3, with the right signal sets, a slightly modified \mathcal{H}_∞ control theory can produce non-conservative results with the most attractive features of the \mathcal{L}_1 approach.

The conclusion drawn is that the \mathcal{L}_∞ signal norm generally provides the best model of the objectives of feedback control systems.

6.3 Uncertain Signal Modelling in Robust Control Theory

III. *Which signal norm provides the best model of uncertain input signals in feedback control systems?*

As discussed in Chapter 2, the presence of signal set lumping in standard \mathcal{H}_∞ control theory means that reasonably accurate models of disturbance/noise/command inputs is impossible *a priori*. The lumping of all uncertain input signals to the system into a single vector which is then measured using the \mathcal{L}_2 norm grossly distorts the true physical situation, since it creates an artificial interdependence between what are essentially independent signals. Carefully choosing weighting functions to obtain accurate models of several independent external disturbance, sensor noise and command inputs is futile because such accurate models would have to be covered by a single unit ball anyway, thereby largely eliminating their descriptive value. In contrast, both the standard \mathcal{L}_1 and the proposed approaches are based on the infinity

vector norm. So they automatically avoid the problem of signal set lumping on the system's inputs.

The conclusion drawn is that the infinity vector norm provides the best model of uncertain input signals in feedback control systems.

6.4 Time Domain Specifications and Frequency Domain Design

IV. *Can time domain specifications be satisfied exactly using frequency domain design methods?*

The signals in the signal set $\mathcal{D}_w^{(s)}$ introduced in Chapter 3 are sinusoids. The signal sets $\mathcal{D}_w^{(1)}$ and $\widehat{\mathcal{D}}_w^{(1)}$ are described in the frequency domain. The resulting induced system norm to be minimized is most naturally expressed in the frequency domain. Thus, like standard \mathcal{H}_∞ control theory, the pedagogy presented in Chapter 3 is very much a frequency domain approach. This is an important feature of the proposed approach, because the engineer can effectively bring his frequency domain experience and intuition to bear on a practical problem. A frequency domain setting for controller design paradigms is favoured intuitively by many engineers familiar with classical design methods. In contrast with standard \mathcal{H}_∞ control theory however, the control specifications in the new pedagogy are expressed and satisfied exactly in the time domain. While this is also the case in the standard \mathcal{L}_1 approach, \mathcal{L}_1 control theory is *not* a frequency domain but a time domain theory, and therefore it seems to suffer at present from a serious lack of design transparency. Finally it is shown in Chapter 3 that the ideas outlined above have a natural extension to \mathcal{H}_2 control theory. Indeed they provide a new deterministic interpretation of \mathcal{H}_2 control theory in the MIMO case.

The conclusion drawn is that slightly modified frequency domain \mathcal{H}_∞ and \mathcal{H}_2 control theories can be used to exactly satisfy time domain specifications.

6.5 Weighting Function Selection and Manipulation in \mathcal{H}_∞ Control theory

V. *How can procedures for the selection and manipulation of weighting functions be made more systematic, transparent and scientific?*

A major problem with robust control theory in general is its reliance on weighting transfer functions. Where are these weights supposed to come from? It is argued in Chapter 3 that the results presented have significant implications for the weight selection problem.

In standard \mathcal{H}_∞ design, the combined impact of the limitations (i) to (iii) described in Chapter 2 is that the designer is obliged to fall back on design thinking which is sub-optimal and/or heuristic. It is argued that the need for viewing weights as ‘tuning knobs’ in present day \mathcal{H}_∞ design and the need for frustrating and time consuming iterations in the design process comes at least partly from these limitations. In short, the impact of (i) to (iii) is to sever the connection between realistic design on the one hand, and the formal mathematical optimization problems described above on the other hand. The results presented in Chapter 3 represent an attempt to narrow this ‘gap’, i.e. that between the engineering aspects and the mathematical aspects of \mathcal{H}_∞ control theory. The mathematical optimization problems of Chapter 3 more faithfully capture the ‘real’ control engineering problem by improving the model on both the input side (III above) and the output side (II above). This new paradigm clarifies the fundamentally different roles played by weighting functions on the input and the output side, and makes possible the approach to weighting function selection and manipulation proposed in Chapter 3.

The conclusion drawn is that the weighting function on the input side W should be viewed as a fixed model of possible uncertain input signals, under the modified \mathcal{H}_∞ paradigm proposed. In this paradigm the output weighting function V may then be used to examine and tune the relative quality of control of each individual element of the output, and to manage the tradeoffs between them. So V enables each output signal z_i to be weighted separately, allowing the relative importance of each to be traded off by tuning the appropriate diagonal element of V . The use of weighting functions on both the input and the output sides is also appropriate when modelling system uncertainty as this allows extra design flexibility in the MIMO case. It is argued that the two viewpoints regarding the roles of the weighting functions (as models

of uncertainty and also as models of control system objectives and tradeoff priorities) are complementary rather than contradictory, but that this distinction needs to be formally recognised. The proposed approach fulfills this objective, resulting hopefully in a more transparent and systematic approach to \mathcal{H}_∞ design.

6.6 Connections between \mathcal{H}_∞ and \mathcal{L}_1 Control Theories

VI. *How ‘far apart’ are the \mathcal{L}_1 and \mathcal{H}_∞ control theories?*

The signal sets $\mathcal{D}_w^{(1)}$ and $\widehat{\mathcal{D}}_w^{(1)}$ described in Chapter 3 are defined as having bounded \mathcal{L}_1 norm in the frequency domain. This may seem a little unnatural at first, and one is left wondering what this set of signals ‘looks like’. Now, since every element of $\mathcal{D}_w^{(s)}$ has time domain amplitude less than or equal to unity, it follows immediately that every element of the closure of its convex hull must also have time domain amplitude less than or equal to unity. Alternatively, letting \mathcal{F}^{-1} denote the inverse Fourier transform, arguments similar to those used in the proofs of Chapter 3 can be used to show directly that

$$\mathcal{F}^{-1}\{\widehat{\mathcal{D}}_w^{(1)}\} \subset \mathcal{D}_w^{(m)} \quad (6.1)$$

by which we mean that

$$\begin{aligned} w(j\omega) &\in \widehat{\mathcal{D}}_w^{(1)} \\ \Rightarrow \mathcal{F}^{-1}\{w(j\omega)\} &= w(t) \in \mathcal{BL}_\infty^n(t) \\ \Rightarrow |w_i(t)| &\leq 1 \quad \forall t, i \end{aligned}$$

Hence, signals in $\widehat{\mathcal{D}}_w^{(1)}$ are also in $\mathcal{BL}_\infty^n(t)$, and so the proposed signal sets have an obvious time domain bound, just like $\mathcal{BL}_\infty^n(t)$. However, the set $\mathcal{BL}_\infty^n(t)$ is larger. A counterexample to equality in eqn. (6.1) is the unit step function. Being infinite dimensional, the set $\widehat{\mathcal{D}}_w^{(1)}$ is still a huge vector space, and it can be argued that it should be rich enough for most practical purposes. So it seems that $\widehat{\mathcal{D}}_w^{(1)}$ can be viewed loosely as being similar to $\mathcal{BL}_\infty^n(t)$, but a little smaller.

The conclusion drawn from this analysis is that the \mathcal{H}_∞ and \mathcal{L}_1 theories are not as far apart as they might seem to be at first glance. Indeed, the analysis in this thesis shows they are quite close in certain senses. The proposed approach uses the same norm as the \mathcal{L}_1 theory on the output side, and the only difference is in the choice of

the (unstructured) signal uncertainty set,

$$\sup_{w(t) \in \mathcal{BL}_\infty^n(t)} \|z(t)\|_\infty \quad \text{Versus} \quad \sup_{w(j\omega) \in \mathcal{BL}_1^n(j\omega)} \|z(t)\|_\infty$$

On the input side, simply replacing $\mathcal{BL}_\infty^n(t)$ with its ‘subset’ $\mathcal{BL}_1^n(j\omega)$ means that the resulting \mathcal{L}_1 type problem (i.e. that of minimizing the worst case $\|z(t)\|_\infty$) leads to a problem which is very close to standard \mathcal{H}_∞ .

It seems remarkable that $\mathcal{F}^{-1}\{\widehat{\mathcal{D}}_w^{(1)}\}$ looks so like $\mathcal{BL}_\infty^n(t)$, (as in eqn. (6.1)), but that the corresponding optimal controllers are so different. The distinction between these two sets is therefore an important question for future research, because it is fundamental to understanding the difference between \mathcal{L}_1 control theory and \mathcal{H}_∞ like control theories.

6.7 A Comparison of the Different Paradigms

VII. *How do the different robust control paradigms compare?*

A brief description of some of the strengths and weaknesses of the different control paradigms is given below in Table 6.1.

Paradigm:	\mathcal{H}_∞	\mathcal{L}_1	New
“Spikes” are prohibited	No	Yes	Yes
Signal set lumping is avoided	No	Yes	Yes
Specification lumping is avoided	No	Yes	Yes
It is a genuinely frequency domain approach	Yes	No	Yes
Optimal continuous time controllers are rational	Yes	No	Yes

Table 6.1: Brief Comparison of Alternative Approaches.

The conclusion drawn from the above table is that a theory which is very close to standard \mathcal{H}_∞ control theory can optimally and non-conservatively minimize maximum

tracking errors in the time domain. The \mathcal{L}_1 theory is one route to achieving this, but it is very much a time domain theory, and seems to suffer from applications difficulties. In contrast, the proposed approach provides a frequency domain theory for achieving the above time domain control objectives, which is therefore closer to the ‘classical’ approaches familiar to every control engineer. In this way, the modified \mathcal{H}_∞ theory proposed seems to capture the most attractive features of the standard \mathcal{H}_∞ and \mathcal{L}_1 approaches.

6.8 Decoupling MIMO Systems for Super-Optimal Robust Controller Design

VIII. *Can super-optimal robust controllers be directly designed by decoupling closed loop MIMO systems?*

In Chapter 4 a design method is presented which may be used to construct \mathcal{H}_∞ , \mathcal{L}_1 and modified \mathcal{H}_∞ optimal controllers which completely decouple the closed loop system, provided the plant is square, stable and minimum-phase. It is shown that these controllers are super-optimal, i.e. optimal (in the appropriate sense) for each loop of the system. Note that in this context the term ‘decoupling’ means that the closed loop transfer function matrix is diagonal (or almost diagonal) – thus each loop of the MIMO system is decoupled from every other loop. In effect the proposed method allows the designer to select the super-optimal controller which decouples the system, from the set of optimal MIMO controllers for the problem. The design problem is transformed from one multivariable problem into a number of independent SISO problems, thus allowing greater transparency and flexibility in the design process. In Chapter 5 the proposed decoupling design method is applied to the HIMAT pitch axis controller design problem. For multivariable plants which are stable but non-minimum-phase, half-decoupling can be achieved by transforming the multivariable design problem into a number of independent MISO problems.

The conclusion drawn is that under certain restrictive conditions, super-optimal robust controllers which decouple the closed loop system can easily be constructed.

6.9 Loopshaping Decoupled MIMO Systems for Improved Performance

VIII. *Is a classical decoupling approach to MIMO control system design useful in the context of modern multivariable robust control theory?*

Classical multivariable design procedures such as Inverse Nyquist Arrays and Characteristic Loci were based on the idea of decoupling the design problem as much as possible, and then applying SISO techniques to achieve satisfactory performance. With the advent of truly multivariable design methods such as \mathcal{H}_∞ control, the idea of decoupling the MIMO problem into a number of SISO problems may have appeared obsolete. In Chapter 5 however, it is shown that decoupling the design problem allows SISO loopshaping techniques to be used to improve MIMO robust controller designs in a number of different ways. Once the initial optimal decoupling controller has been calculated cascade controllers can be used to improve robust performance and meet time domain objectives. SISO loopshaping is a well established technique in robust control – it allows the designer a great deal of flexibility and provides much needed insight into the nature of the difficulties inherent in the particular problem. Multivariable loopshaping on the other hand is a decidedly more complex proposition. Decoupling the problem allows the application of SISO loopshaping techniques to MIMO systems. Finally the Sendzimir mill shape control problem discussed in Chapter 5 illustrates the advantages of using the singular value decomposition to decouple ill-conditioned plants prior to \mathcal{H}_∞ design.

The conclusion drawn is that attempting to decouple the closed loop system as part of the design process makes sense from a classical *and* a robust control point of view.

6.10 Directions for Future Research

The work completed in this thesis naturally suggests some fruitful avenues for further research. The paradigm for optimal robust controller synthesis presented in Chapter 3 proposes some new optimisation problems, which at present are unsolved analytically. However since these problems are convex, sub-optimal solutions can be generated using numerical methods, for example by using the convex optimisation approach detailed in [6]. Thus one obvious direction for future research is in the development

of analytical and/or customised numerical solutions to these optimisation problems.

Another open problem is the issue of robust performance in the proposed paradigm, since the optimisation problems involving the B and C norms introduced in Chapter 3 guarantee certain levels of nominal performance only. Many important questions concerning the effect of system uncertainty (whether structured or unstructured) on control performance in the time domain are open, in both analysis and synthesis.

Finally it has been argued above that the quality of control achieved by a feedback system depends to a large extent on the way in which uncertainty is modelled in the design process. In the case of signal uncertainty, new signal sets have been proposed in this thesis with the aim of more faithfully capturing the physical realities in which control systems operate. Ultimately however, the type and level of uncertain signals acting on a system will depend on the particular environment in which it is operating. Wind gusts on the wings of an aircraft for example will certainly have different physical characteristics than wave motion acting on the hull of a ship. Therefore the development of formalised identification procedures, which would produce applications specific models of uncertain signals for use in robust controller design would be highly desirable.

Bibliography

- [1] D. G. Bates and A. M. Holohan, " \mathcal{H}_∞ Control Theory Solves an \mathcal{L}_1 Problem", *Oral Presentation, 3rd SIAM Conference on Control and its Applications*, St. Louis MI, April 1995.
- [2] D. G. Bates and A. M. Holohan, "Non-Conservative Minimisation of Maximum Tracking Errors in the Time Domain Using \mathcal{H}_∞ Control theory", *in preperation*, 1996.
- [3] D. G. Bates and A. M. Holohan, "A Decoupling Design Method for Super-Optimal \mathcal{H}_∞ Control", *Poster Presentation, Euraco Network Workshop on Robust and Adaptive Control*, Dublin, Ireland, 1994.
- [4] D. G. Bates and A. M. Holohan, "A Decoupling Design Method for Super-Optimal Robust Control", *in preperation*, 1996.
- [5] D. G. Bates, J. V. Ringwood and A. M. Holohan, "Robust Shape Control in a Sendzimir Cold-Rolling Steel Mill", *to appear in Proc. IFAC World Congress*, San Francisco, 1996.
- [6] S. P. Boyd and C. H. Barratt, "Linear Controller Design", Prentice Hall, 1991.
- [7] B. D. O. Anderson and J. B. Moore, "Optimal Control: Linear Quadratic methods", Prentice Hall, 1989.
- [8] G. Zames, "Feedback and Optimal Sensitivity: Model Reference Transformations, Multiplicative Seminorms, and Approximate Inverses", *IEEE Transactions on Automatic Control*, Vol. AC-26, pp 301-320, April 1981.
- [9] J. C. Doyle, "A Review of μ for Case Studies in Robust Control", *in Proc. IFAC 10th World Congress*, Munich, 1987.

- [10] M. A. Dahleh and I. J. Diaz-Babillo, "Control of Uncertain Systems", Prentice Hall, 1995.
- [11] G. Zames, "On the Input-Output Stability of Time-Varying Non-Linear Feedback Systems", *IEEE Transactions on Automatic Control*, Part 1: Vol. AC-11, pp. 228-238, April 1966, Part 2: Vol. AC-11, pp. 465-476, July 1966.
- [12] C. A. Desoer and M. Vidyasager, "Feedback Systems: Input-Output Properties, Academic Press, 1975.
- [13] M. Green and D. J. N. Limebeer, "Linear Robust Control", Prentice Hall, 1994.
- [14] A. L. Tits and M. K. H. Fan, "On the Small- μ Theorem, *Automatica*, Vol. 31, pp. 1199-1201.
- [15] J. C. Doyle and G. Stein, "Multivariable Feedback Design: Concepts for a Classical/Modern Synthesis, *IEEE Transactions on Automatic Control*, Vol. AC-26, pp. 4-16, Feb. 1981.
- [16] J. B. Garnett, "Bounded Analytic Functions", Academic Press, 1981.
- [17] Y. V. Genin and S. Y. Kung, "A Two-Variable Approach to the Model Reduction Problem with Hankel Norm Criterion", *IEEE Transactions on Circuits and Systems*, Vol 28, pp. 912-924, Sept. 1981.
- [18] G. Zames and B. A. Francis, "Feedback, Minimax Sensitivity and Optimal Robustness", *IEEE Transactions on Automatic Control*, Vol. AC-28, pp 586-601, May 1983.
- [19] P. Duren, "Bounded Analytic Functions", Academic Press, 1981.
- [20] D. G. Luenberger, "Optimisation by Vector Space Methods", Wiley, 1969.
- [21] A. M. Holohan and M. G. Safonov, "Neoclassical Control Theory: A Functional Analysis Approach to Optimal Frequency Domain Controller Design", in *Control and Dynamic Systems*, Academic Press, Ed. by C. T. Leondes, Vol. 50, pp. 297-329, 1992.
- [22] A. M. Holohan and M. G. Safonov, "Nominal and Robust Loop Shaping", *Proc. American Control Conference*, Chicago, Ill, pp. 901-905, June 1992.

- [23] K. Glover, "All Optimal Hankel-norm Approximations of Linear Multivariable Systems and their \mathcal{L}_∞ -error Bounds", *International Journal of Control*, Vol. 39, No. 6, pp. 1115-1193, June 1984.
- [24] J. C. Doyle, K. Glover, P. P. Khargonekar and B. A. Francis, "State-Space Solutions to Standard \mathcal{H}_2 and \mathcal{H}_∞ Control Problems", *IEEE Transactions on Automatic Control*, Vol. AC-34, No. 8, pp. 831-846, Aug. 1989.
- [25] H. Kwakernaak, "Minimax Frequency Domain Performance and Robustness Optimization Of Linear Feedback Systems", *IEEE Transactions on Automatic Control*, Vol. AC-30, pp. 994-1004, Oct. 1985.
- [26] H. Kwakernaak, "A Polynomial Approach to Minimax Frequency Domain Optimization of Multivariable Feedback Systems", *International Journal of Control*, Vol. 44, No. 1, pp. 117-156, 1986.
- [27] D. Sarason, "Generalised Interpolation in \mathcal{H}_∞ ", Transactions of the American Mathematics Society, Vol. 127, pp. 179-203, 1967.
- [28] B. A. Francis and G. Zames, "On \mathcal{H}_∞ -Optimal Sensitivity Theory for SISO Feedback Systems", *IEEE Transactions on Automatic Control*, Vol. AC-29, Jan. 1984.
- [29] J. S. Freudenberg and D. P. Looze, "An Analysis of \mathcal{H}_∞ Optimization Design Methods", *IEEE Transactions on Automatic Control*, Vol. AC-31, Mar. 1986.
- [30] J. L. Stoustrup, H. Niemann and A. Saberi, "Robust Almost Disturbance Decoupling", *Proc. IEEE Conf. on Decision and Control*, New Orleans, Louisiana, 1995.
- [31] T. Zhou, M. Fujita and F. Matsumura, "Robust Control of a Two-Axis, Magnetic Suspension, Flexible Beam System Based on \mathcal{H}_∞ Optimisation Theory", *International Journal of Robust and Nonlinear Control*, 1992.
- [32] T. Liu, J. Shi and C. Liu, "Robust Controller Design and Efficiency Analysis for a Brushless Servo System", *Journal of the Chinese Institute of Engineers*, 1991.
- [33] J. S. Freudenberg and D. P. Looze, "Right Half Plane Poles and Zeros and Design Tradeoffs in Feedback Systems", *IEEE Transactions on Automatic Control*, Vol. AC-30, June 1985.

- [34] J. G. Owens and G. Zames, "Duality Theory of Robust Disturbance Attenuation", *Automatica*, Vol. 29, pp. 695-705, 1993.
- [35] J. G. Owens and G. Zames, "Duality Theory for MIMO Robust Disturbance Attenuation", *IEEE Transactions on Automatic Control*, Vol. 38, pp. 743-752, 1993.
- [36] J. C. Doyle, "Synthesis of Robust Controllers and Filters", *Proc. IEEE Conf. on Decision and Control*, pp. 109-114, Dec. 1983.
- [37] M. G. Safonov, "Optimal Diagonal Scaling for Infinity Norm Optimisation", *Systems and Control Letters*, Vol. 7, pp. 257-260, July 1986.
- [38] M. G. Safonov and J. C. Doyle, "Minimizing Conservativeness of Robustness Singular Values", in *Multivariable Control*, Ed. S. G. Tzafestas, D. Reidel Publishing Company, pp. 197-207, 1984.
- [39] J. S. Bird and B. A. Francis, "On the Robust Disturbance Attenuation Problem", *Proc. IEEE Conf. on Decision and Control*, Athens, Greece, pp. 1804-1809, Dec. 1986.
- [40] S. D. O'Young and B. A. Francis, "Optimal Performance and Robust Stabilization", *Automatica*, Vol 22, No. 2, pp. 171-183, 1986
- [41] F. M. Callier and C. A. Desoer, "An Algebra of Transfer Functions of Distributed Linear Time Invariant Systems", *IEEE Transactions on Circuits and Systems*, Vol. CAS-25, Sept. 1978.
- [42] M. A. Dahleh and J. B. Pearson "l¹-optimal Compensators for Continuous-Time Systems", *IEEE Transactions on Automatic Control*, Vol. AC-32, pp. 889-895, Oct. 1987.
- [43] M. A. Dahleh and J. B. Pearson "Optimal Rejection of Persistent Disturbances, Robust Stability, and Mixed Sensitivity Minimization", *IEEE Transactions on Automatic Control*, Vol. AC-33, pp. 722-731, 1988.
- [44] M. A. Dahleh and I. J. Diaz-Bobillo, "Control of Uncertain Systems", Prentice Hall, 1995.

- [45] M. A. Dahleh and Y. Ohta, "A Necessary and Sufficient Condition for Robust BIBO Stability", *Systems and Control Letters*, Vol. 11, pp. 271-275, 1988.
- [46] F. Blanchini and M. Sznajder, "Rational \mathcal{L}_1 Suboptimal Compensators for Continuous-Time Systems", *IEEE Transactions on Automatic Control*, Vol. AC-39, pp. 1487-1492, July. 1994.
- [47] Y. Ohta, H. Maeda and S. Kodama, "Rational Approximation of \mathcal{L}_1 Optimal Controllers for SISO systems", *IEEE Transactions on Automatic Control*, Vol. AC-37 pp. 1683-1691, 1992.
- [48] I. J. Diaz-Bobillo and M. A. Dahleh, "Minimization of the Maximum Peak-to-Peak Gain: The General Multiblock Problem", *IEEE Transactions on Automatic Control*, Vol. AC-38, pp. 1459-1482, Oct. 1993.
- [49] D. G. Luenberger, "Linear and Nonlinear Programming", Addison-Wesley, 1973.
- [50] M. A. Dahleh and J. B. Pearson, " l_1 Optimal Feedback Controllers for Discrete Time Systems", *Proc. ACC*, Seattle, pp. 1964-1968, 1986.
- [51] M. A. Dahleh and J. B. Pearson " l^1 -optimal Feedback Controllers for MIMO Discrete-Time Systems", *IEEE Transactions on Automatic Control*, Vol. 32, pp. 314-322, April 1987.
- [52] M. A. Dahleh and M. H. Khammash "Controller Design for Plants with Structured Uncertainty", *Automatica*, Vol. 29, pp. 37-56, 1993.
- [53] W. Rudin, "Real and Complex Analysis", McGraw Hill, 1987.
- [54] K. Zhou, J. C. Doyle and K. Glover, "Robust and Optimal Control", Prentice Hall, 1995.
- [55] S. P. Boyd, V. Balakrishnan, C. H. Baratt, N. Khraishi, X. Li, D. Meyer and S. Norman, "A New CAD Method and Associated Architectures for Linear Controllers", *IEEE Transactions on Automatic Control*, Vol. AC-33, pp. 268-283, March 1988.
- [56] S. P. Boyd, C. H. Baratt and S. Norman, "Linear Controller Design: Limits of Performance via Convex Optimisation", *Proc. IEEE*, Vol. 78, pp. 529-574, March 1990.

- [57] A. M. Holohan, "On the SISO Optimal Robust Disturbance Attenuation Problem", *in preperation*.
- [58] J. A. Donnellan and A. M. Holohan, "Convex Optimisation for Controller Design", *Poster Presentation, 3rd SIAM Conference on Control and its Applications*, St. Louis MI, April 1995.
- [59] H. Kwakernaak and R. Sivan, "Linear Optimal Control Systems", Wiley, 1972.
- [60] M. Vidyasager, "Optimal Rejection of Persistent Bounded Disturbances", *IEEE Transactions on Automatic Control*, Vol. AC-31, pp. 527-534, June 1986.
- [61] P. P. Kwakernaak and M. A. Rotea, "Mixed \mathcal{H}_2 / \mathcal{H}_∞ Control: A Convex Optimisation Approach", *IEEE Transactions on Automatic Control*, Vol. AC-36, pp. 824-837, July 1991.
- [62] A. A. Stoorvogel, "The Robust \mathcal{H}_2 Control Problem: A Worst Case Design", *IEEE Transactions on Automatic Control*, Vol. AC-38, pp. 1358-1370, Sept. 1993.
- [63] A. Sideris and H. Rotstein, "Single-input-Single-output \mathcal{H}_∞ -control with Time Domain Constraints", *Automatica*, Vol. 29, pp. 969-983, 1993.
- [64] M. C. Tsai, D. W. Gu and I. Postlethwaite, "A State Space Approach to Super-Optimal \mathcal{H}_∞ Control Problems", *IEEE Transactions on Automatic Control*, Vol. AC-33, pp. 833-843, Sept. 1988.
- [65] F. B. Yeh and T. S. Hwang, "A computational Algorithm for the Super-Optimal Solution of the Model Matching Problem", *Systems and Control Letters*, Vol. 11, pp. 203-211, 1988.
- [66] D. J. N. Limbeer, G. D. Halikias and K. Glover, "State Space Algorithm for the Computation of Superoptimal Matrix Interpolation Functions", *International Journal of Control*, Vol. 50, pp. 2431-2466, 1989.
- [67] P. O. Nyman, "A Super-Optimization Method for Four Block Problems", *SIAM Journal of Control and Optimisation*, Vol. 32, pp. 86-115, Jan. 1994.
- [68] C. A. Desoer, R. W. Liu, J. Murray and R. Saeks, "Feedback System Design: The Fractional Representation Approach to Analysis and Synthesis", *IEEE Transactions on Automatic Control*, Vol AC-25, pp. 399-412, June 1980.

- [69] J. Stoustrup and H. Niemann, "Sensitivity Synthesis for MIMO Systems: A Multi Objective \mathcal{H}_∞ Approach", in *Proc. ACC*, Seattle, Washington, pp. 1448-1452, 1990.
- [70] A. Packard, J. C. Doyle and G. Balas, "Linear, Multivariable Robust Control With a μ Perspective", *Journal of Dynamic Systems, Measurement, and Control*, Vol. 115, pp. 426-438, June 1993.
- [71] M. G. Safonov and R. Y. Chiang, "Robust Control Toolbox", *for use with MATLAB* ©The Mathworks, 1988
- [72] J. M. Maciejowski, "Multivariable Feedback Design", Addison Wesley, 1989.
- [73] M. G. Safonov and R. Y. Chiang, "A Schur Method for Balanced-Truncation Model Reduction", *IEEE Transactions on Automatic Control*, Vol. AC-34, pp. 729-733, July 1989.
- [74] J. C. Doyle, B. A. Francis and A. R. Tannenbaum, "Feedback Control Theory", Macmillan Publishing Company, New York, 1992
- [75] I. Postlethwaite, J. L. Lin and D. W. Gu, "A Loop-Shaping Approach to Robust Performance for SISO Systems", *Transactions of The Institute of Measurement and Control*, Vol. 13, No. 5, pp. 262-268, 1991.
- [76] H. W. Bode, "Network Analysis and Feedback Amplifier Design", Van Nostrand, New York, 1945.
- [77] J. W. Helton, "Worst Case Analysis in the Frequency Domain: The \mathcal{H}_∞ Approach to Control", *IEEE Transactions on Automatic Control*, Vol. AC-30, pp. 1154-1170, 1985.
- [78] G. Balas, J. C. Doyle, K. Glover, A. Packard and R. Smith, "The μ Analysis and Synthesis Toolbox", *for use with MATLAB*, ©The Mathworks, 1991.
- [79] S. Skogestad, M. Morari and J. C. Doyle, "Robust Control of Ill-Conditioned Plants: High-Purity Distillation", *IEEE Transactions on Automatic Control*, Vol. AC-33, pp. 1092-1105, Dec. 1988.

- [80] J. V. Ringwood and M. J. Grimble, "Shape Control in Sendzimir Mills using both Crown and Intermediate Roll Actuators", *IEEE Transactions on Automatic Control*, Vol. AC-35, 1990.
- [81] J. V. Ringwood, D. H. Owens and M. J. Grimble, "Feedback Design of a Canonical Multivariable System with application to Shape Control in Sendzimir Mills", in *Proc. ACC*, San Diego, 1990.
- [82] G. W. D. M. Gunawardene, "Static Model Development for the Sendzimir Cold-Rolling Mill", *Ph.D. Thesis, Sheffield City Polytechnic*, 1982.
- [83] J. V. Ringwood, "Diagonalisation of a Class of Multivariable Systems via an Actuator Linearisation Technique", in *Proc. IMC-11*, Belfast, 1994.
- [84] M. G. Safonov, "Stability and Robustness of Multivariable Feedback Systems", MIT Press, Cambridge, MA, 1980.